

NASA CONTRACTOR
REPORT

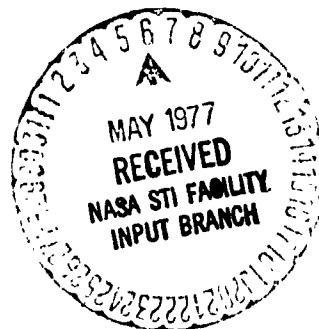
NASA CR-150220

(NASA CR-150220) WIND SHEAR AND WET AND DRY THERMODYNAMIC INDICES AS PREDICTORS OF THUNDERSTORM MOTION AND SEVERITY AND APPLICATION TO THE AVE 4 EXPERIMENTAL DATA (Tennessee Univ. Space Inst., Tullahoma.) N77-21801 HC A50/MF A01 Unclass G3/47 24950

WIND SHEAR AND WET AND DRY THERMODYNAMIC INDICES AS
PREDICTORS OF THUNDERSTORM MOTION AND SEVERITY AND
APPLICATION TO THE AVE 4 EXPERIMENTAL DATA

By James R. Connell and Lillian Ey
University of Tennessee Space Institute
Tullahoma, Tennessee

March 1977



Prepared for
NASA - GEORGE C. MARSHALL SPACE FLIGHT CENTER
Marshall Space Flight Center, Alabama 35812

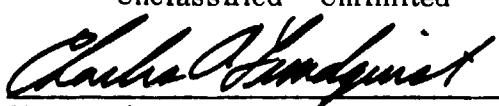
1. REPORT NO. NASA CR-150220	2. GOVERNMENT ACCESSION NO.	3. RECIPIENT'S CATALOG NO.	
4. TITLE AND SUBTITLE Wind Shear and Wet and Dry Thermodynamic Indices as Predictors of Thunderstorm Motion and Severity and Application to the AVE IV Experimental Data		5. REPORT DATE March 1977	6. PERFORMING ORGANIZATION CODE
		8. PERFORMING ORGANIZATION REPORT #	
7. AUTHOR(S) James R. Connell and Lillian Ey		10. WORK UNIT NO.	
9. PERFORMING ORGANIZATION NAME AND ADDRESS The University of Tennessee Space Institute Tullahoma, Tennessee		11. CONTRACT OR GRANT NO. NAS8-31718	
		13. TYPE OF REPORT & PERIOD COVERED Contractor	
12. SPONSORING AGENCY NAME AND ADDRESS National Aeronautics and Space Administration Washington, D. C. 20546		14. SPONSORING AGENCY CODE	
15. SUPPLEMENTARY NOTES Prepared under the technical monitorship of the Atmospheric Sciences Division, Space Sciences Laboratory, NASA/Marshall Space Flight Center			
16. ABSTRACT <p>Two types of parameters are computed and mapped for use in assessing their individual merits as predictors of occurrence and severity of thunderstorms. The first group is comprised of equivalent potential temperature, potential temperature, water vapor mixing ratio, and wind speed. Equivalent potential temperature maxima and strong gradients of equivalent potential temperature at the surface correlate well with regions of thunderstorm activity. The second type comprised of the energy index, shear index, and energy shear index, incorporate some model dynamics of thunderstorms, including nonthermodynamic forcing. The energy shear index is found to improve prediction of tornadic and high-wind situations slightly better than other indices.</p> <p>It is concluded that further development and refinement of nonthermodynamic aspects of predictive indices are definitely warranted. Some specific recommendations for further work are made which involve looking at atmospheric structure in finer detail, with more physical insight, and using correlation techniques for formulating the best predictor indices.</p>			
17. KEY WORDS		18. DISTRIBUTION STATEMENT Unclassified - Unlimited  Charles A. Lundquist Director, Space Sciences Laboratory	
19. SECURITY CLASSIF. (of this report) Unclassified	20. SECURITY CLASSIF. (of this page) Unclassified	21. NO. OF PAGES 116	22. PRICE NTIS

TABLE OF CONTENTS

	Page
I. Introduction	1
II. Synoptic Conditions	2
III. The Thunderstorm Model	42
IV. The Predictive Indices	46
V. Applications of Indices to AVE IV Data	58
VI. Summary of Results	97
VII. Conclusions and Recommendations	97
Appendix A. Computer Program and Program Checkout	100
References	113

I. Introduction

The mechanisms of development of severe thunderstorms are not well understood. Rapid developments of storms and changes in atmospheric conditions can occur over small time and space scales, greatly influencing local weather and sometimes producing localized severe weather events. By providing atmospheric sounding data at 3-hour intervals rather than the usual twelve-hour intervals, the AVE experiments allow finer time scale resolution of weather features and the possibility of more adequate understanding and prediction of processes.

The objectives of this report are:

- 1) To present a time series of maps of atmospheric parameters as measured for the AVE IV experiment.
- 2) To present a thunderstorm model which incorporates mesoscale vortices.
- 3) To explain a severe weather predictive index developed by Eagleman on the basis of a vortex model.
- 4) To present results of the application of this index to the AVE IV data.
- 5) To compare these results with the results from applying presently used predictive indices.
- 6) To suggest modifications of the predictive index.

II. Synoptic Conditions

To determine the synoptic patterns of the thermodynamic and kinetic variables, surface maps and 500 mb charts were drawn for each time of the AVE IV rawinsonde flights of equivalent potential temperature, water vapor mixing ratio, potential temperature, and the magnitudes of the wind speed.

Figure 1 contains the surface maps and 500 mb charts for 0000 GMT, April 24, 1975. The surface map shows that much of the Central United States was covered with potentially warm, moist air. Values of water vapor mixing ratio in excess of 14 g/kg were found in much of southeastern Texas and southern Louisiana. Mixing ratios of 10 and above were found throughout most of the Central Plains. Potential temperatures ranged between 295°K and 310°K across most of the experiment area. Maximum surface wind speeds were located in southern Texas and in a band across Oklahoma, central Missouri, southern Illinois, and Indiana, into West Virginia and Pennsylvania.

The 500 mb chart shows the maximum values of mixing ratio extending through the eastern U.S. from Louisiana to Pennsylvania. Maximum values of potential temperature are also in this area. Maximum wind speeds are in West Virginia, Pennsylvania, and Ohio.

Figure 2 shows variable fields at 600 GMT, April 24, 1975. At the surface, large gradients of mixing ratio and equivalent potential temperature exist over Central Texas and Oklahoma and Kansas, with values of w varying from 4 to 16 across Texas. Potential temperatures over the area are 5° to 10°K lower than at the previous sounding time. Wind speeds are also lower, with a local maximum at Topeka.

At the upper level, the area of maximum w has moved to the east and south. Potential temperature lines have moved southward, and the maximum wind speeds are over the Mississippi River basin.

Figure 3 contains the surface map and 500 mb chart for 1200 GMT April 24, 1975. The large surface gradients of w and θ_e remain over western Texas, with an intrusion of dry, potentially cool air into northern Texas. Lines of potential temperature have moved further south and west. At 500 mb this cooling is also present. The location of maximum winds has changed little. The analysis of the area around Monette, Missouri, may not be a measure of synoptic conditions because the sonde was released during a rainstorm.

Figure 4 shows the atmospheric conditions at 1500 GMT April 24. At the surface the intrusion of warm, dry air is still over northern Texas. Lines of potential temperature have moved northward in the eastern section of the country. Increased wind speeds are also evident. There is no feature at the 500 mb level corresponding to the high surface gradients of θ_e and w over Texas. Lines of θ have moved north in the East and South.

At the surface the potentially warm air has moved further into Texas. At 1800, as shown in Figure 5, areas of high moisture have moved slightly eastward.

At the 500 mb level, patterns are consistent with those of the last flight. The area of maximum θ_e has moved eastward from Indiana to West Virginia. Figure 6 contains the surface maps and 500 mb charts for 2100 GMT April 24, 1975. A localized maximum of θ_e and w is present at the surface at Shreveport, Louisiana. Potentially warm air continues to

move eastward across Texas. At the 500 mb level the moisture maximum has spread and is now centered over West Virginia and Kentucky. Figure 7 contains the surface map and 500 mb chart for 0000 GMT April 25, 1975. The localized maxima are no longer present in Louisiana at the surface. At the 500 mb level the maximum of θ_e has moved over Tennessee, Kentucky, and surrounding areas. Figure 8 shows the surface map and 500 mb chart for 600 GMT, April 25, 1975. Strong gradients of equivalent potential temperature and mixing ratio occur in Texas at the surface. Potential temperatures are 5° to 10° K cooler over most of the experiment area than at the previous sounding. At the 500 mb level an area of relatively moist air is centered just west of the Mississippi River, and potentially cooler air has moved into the northern states. Figure 9 shows the surface map and 500 mb chart for 1200 GMT April 25, 1975. The patterns have changed little at the surface from the previous sounding. Potentially cooler air has moved into Texas. At the 500 mb level the area of maximum mixing ratio has moved eastward and the high velocity winds are centered over Middle Tennessee and Northern Alabama.

A number of severe weather events of various types occurred during the AVE experiment. These include tornadoes, damaging winds, hailstorms, flash floodings, and funnel clouds. A complete description of the severe events is given by Turner [1976]. For the purpose of this report a severe event is defined to be a tornado that touches down, a wind with speeds over 50 miles per hour, or a hailstorm with stones greater than 0.5 inches in diameter. A map of the locations and types of severe events is given in Figure 10. The reported severe hail events are shown on the north and west edges of the severe weather region and tornado and high winds are shown in the center, south and eastern portion.

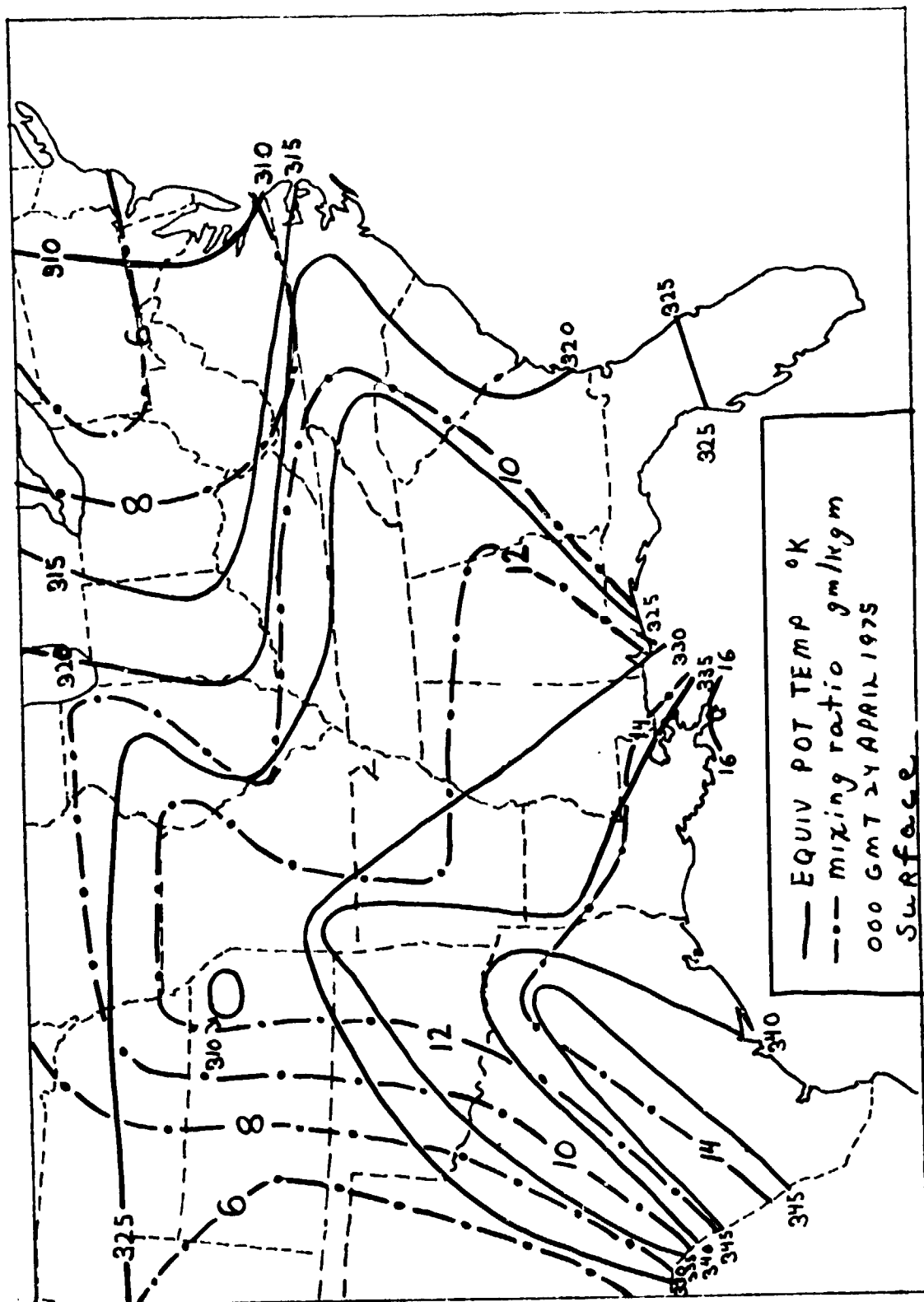


Figure 1a. Surface map of equivalent potential temperature and water vapor mixing ratio at 0000 GMT April 24, 1975.

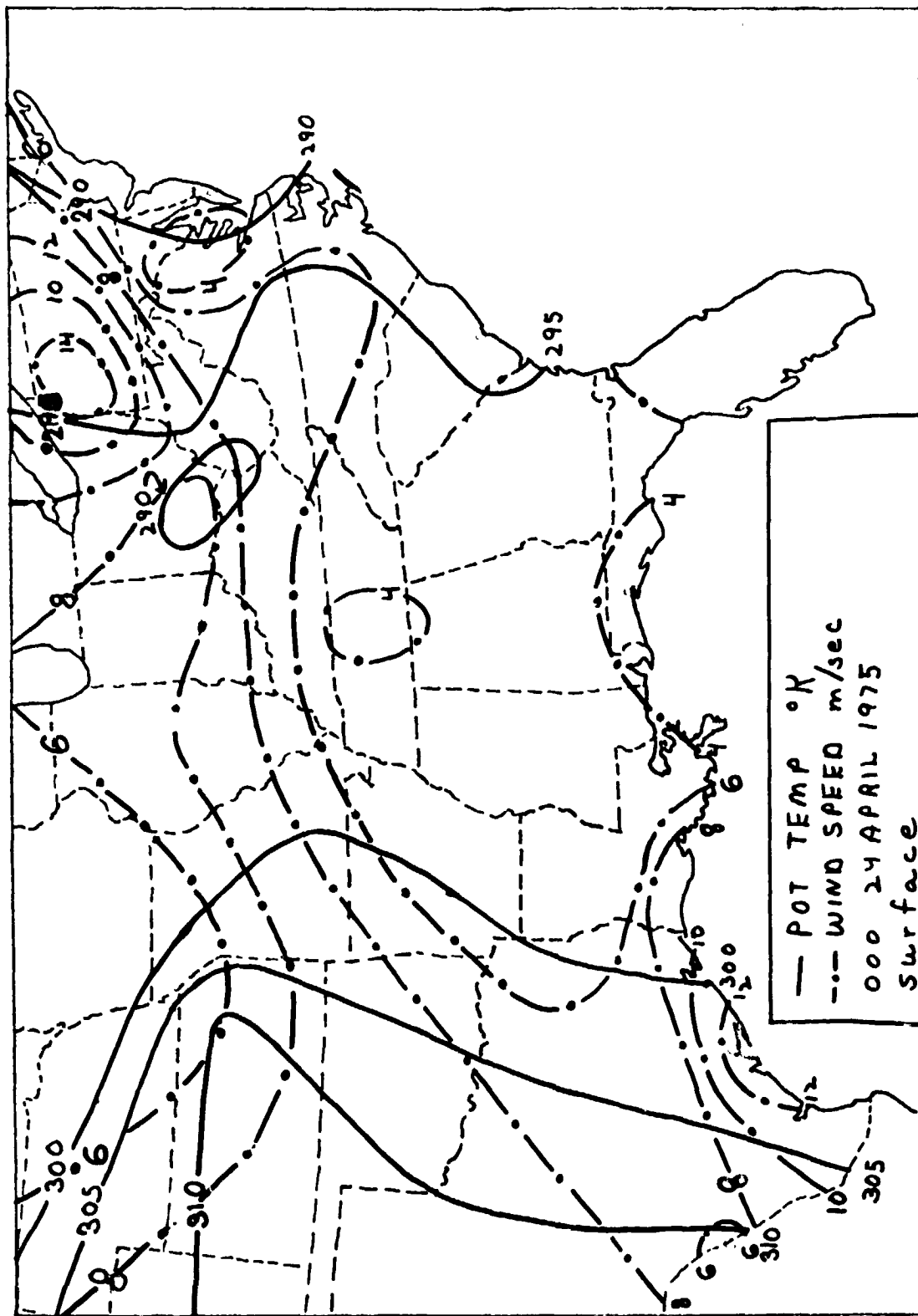


Figure 1b. Surface map of potential temperature and wind speed at 0000 GMT April 24, 1975.

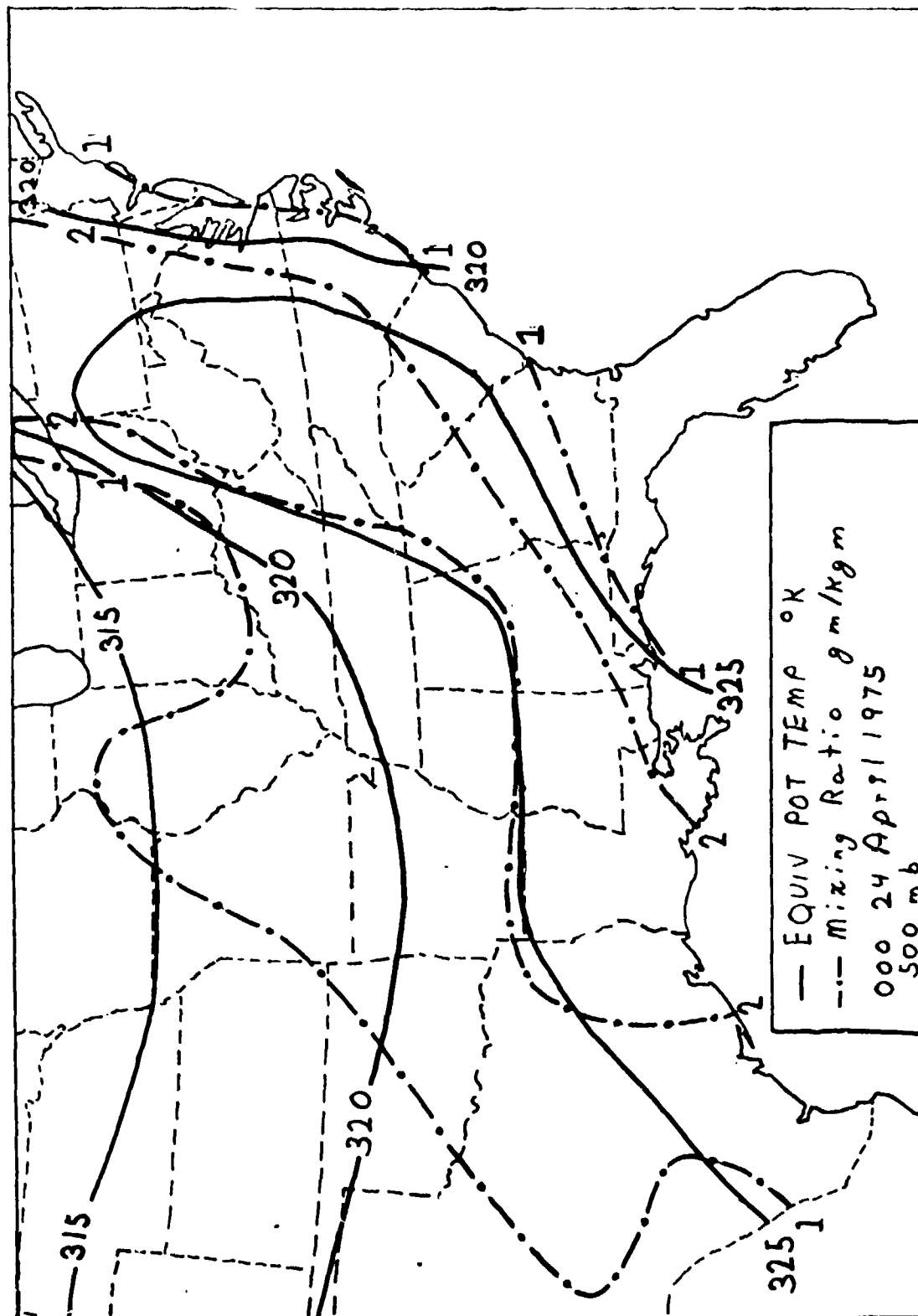


Figure 1c. 500 mb chart of equivalent potential temperature and water vapor mixing ratio at 0000 GMT April 24, 1975.

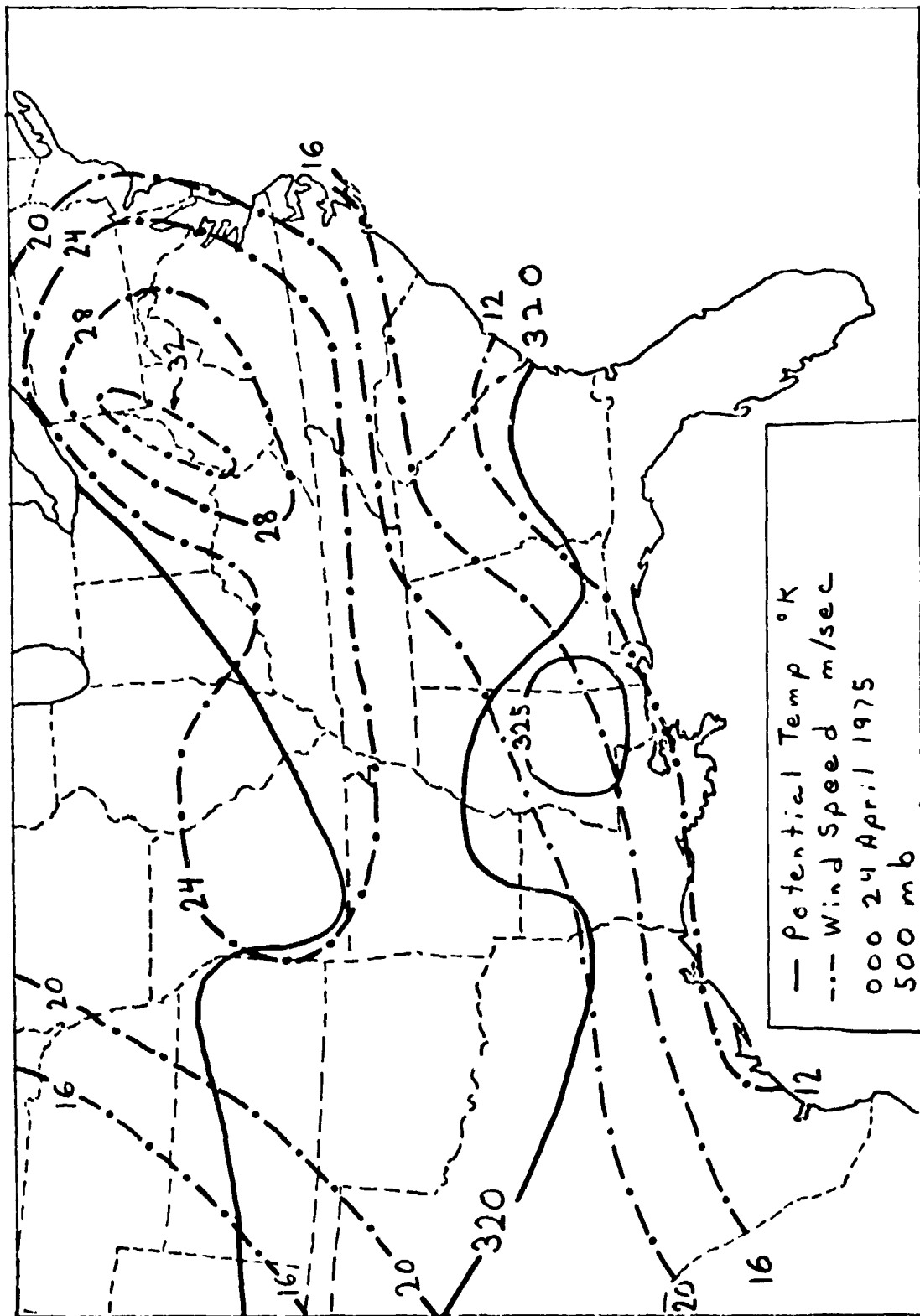


Figure 1d. 500 mb chart of potential temperature and wind speed at 0000 GMT April 24, 1975.

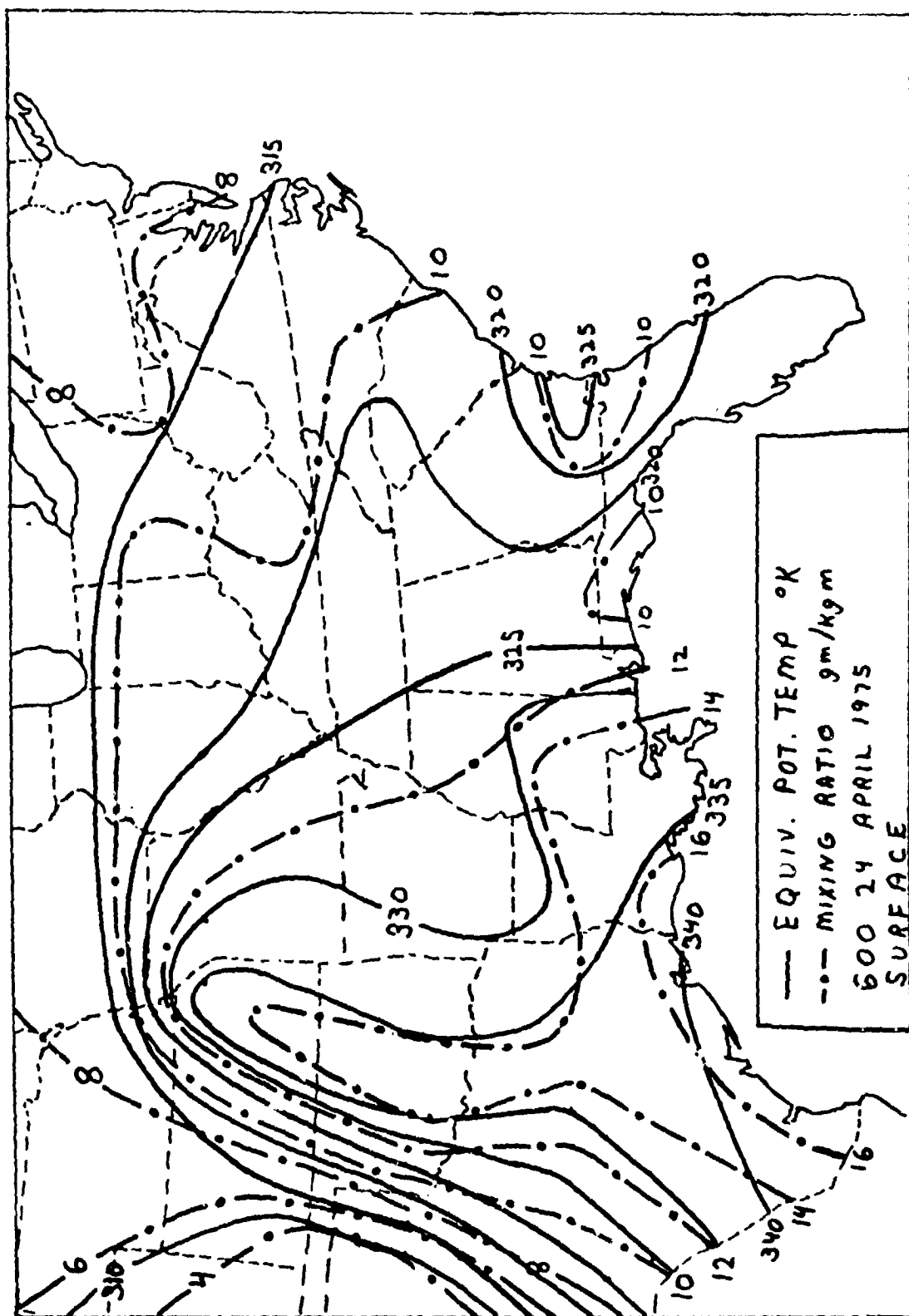


Figure 2a. Surface map of equivalent potential temperature and water vapor mixing ratio at 600 GMT April 24, 1975.

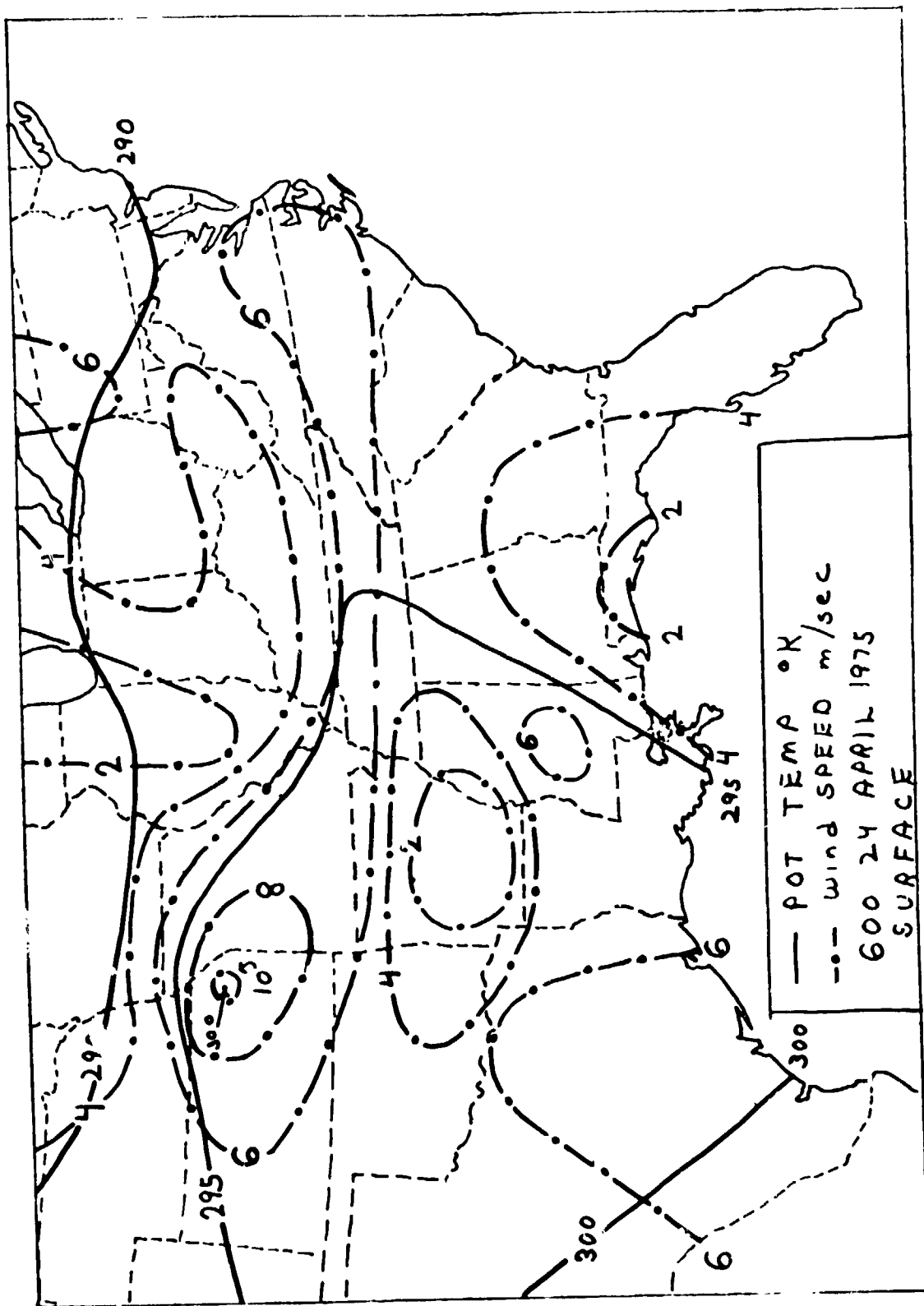


Figure 2b. Surface map of potential temperature and wind speed at 600 GMT April 24, 1975.

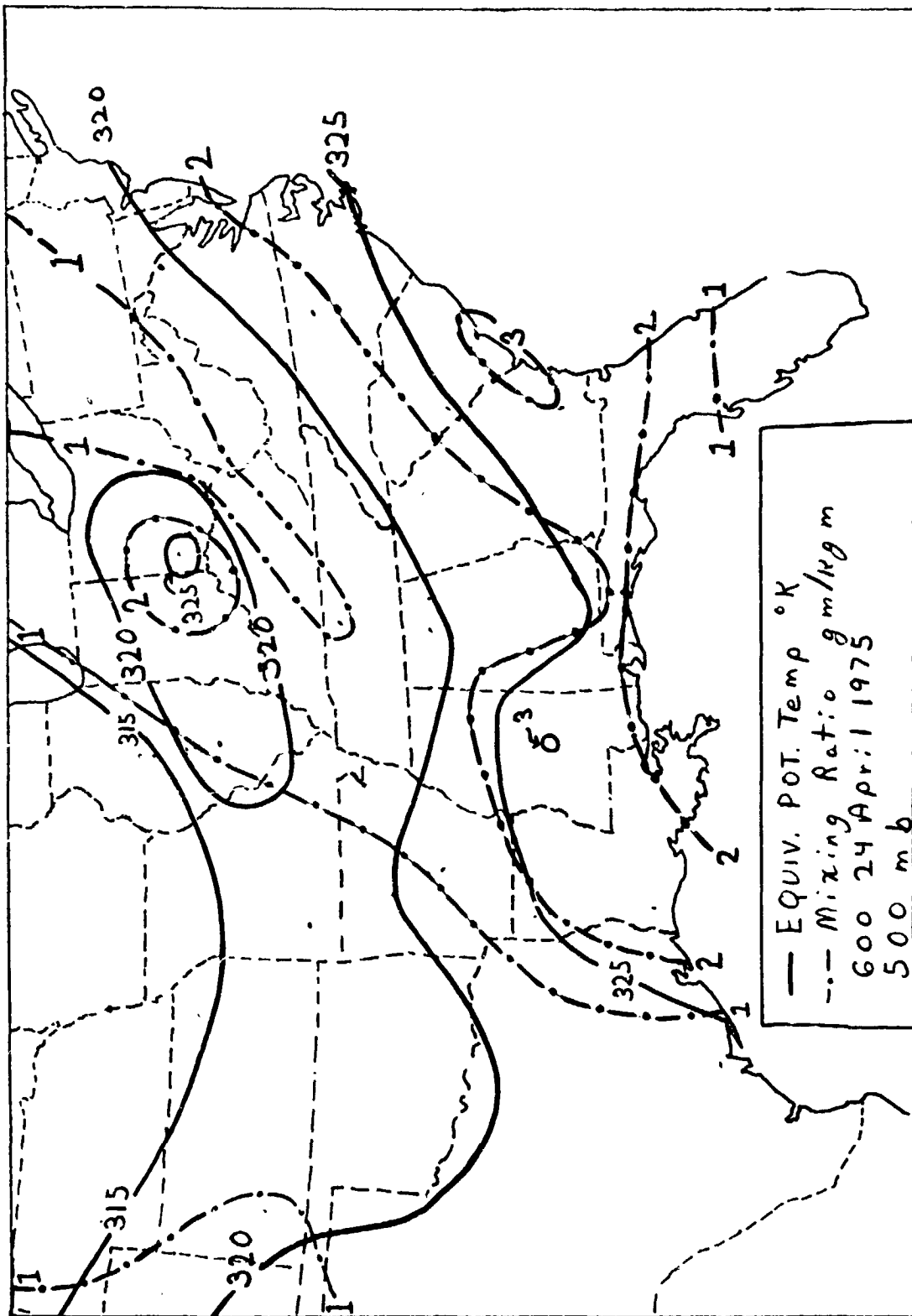


Figure 2c. 500 mb chart of equivalent potential temperature and water vapor mixing ratio at 600 GMT April 24, 1975.

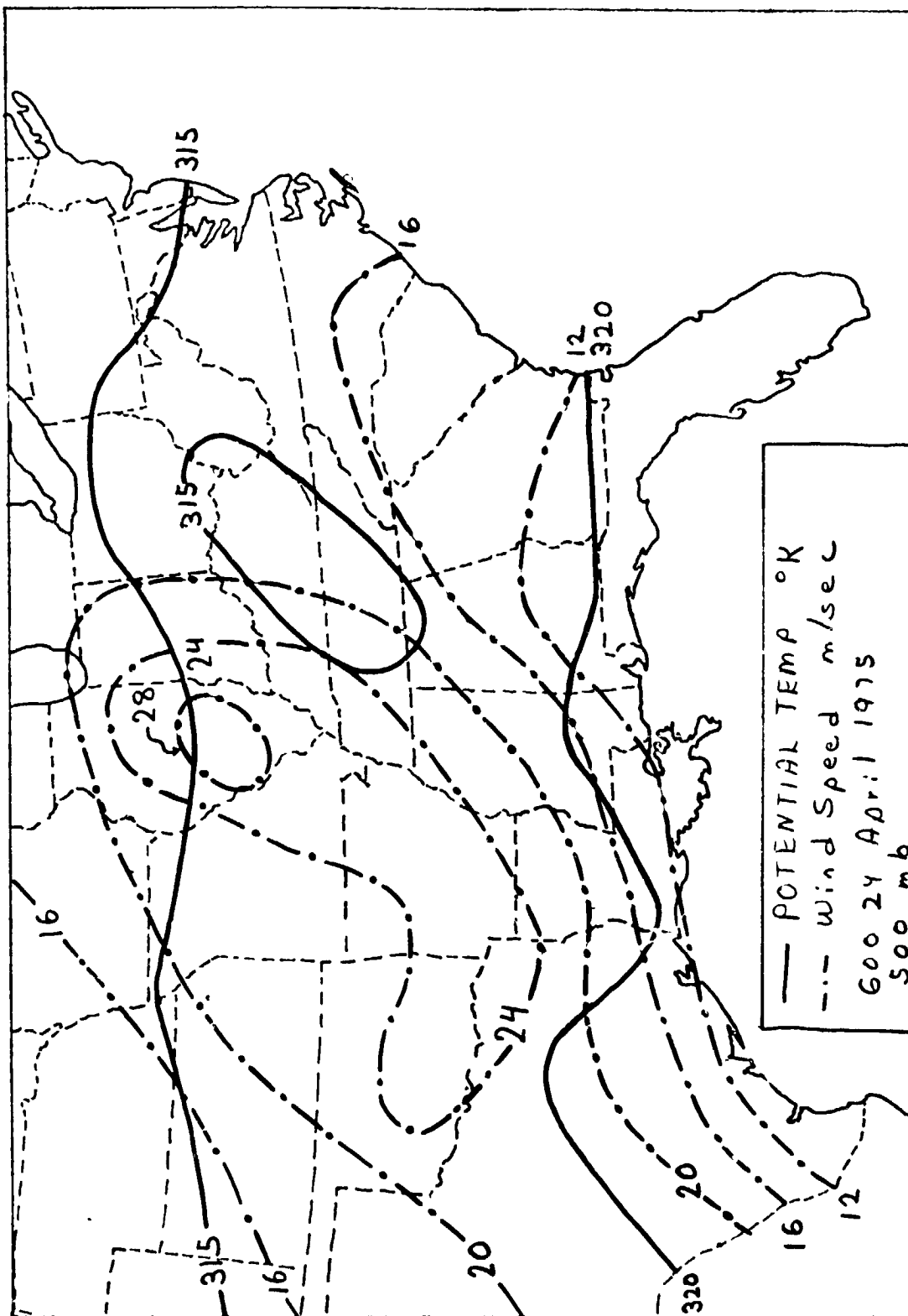


Figure 2d. 500 mb chart of potential temperature and wind speed at 600 GMT April 24, 1975.

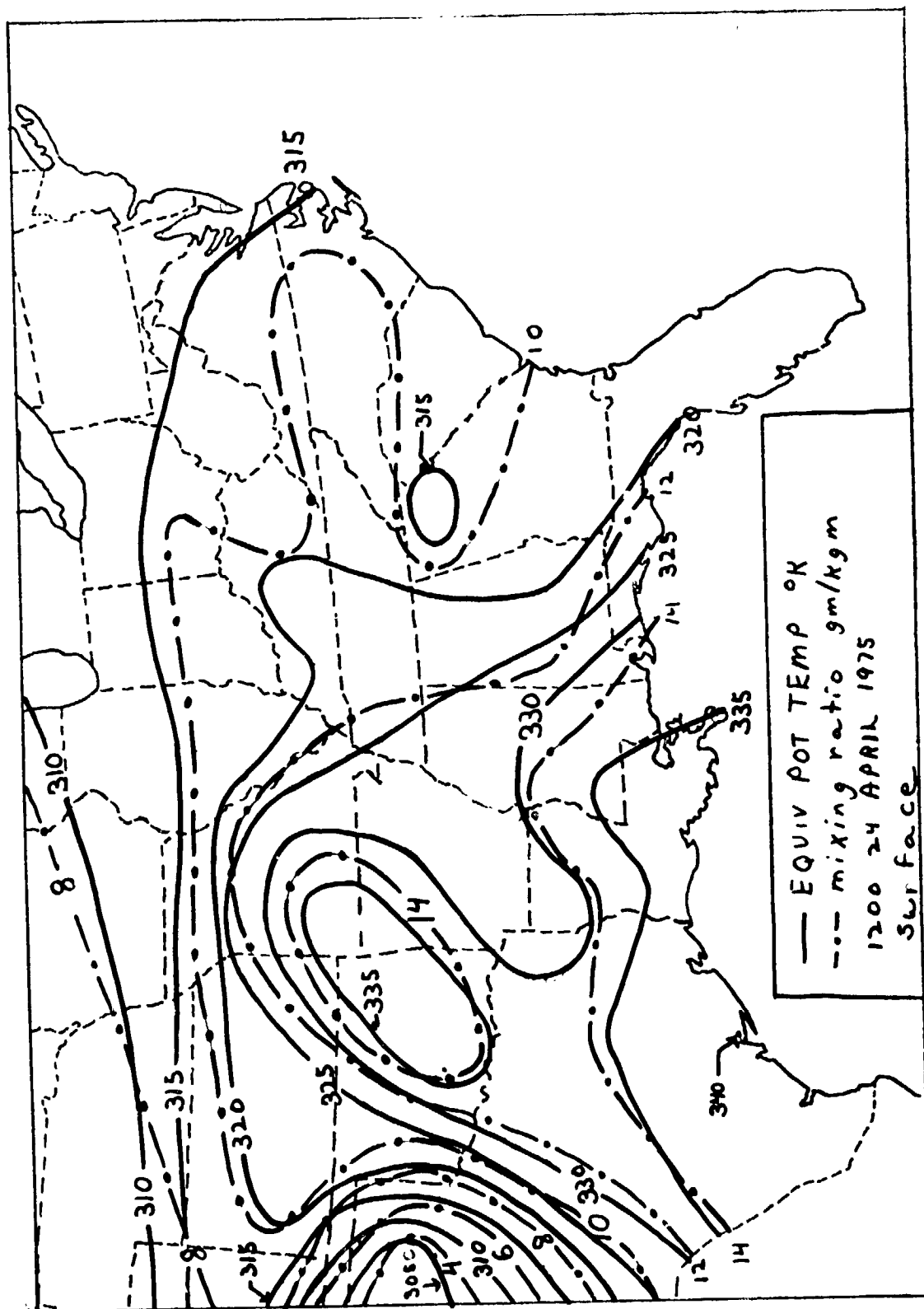


Figure 3a. Surface map of equivalent potential temperature and water vapor mixing ratio at 1200 GMT April 24, 1975.

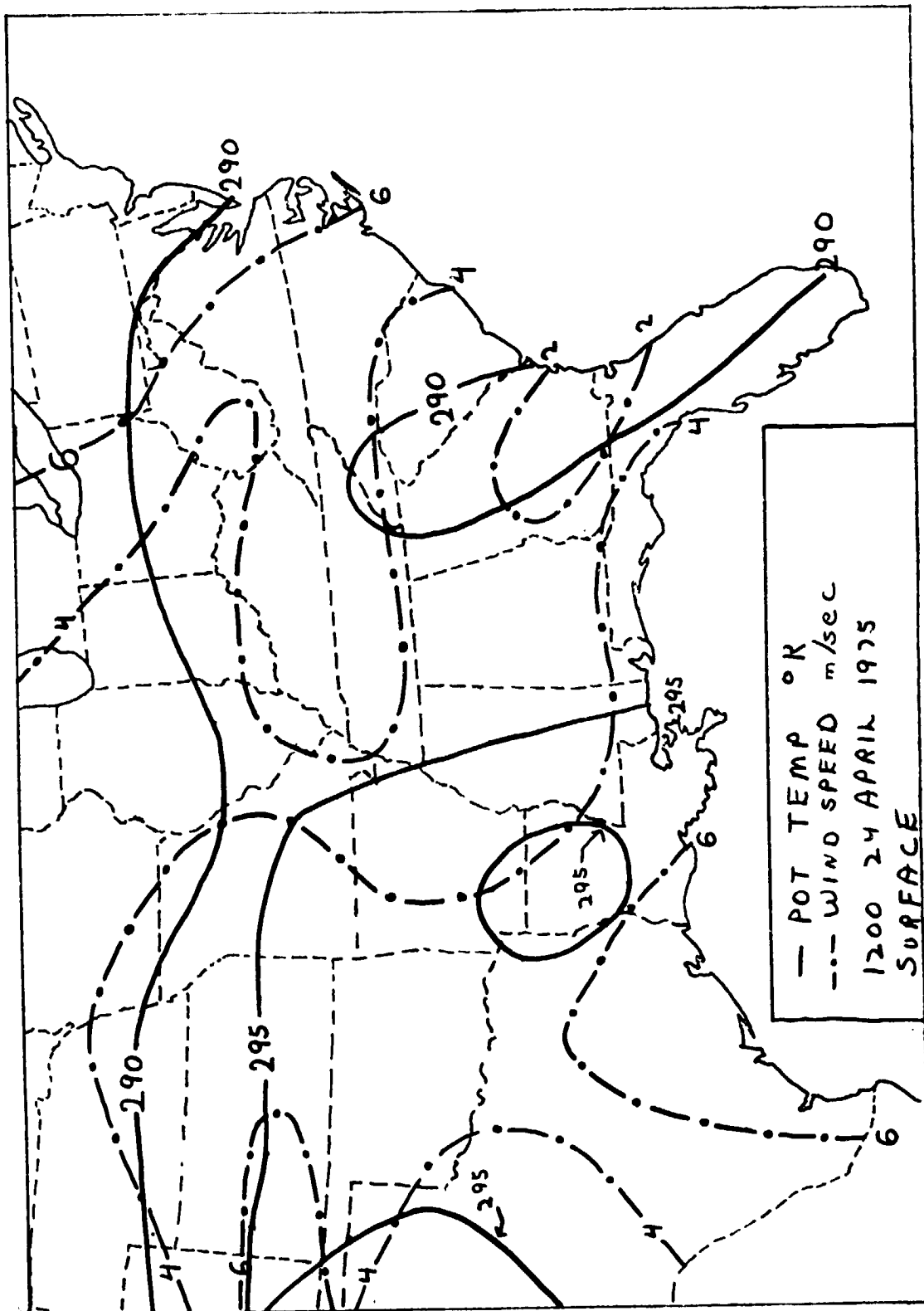


Figure 3b. Surface map of potential temperature and wind speed at 1200 GMT April 24, 1975.

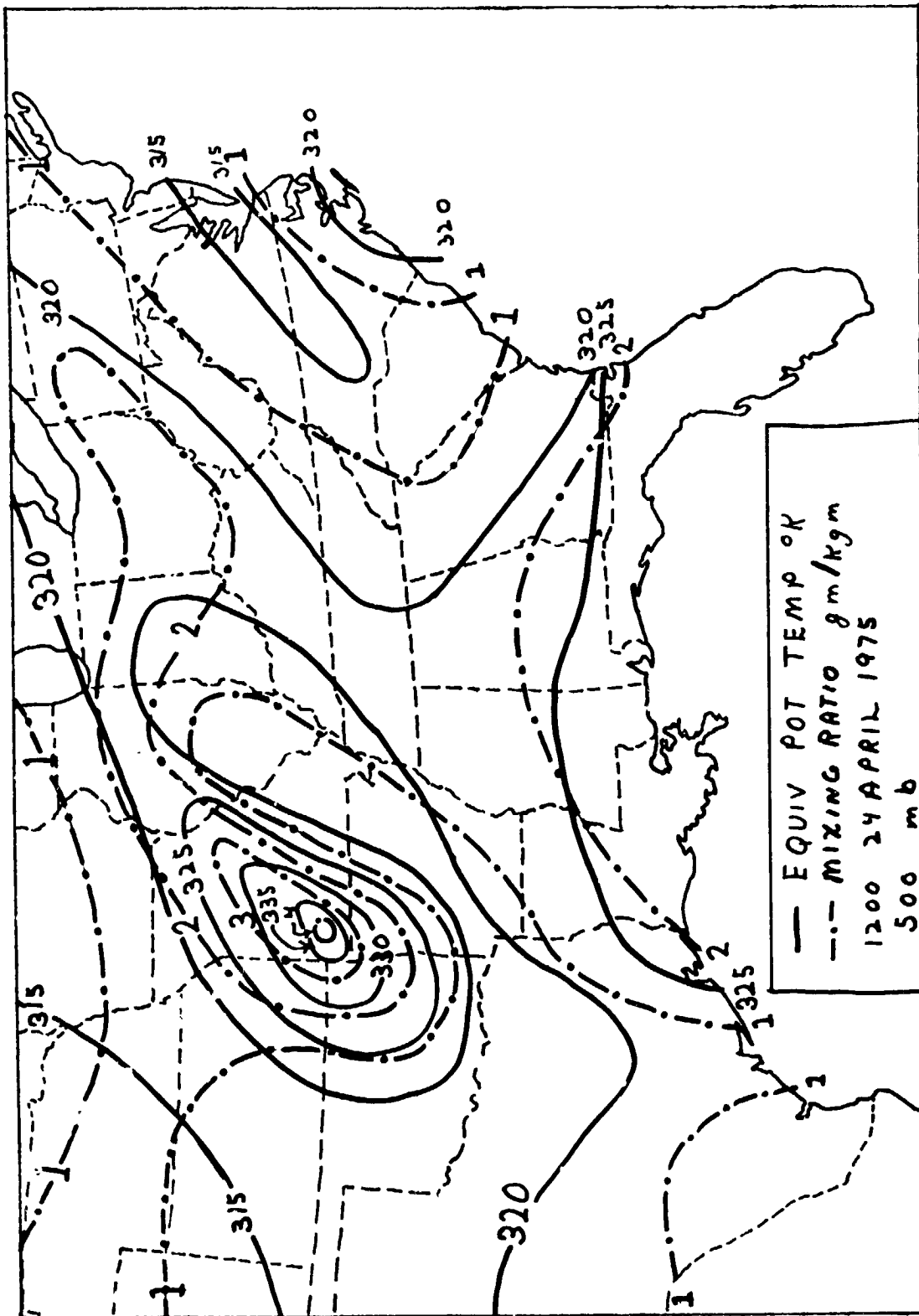


Figure 3c. 500 mb chart of equivalent potential temperature and water vapor mixing ratio at 1200 GMT April 24, 1975.

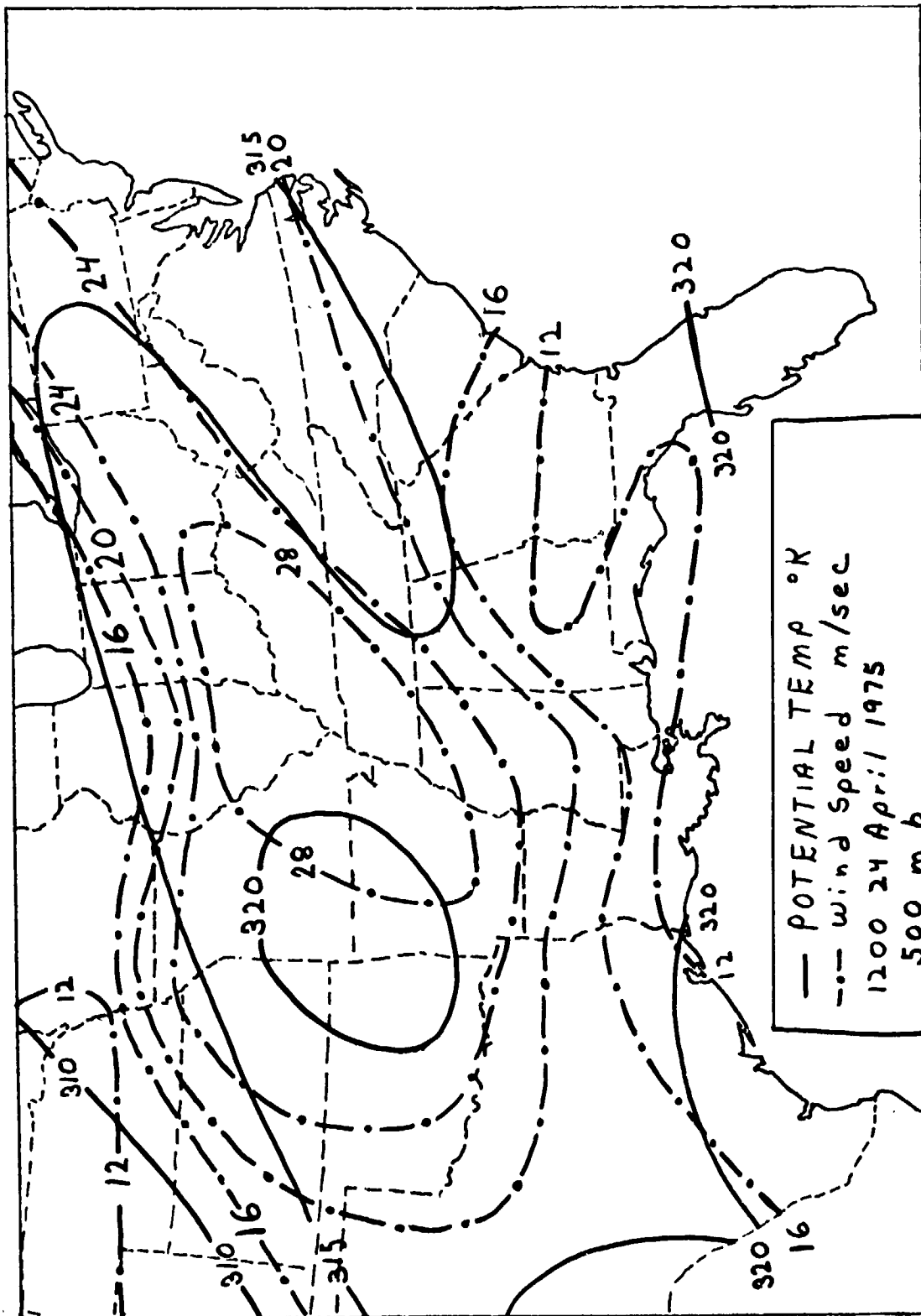


Figure 3d. 500 mb chart of potential temperature and wind speed at 1200 GMT April 24, 1975.

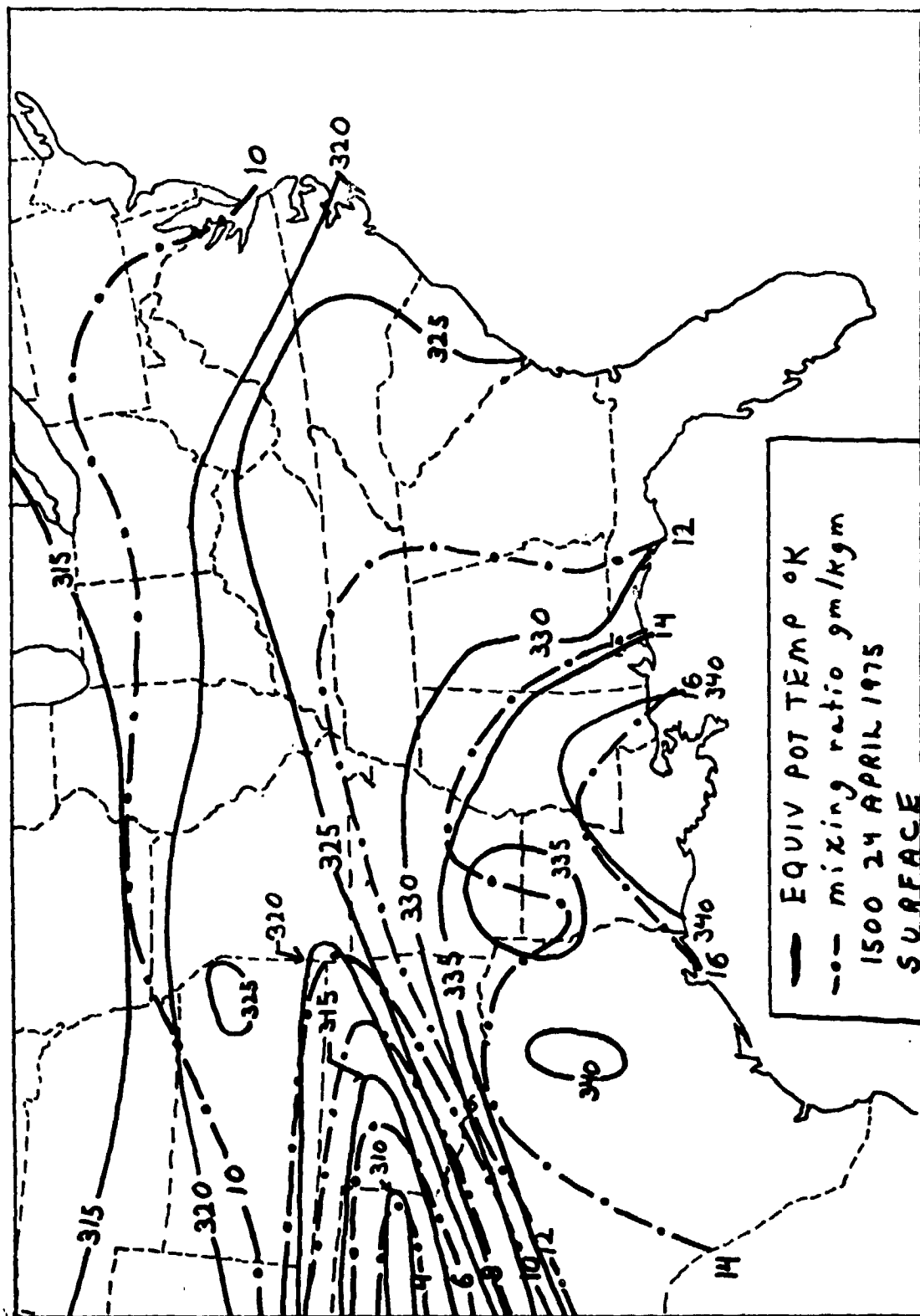


Figure 4a. Surface map of equivalent potential temperature and water vapor mixing ratio at 1500 GMT April 24, 1975.

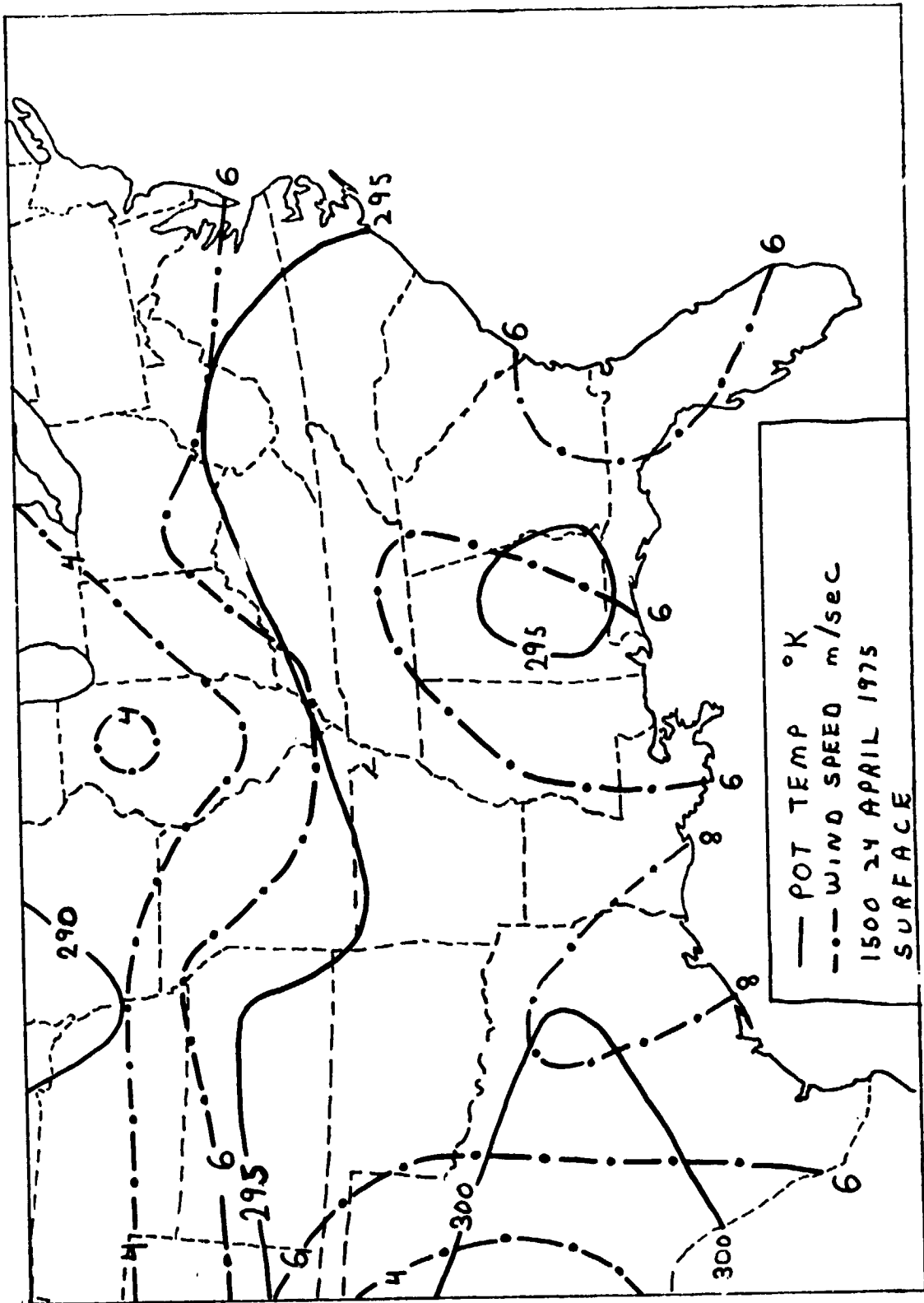


Figure 4b. Surface map of potential temperature and wind speed at 1500 GMT April 24, 1975.

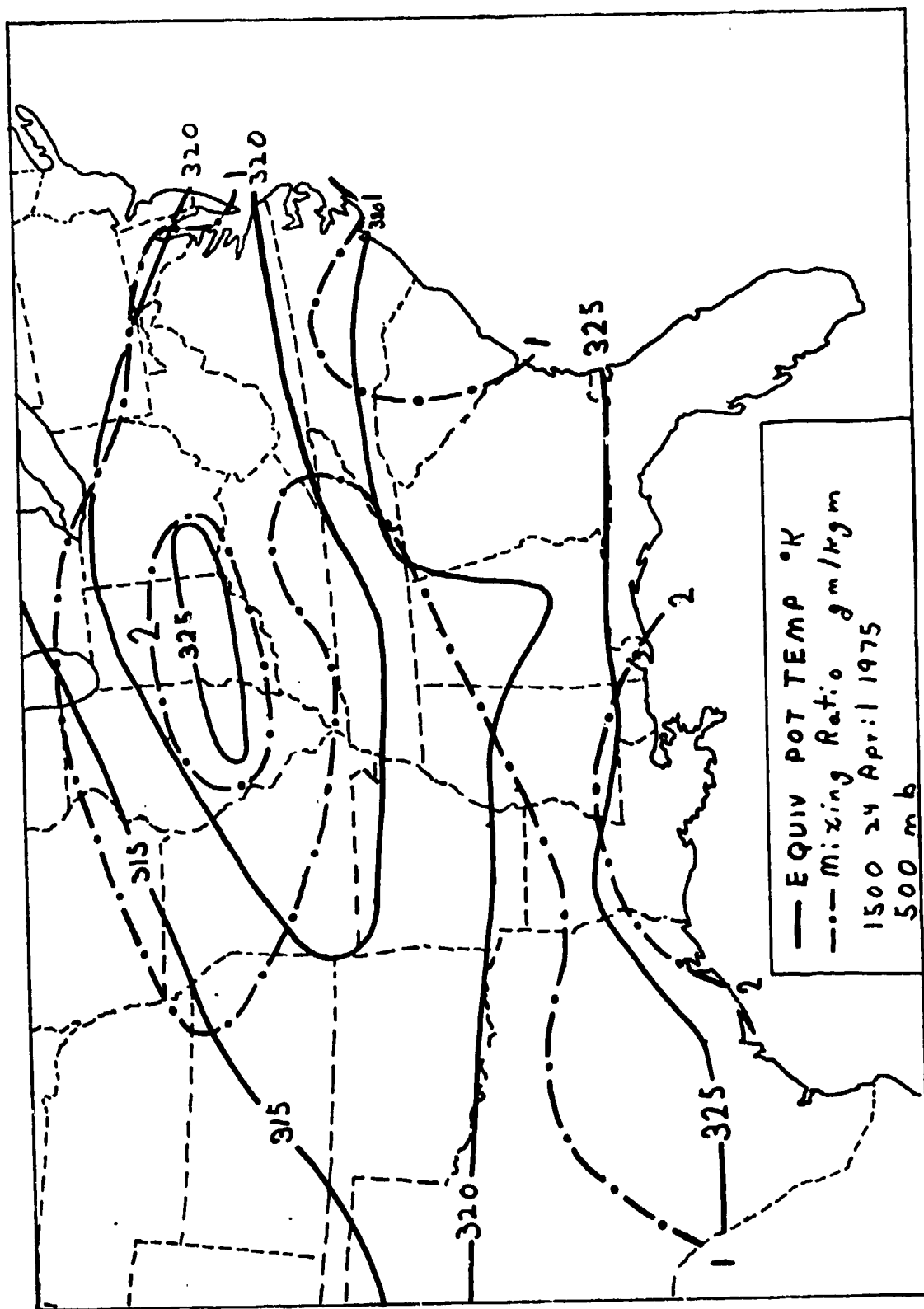


Figure 4c. 500 mb chart of equivalent potential temperature and water vapor mixing ratio at 1500 GMT April 24, 1975.

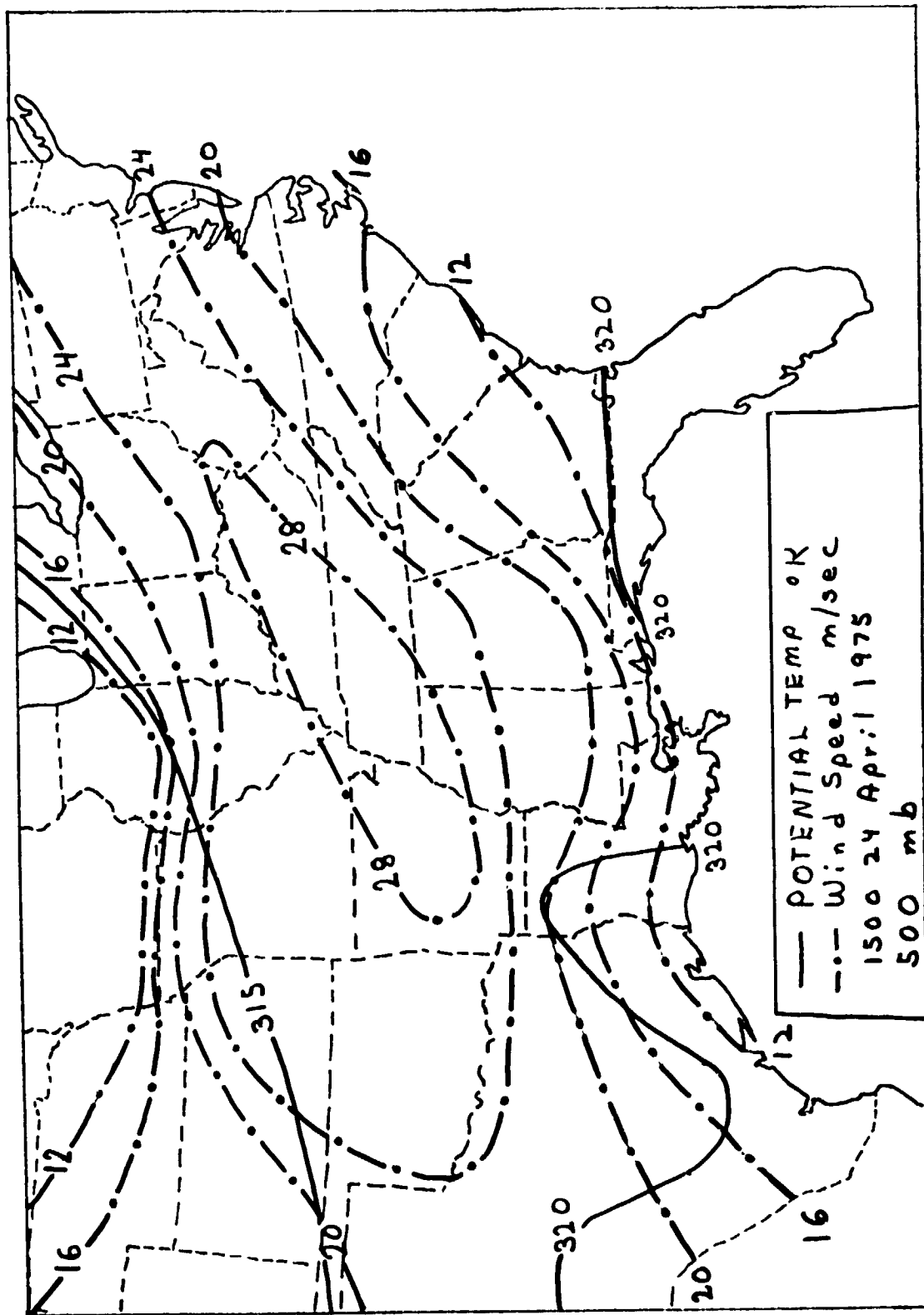


Figure 4d. 500 mb chart of potential temperature and wind speed at 1500 GMT April 24, 1975.

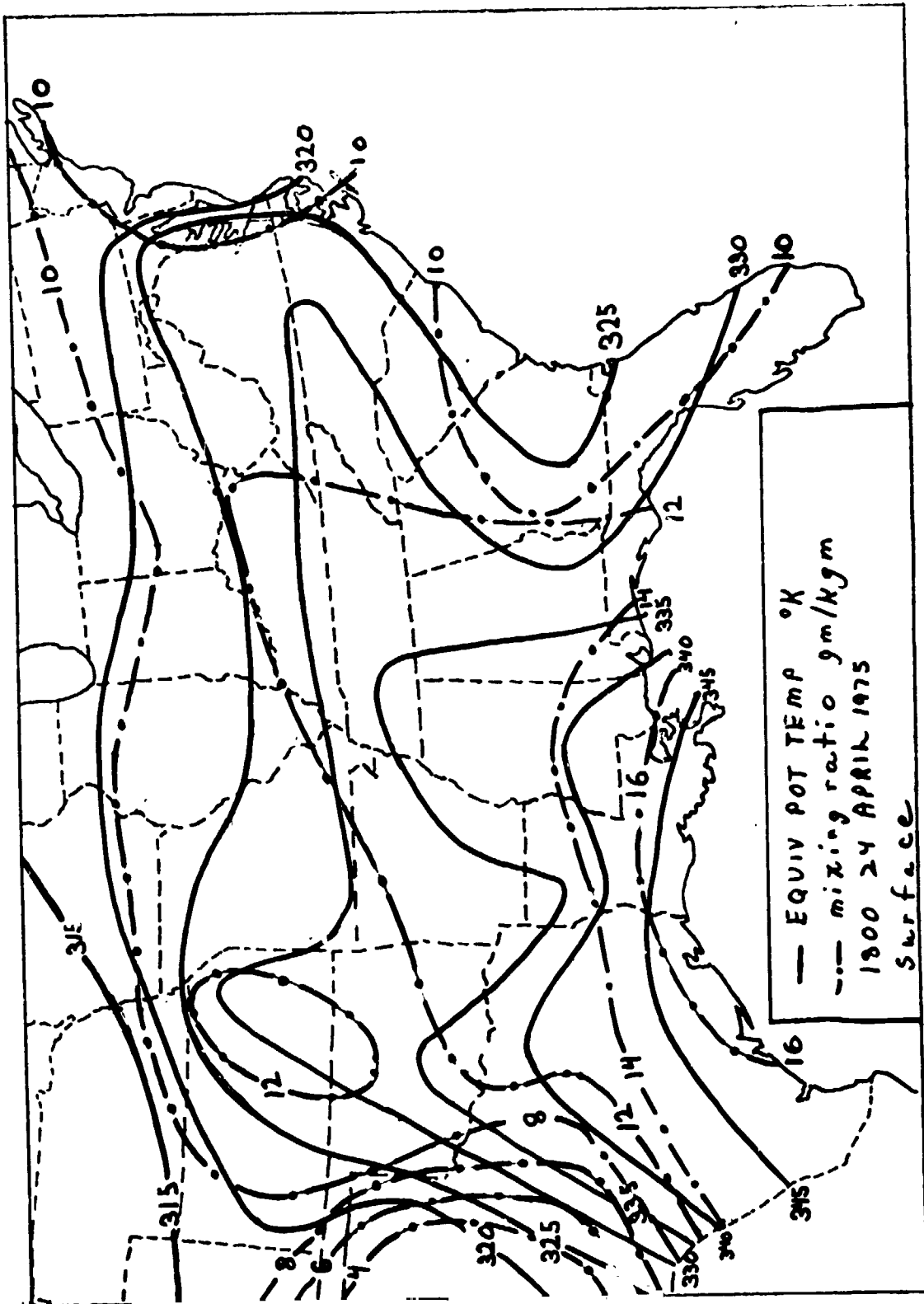


Figure 5a. Surface map of equivalent potential temperature and water vapor mixing ratio at 1800 GMT April 24, 1975.

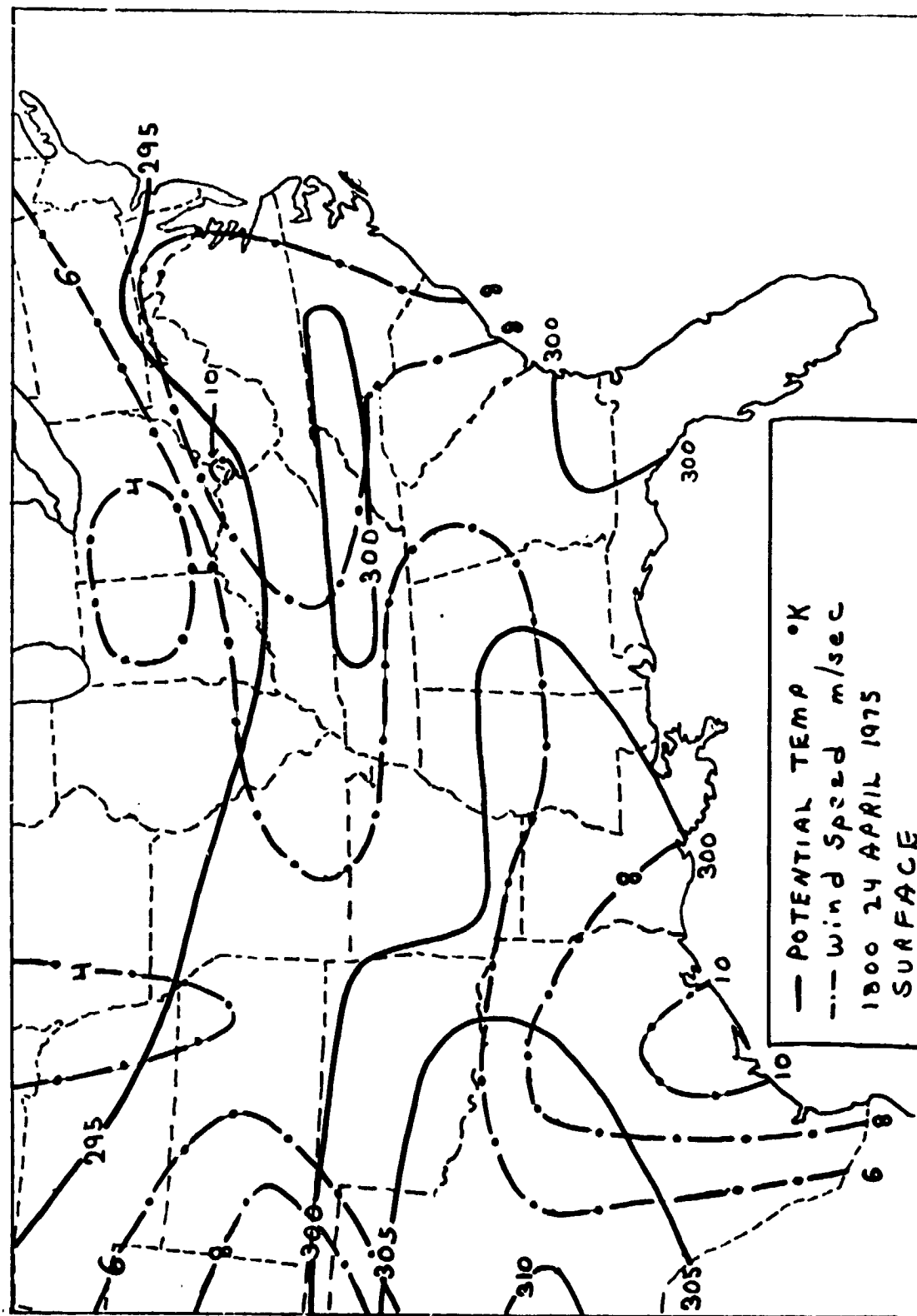


Figure 5b. Surface map of potential temperature and wind speed at 1800 GMT April 24, 1975.

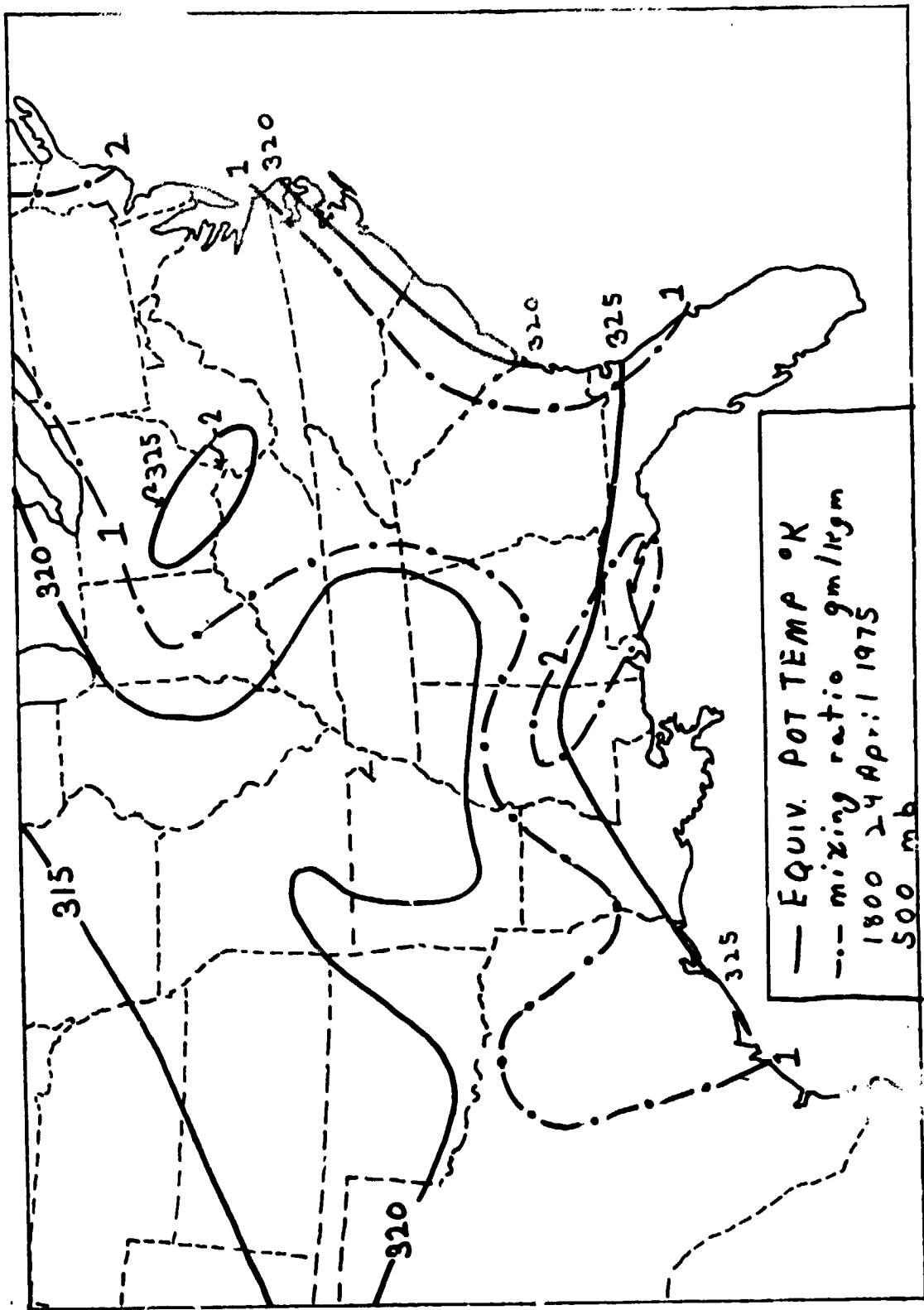


Figure 5c. 500 mb chart of equivalent potential temperature and water vapor mixing ratio at 1800 GMT April 24, 1975.

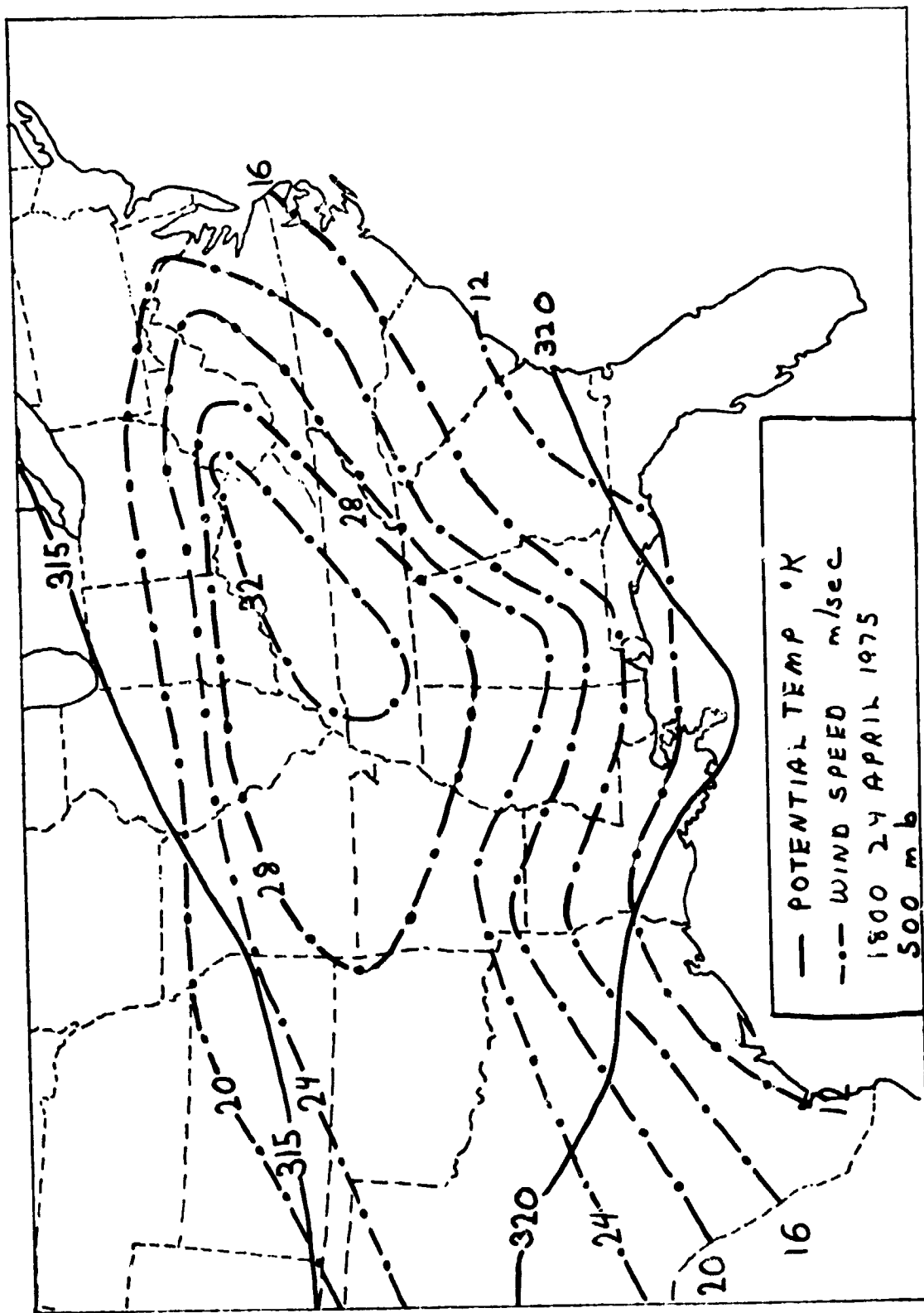


Figure 5d. 500 mb chart of potential temperature and wind speed at 1800 GMT April 24, 1975.

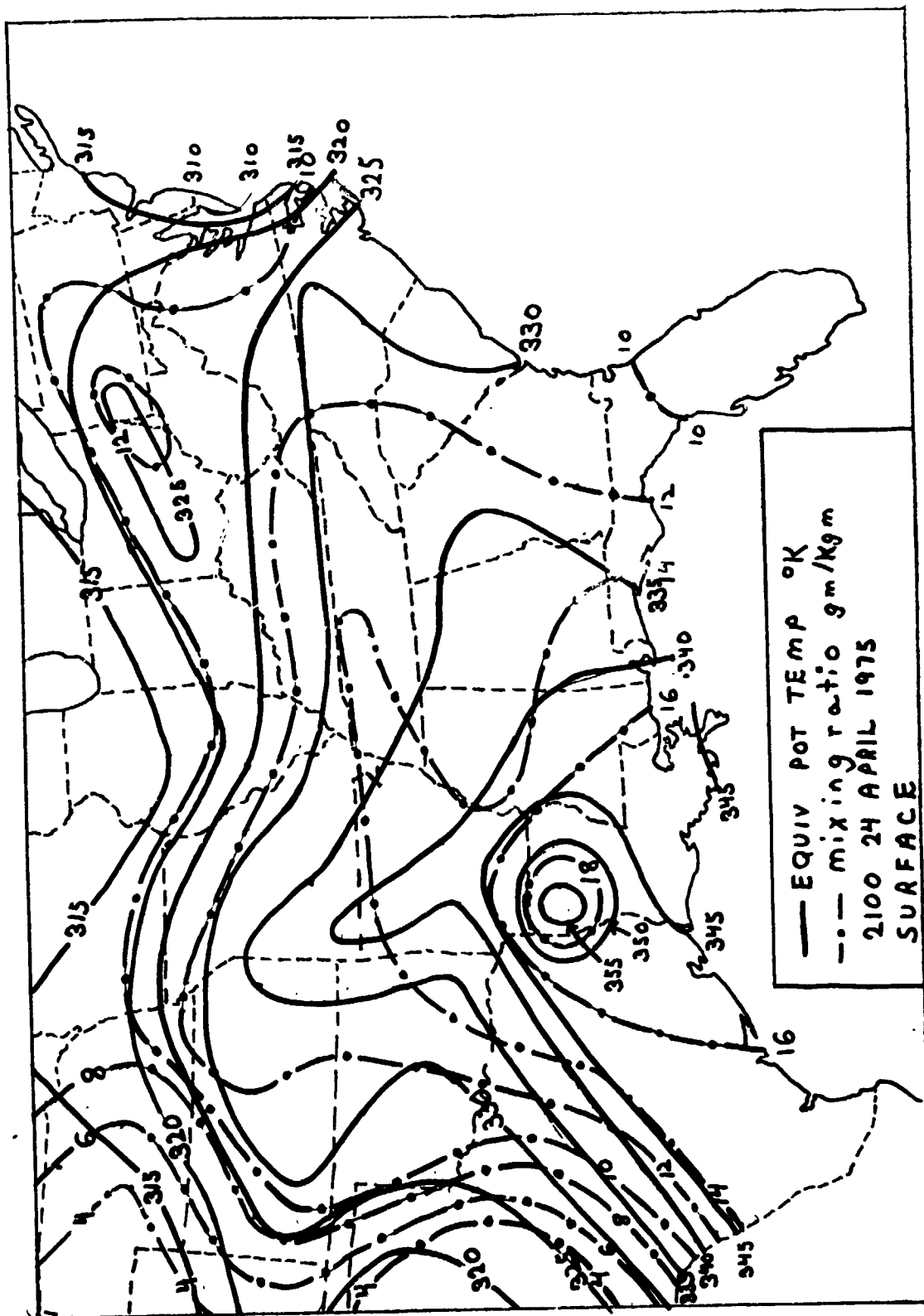


Figure 6a. Surface map of equivalent potential temperature and water vapor mixing ratio at 2100 GMT April 24, 1975.

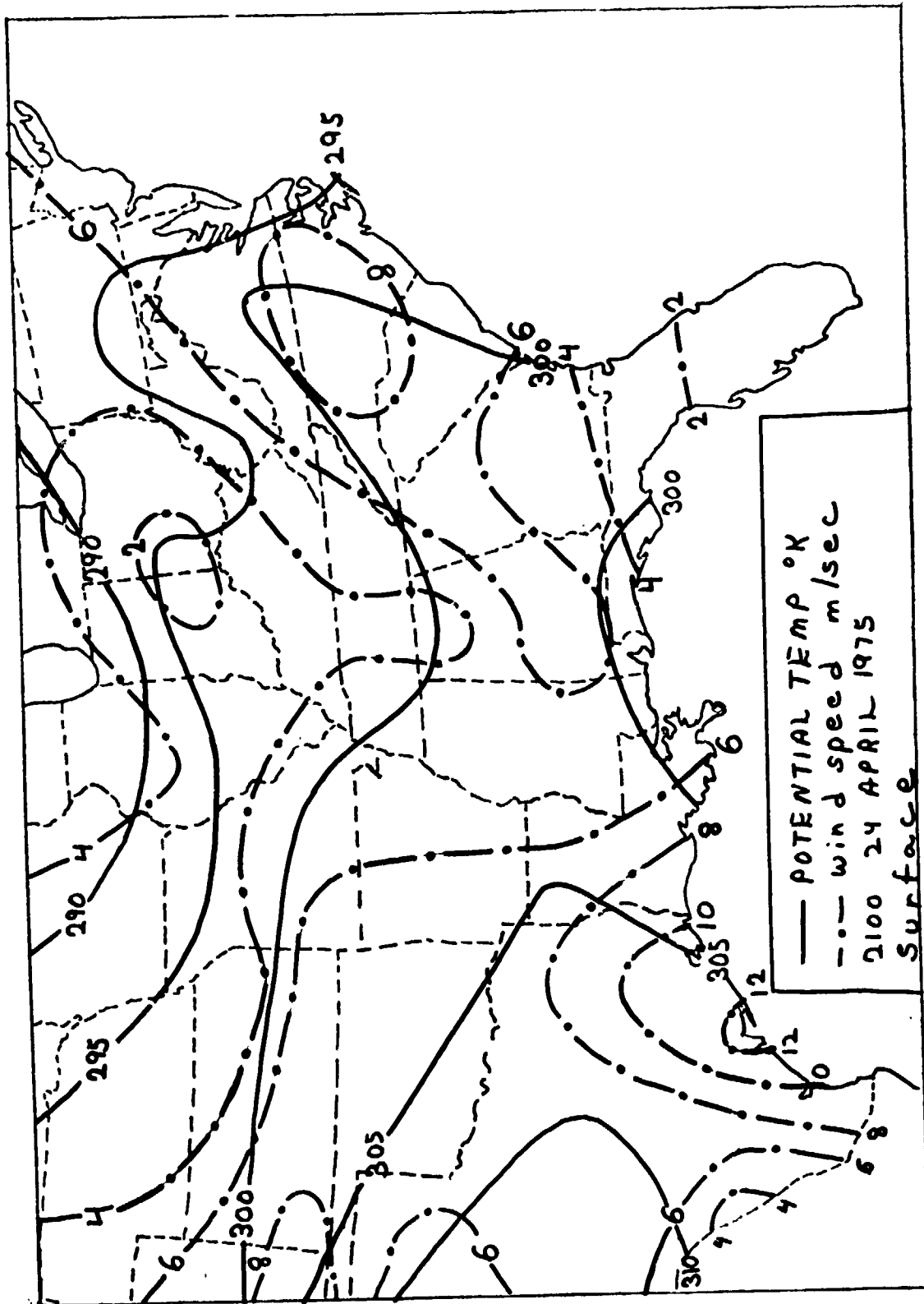


Figure 6b. Surface map of potential temperature and wind speed at 2100 GMT April 24, 1975.

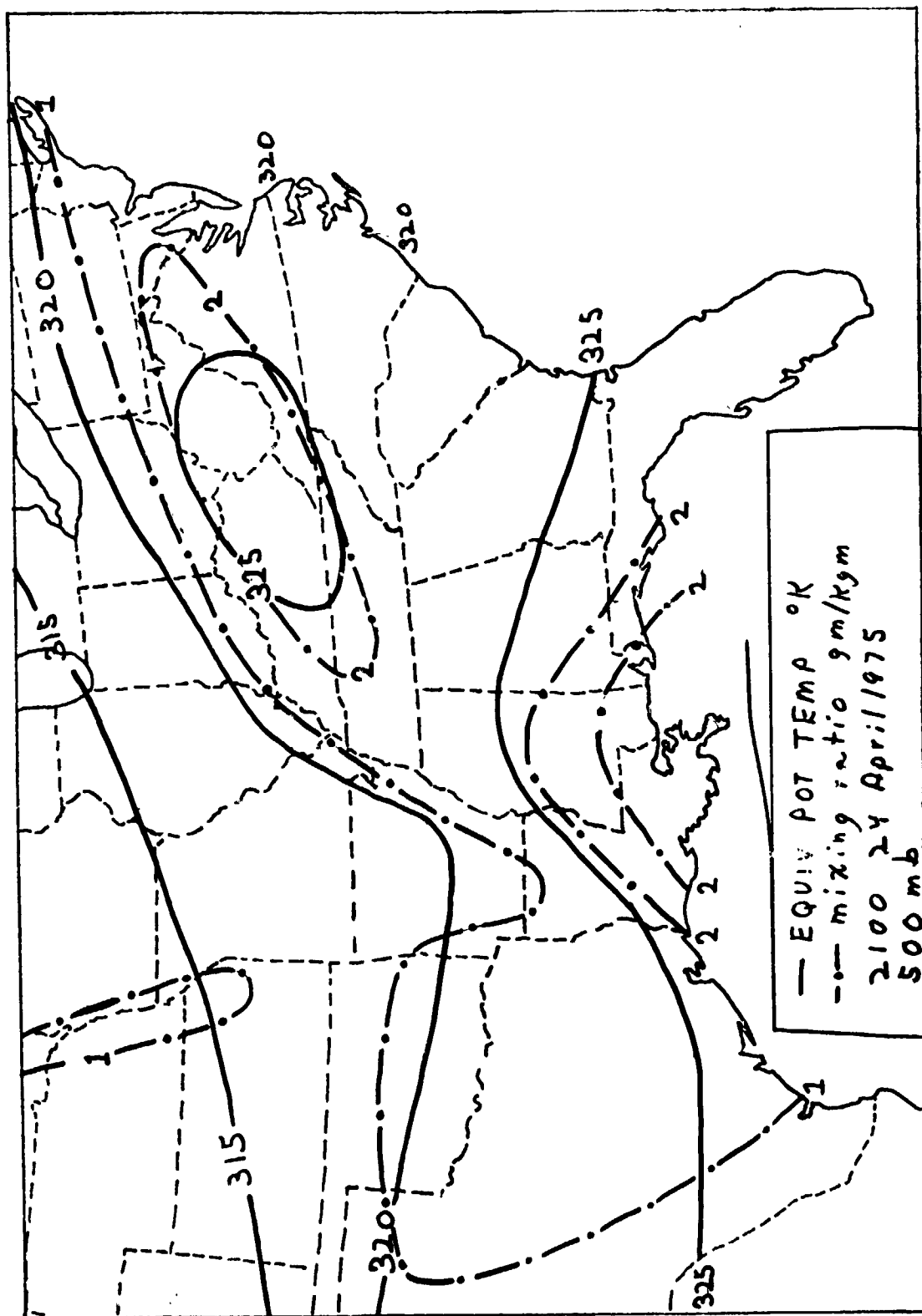


Figure 6c. 500 mb chart of equivalent potential temperature and water vapor mixing ratio at 2100 GMT April 24, 1975.

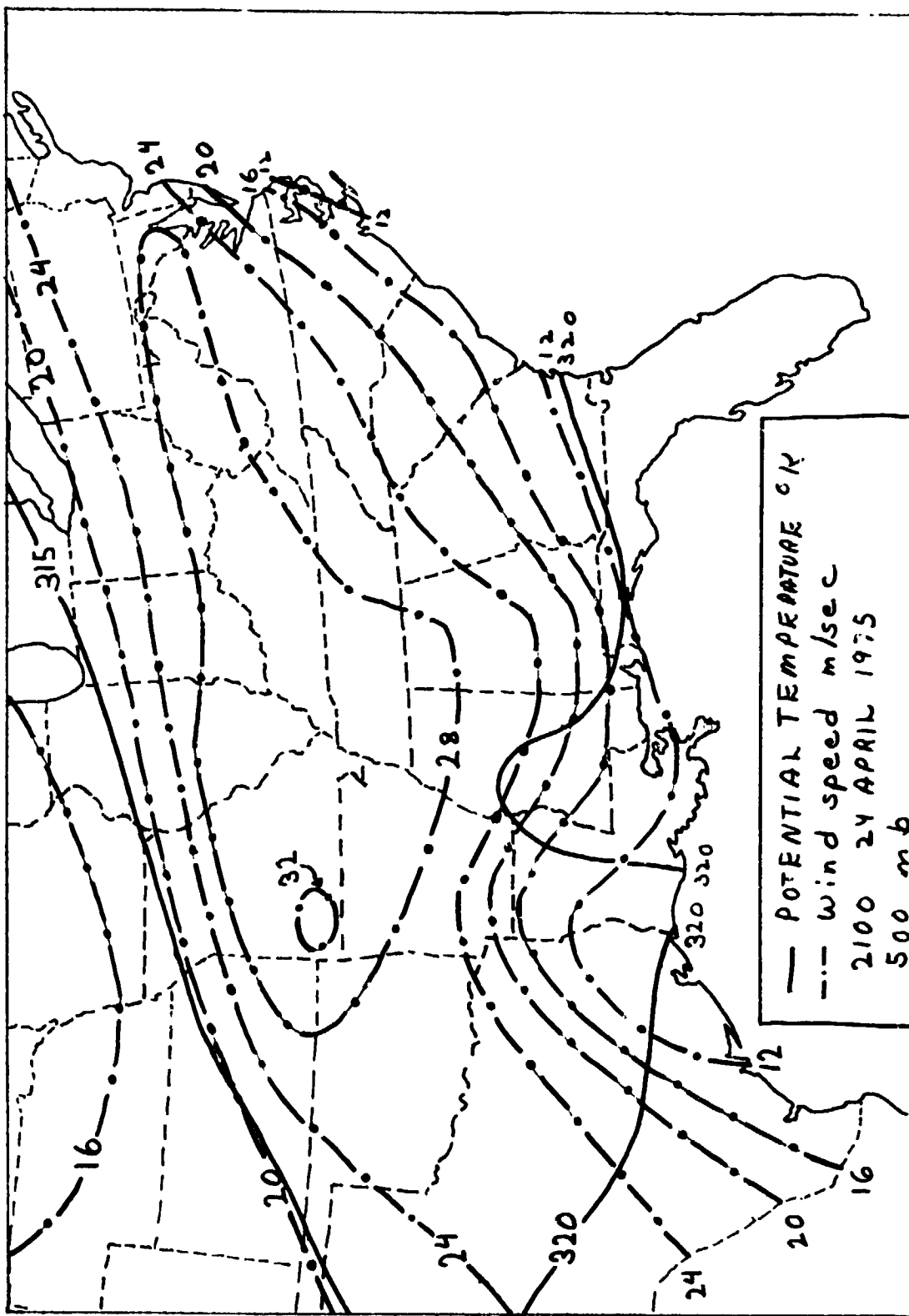


Figure 6d. 500 mb chart of potential temperature and wind speed at 2100 GMT April 24, 1975.

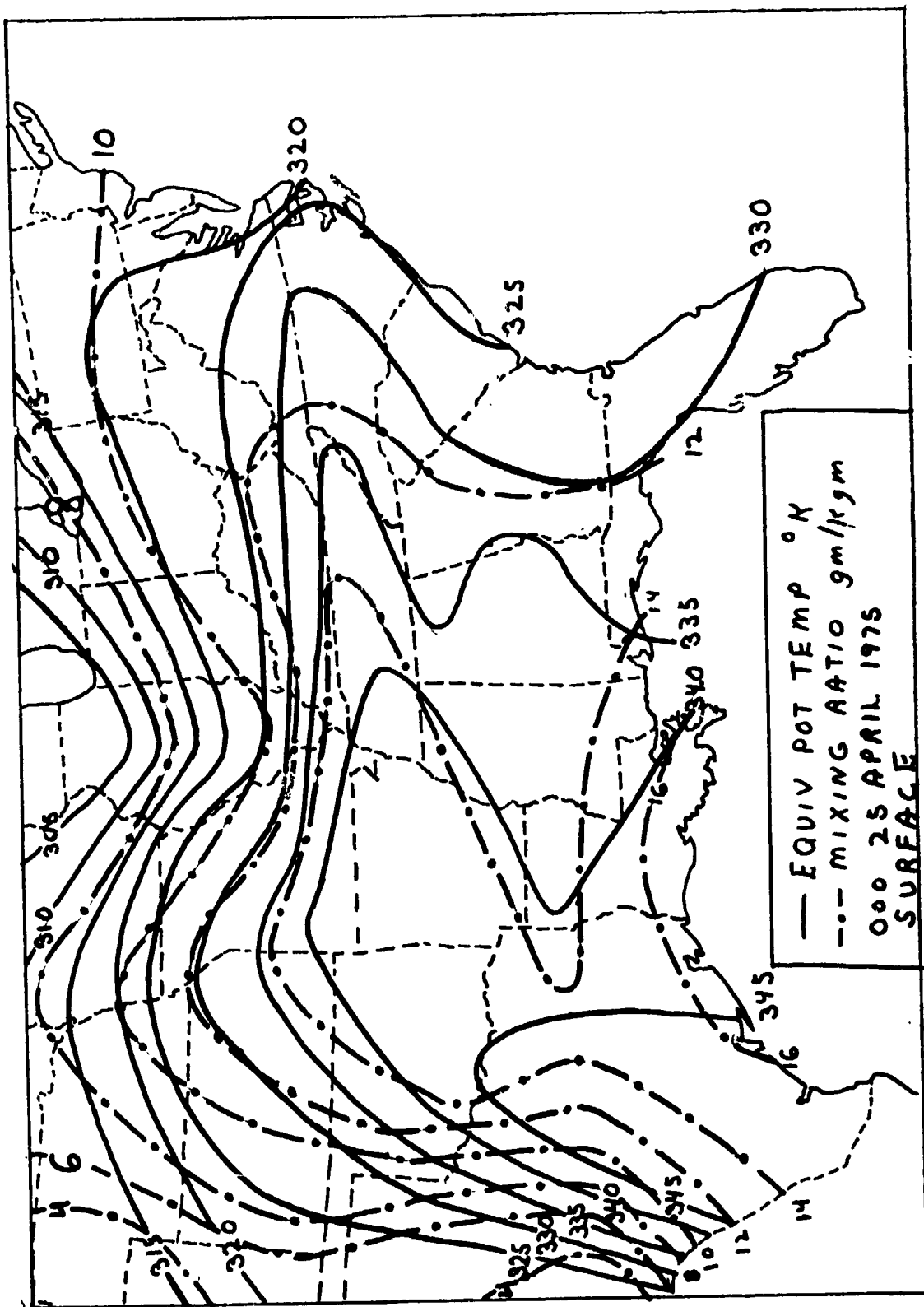


Figure 7a. Surface map of equivalent potential temperature and water vapor mixing ratio at 0000 GMT April 25, 1975.

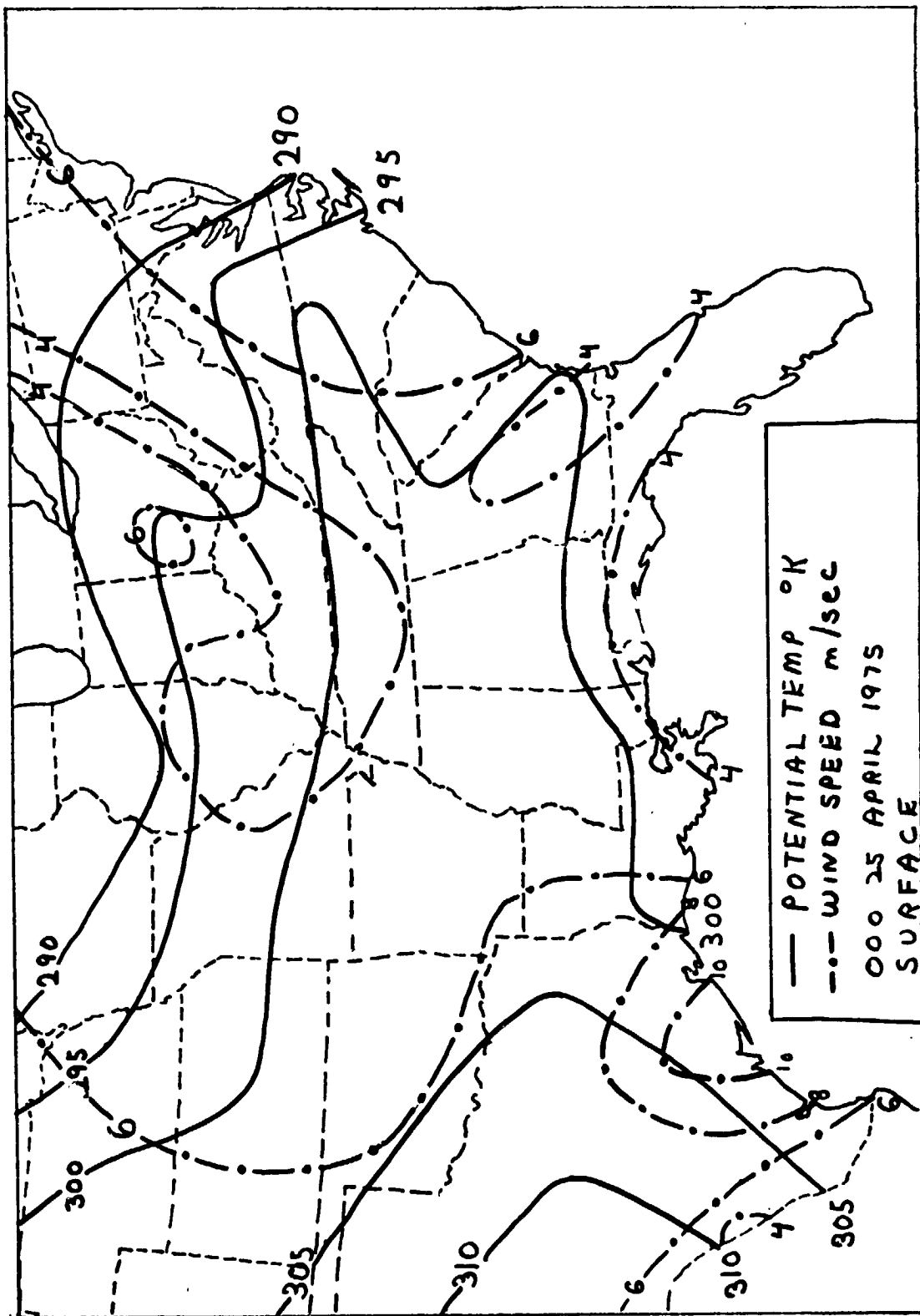


Figure 7b. Surface map of potential temperature and wind speed at 0000 GMT April 25, 1975.

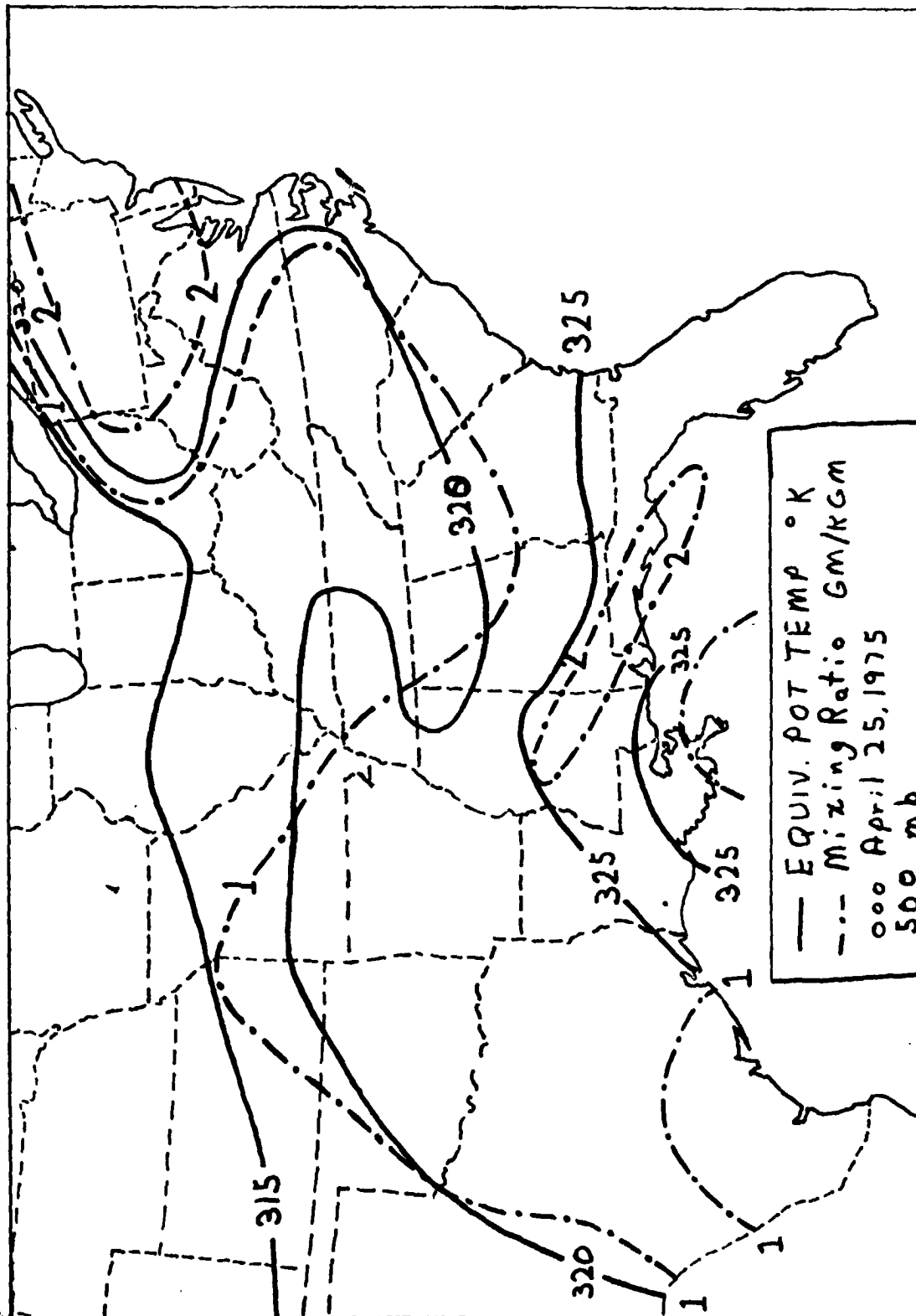


Figure 7c. 500 mb chart of equivalent potential temperature and water vapor mixing ratio at 0000 GMT April 25, 1975.

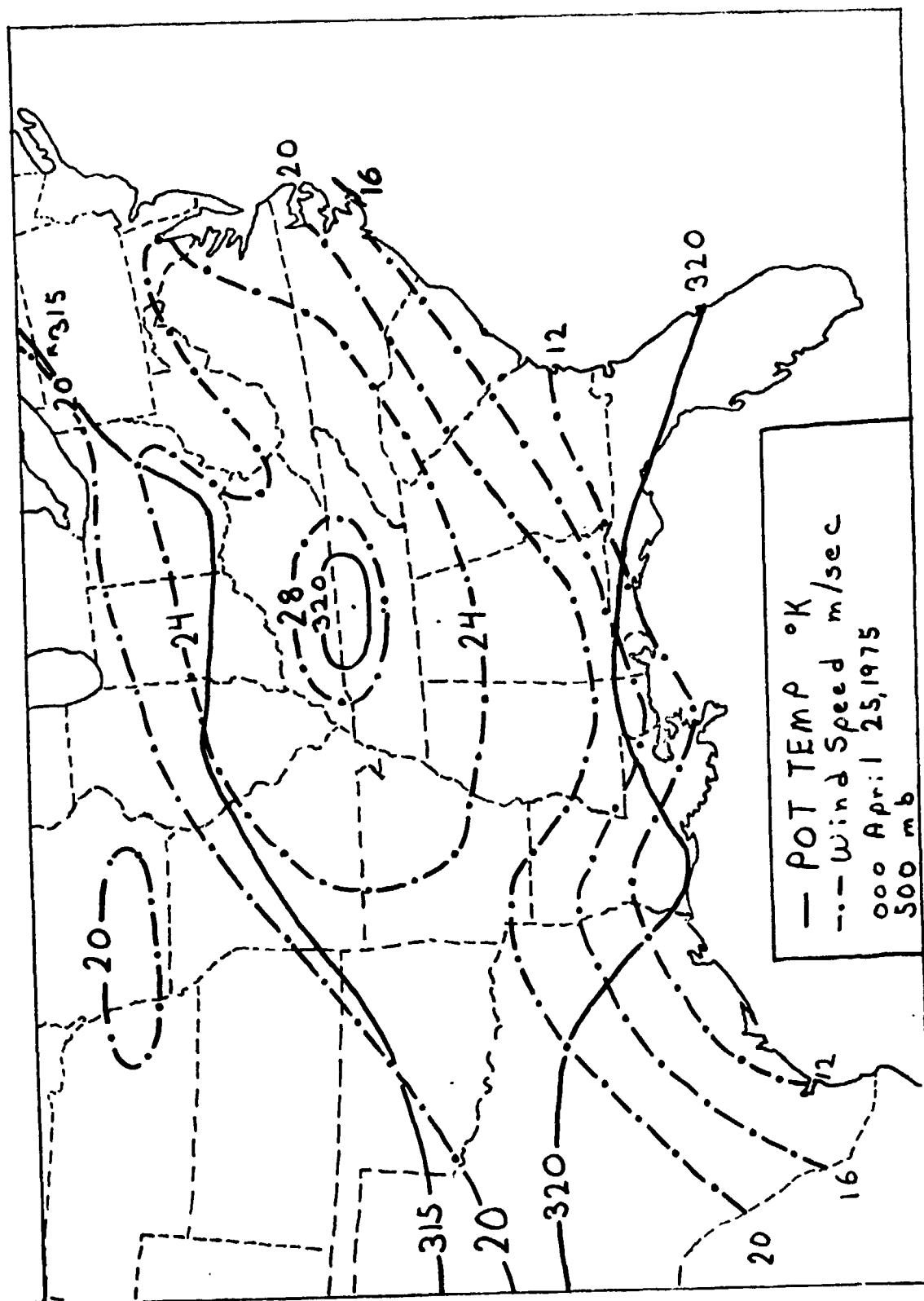


Figure 7d. 500 mb chart of potential temperature and wind speed at 0000 GMT April 25, 1975.

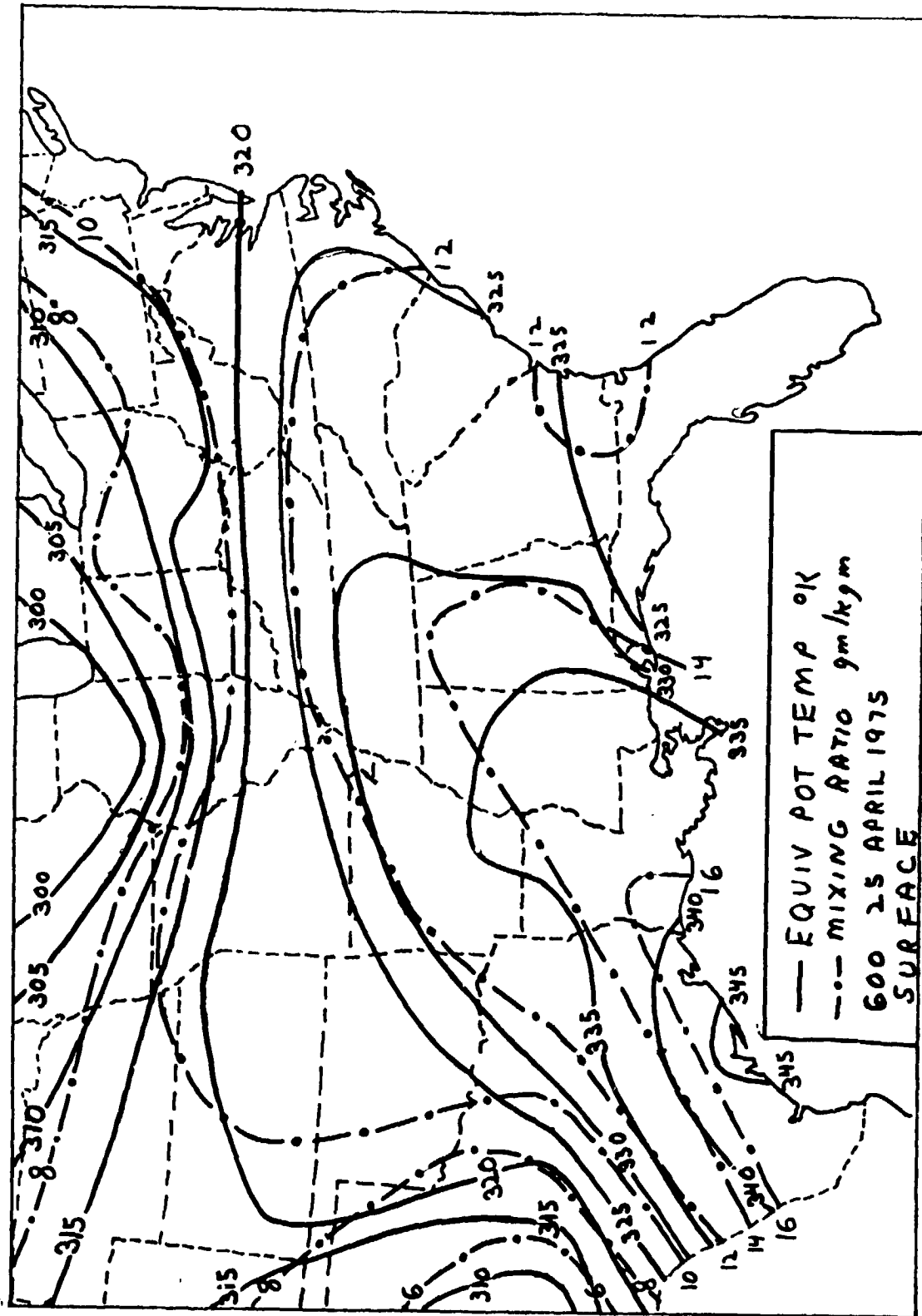


Figure 8a. Surface map of equivalent potential temperature and water vapor mixing ratio at 600 GMT April 25, 1975.

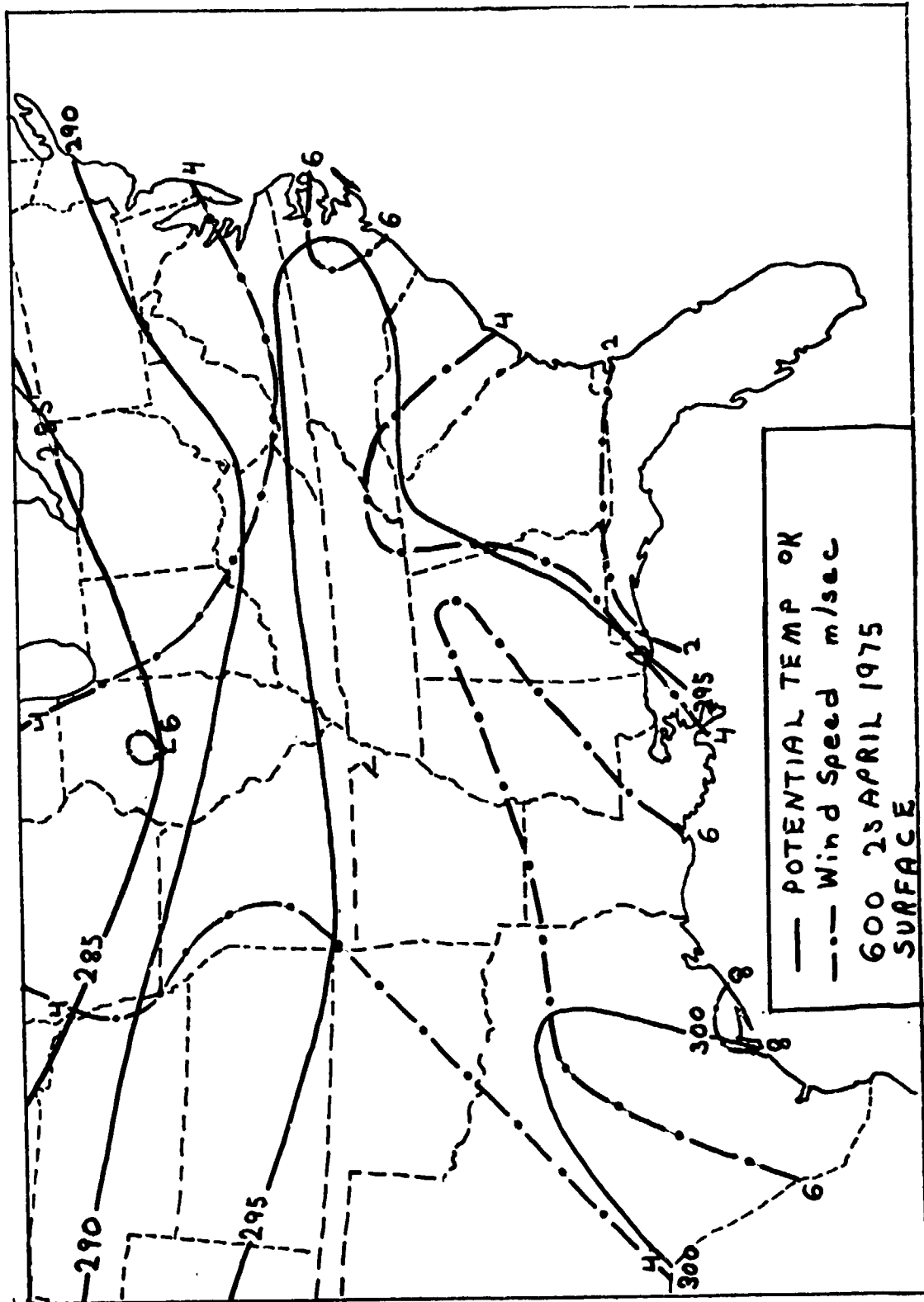


Figure 8b. Surface map of potential temperature and wind speed at 600 GMT April 25, 1975.

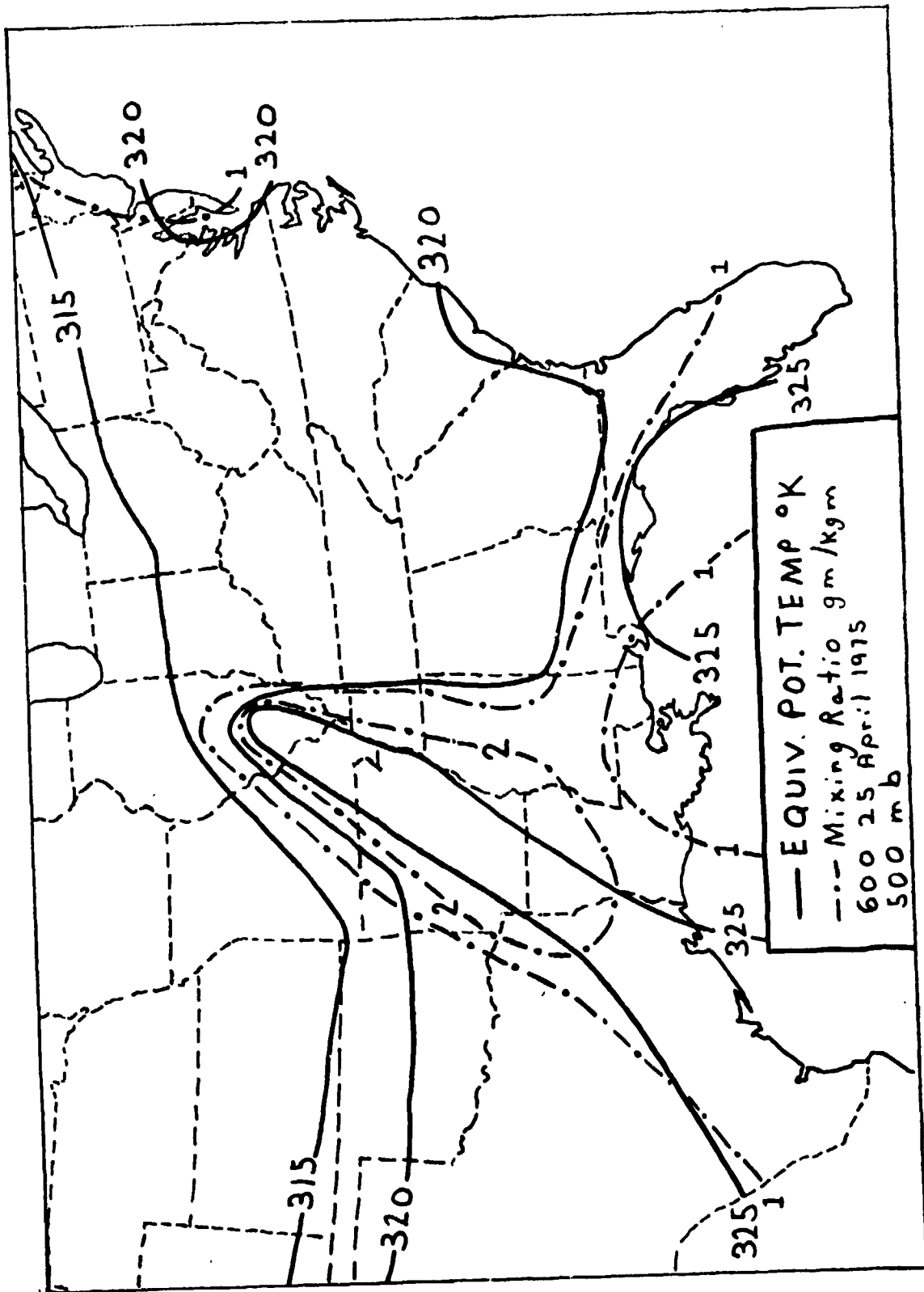


Figure 8c. 500 mb chart of equivalent potential temperature and water vapor mixing ratio at 600 GMT April 25, 1975.

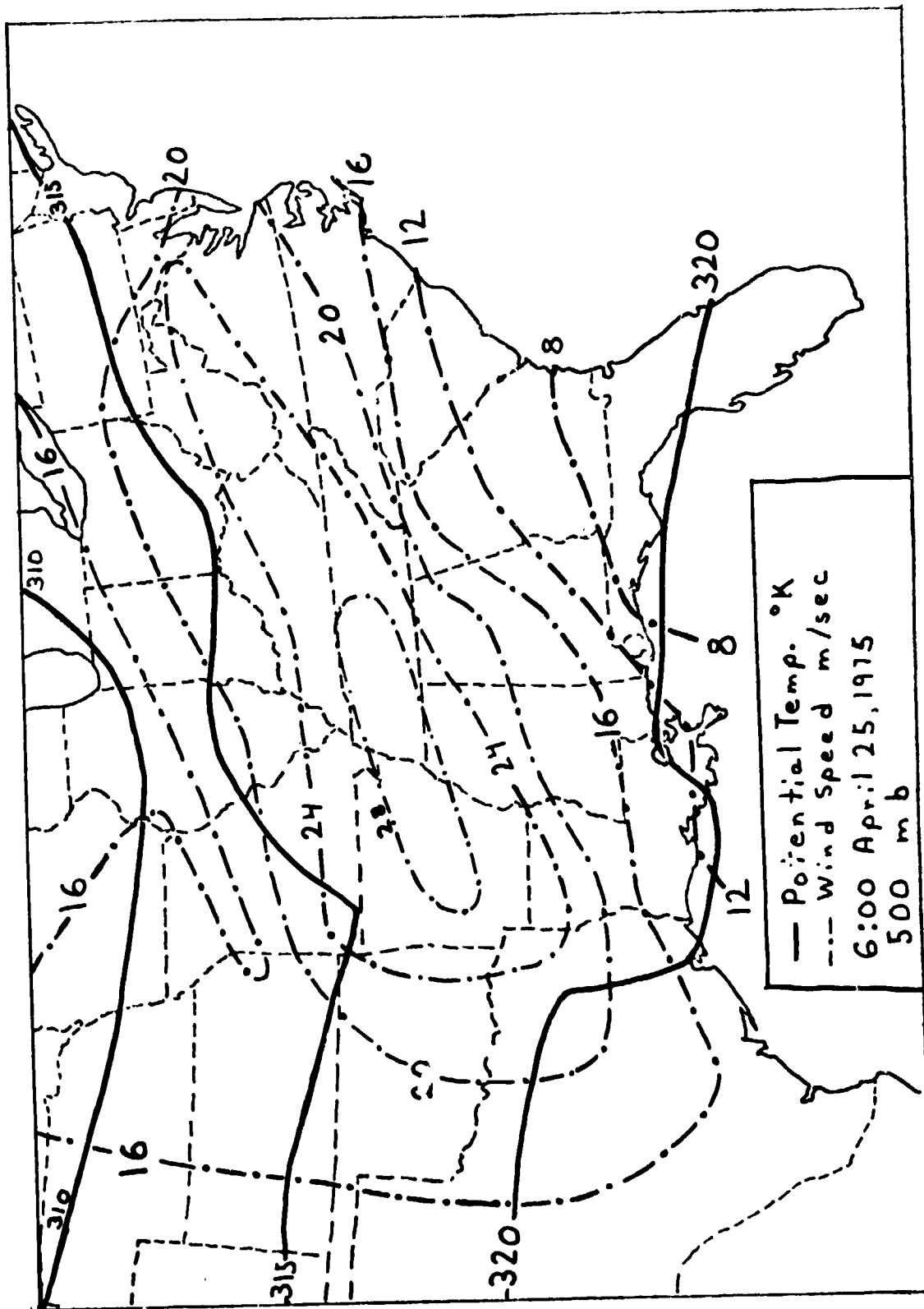


Figure 8d. 500 mb chart of potential temperature and wind speed at 600 GMT April 25, 1975.

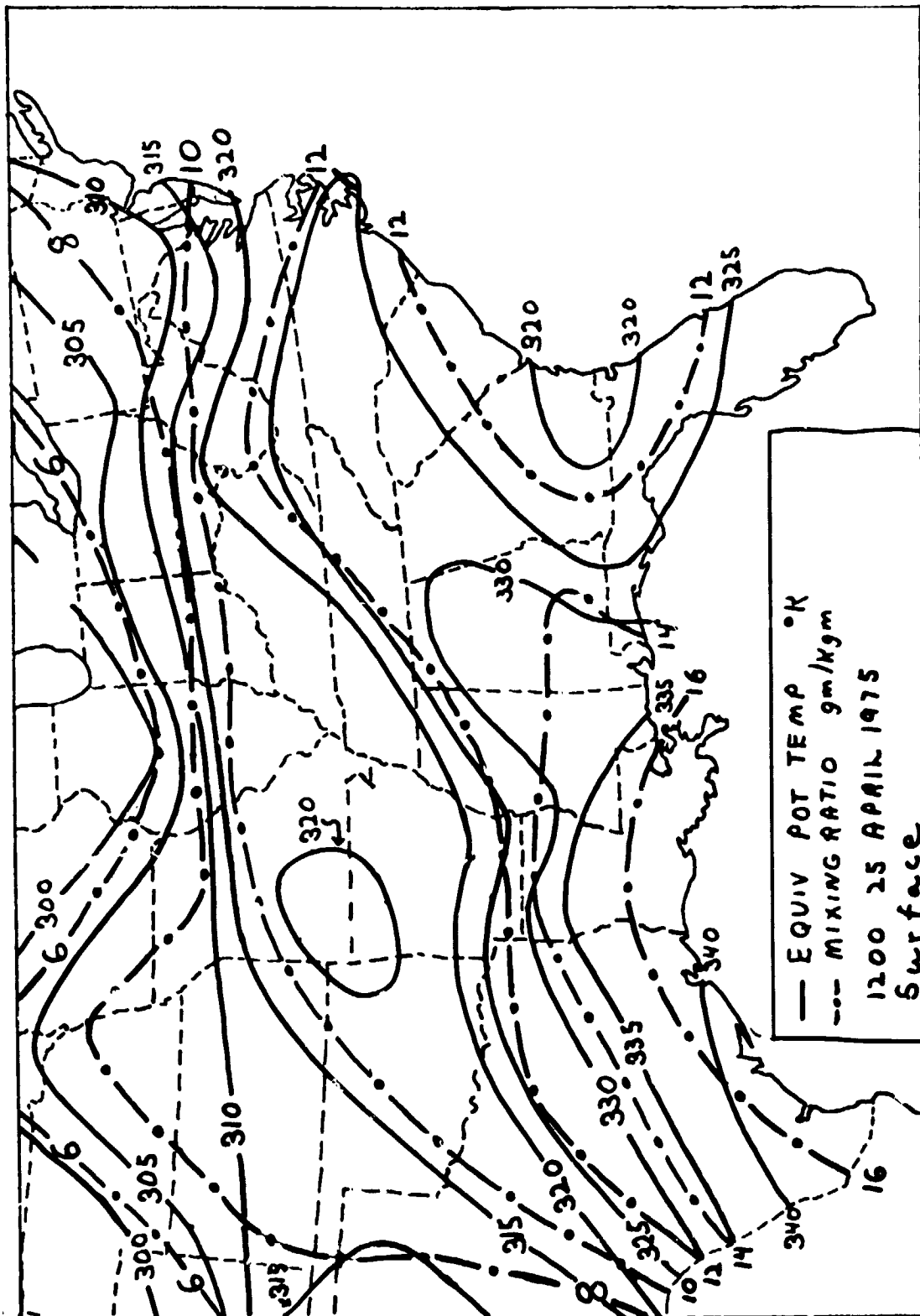


Figure 9a. Surface map of equivalent potential temperature and water vapor mixing ratio at 1200 GMT April 25, 1975.

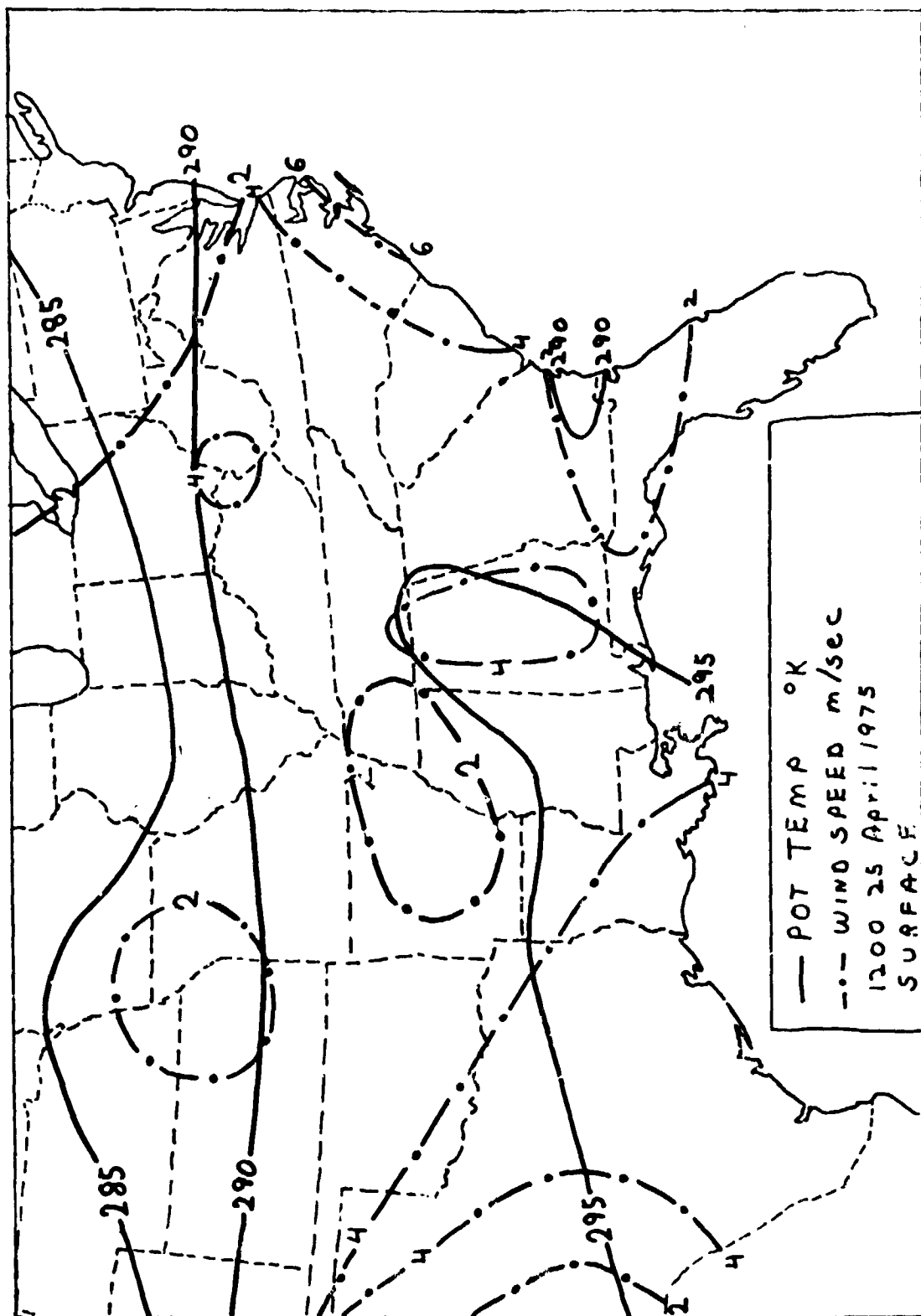


Figure 9b. Surface map of potential temperature and wind speed at 1200 GMT April 25, 1975.

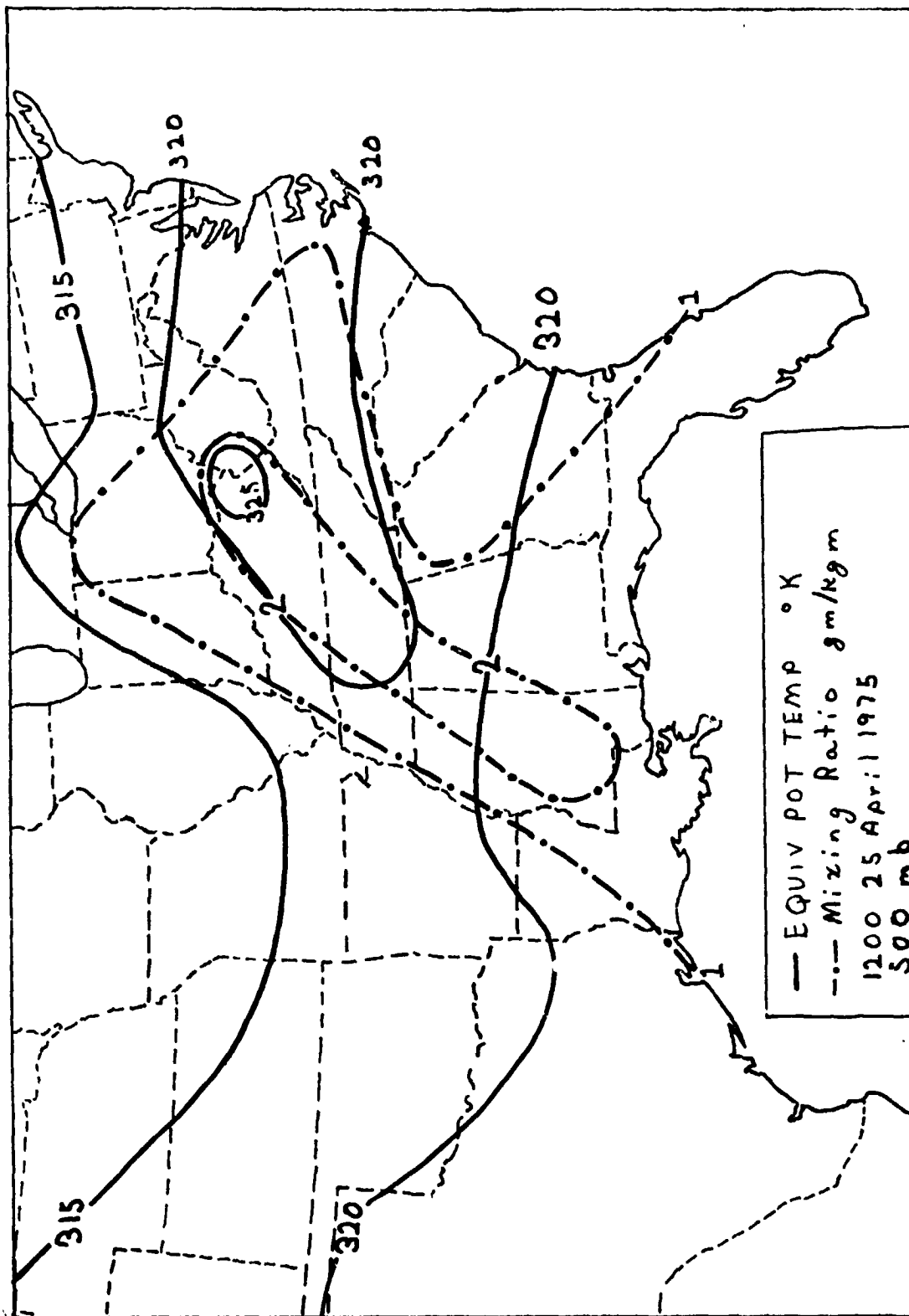


Figure 9c. 500 mb chart of equivalent potential temperature and water vapor mixing ratio at 1200 GMT April 25, 1975.

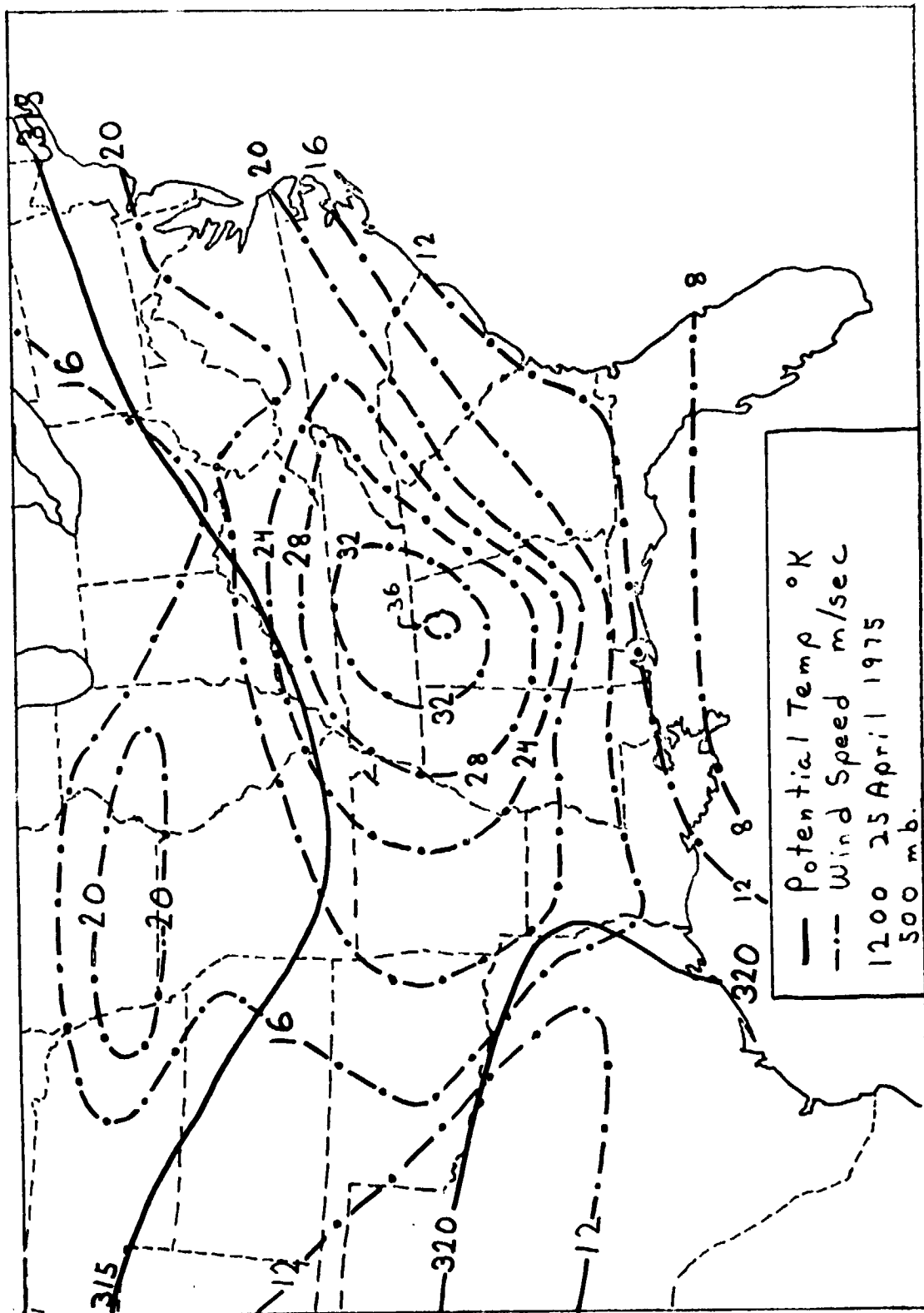
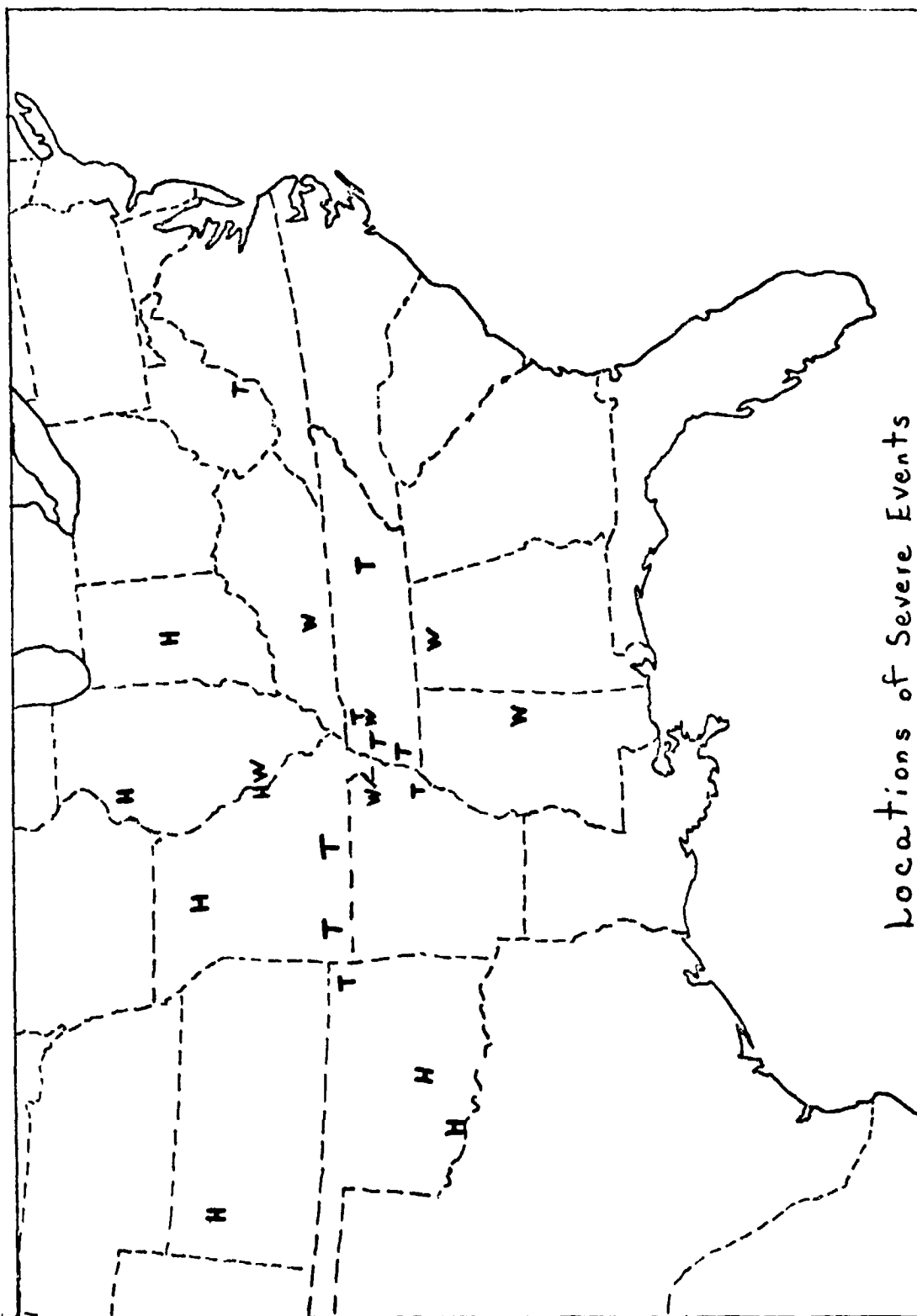


Figure 9d. 500 mb chart of potential temperature and wind speed at 1200 GMT April 25, 1975.



Locations of Severe Events

Figure 10. Location and nature of severe events during the AVE IV experiment. H = hail greater than 0.5 inch in diameter; T = tornadoes; W = wind speeds in excess of 50 mph.

III. The Thunderstorm Model

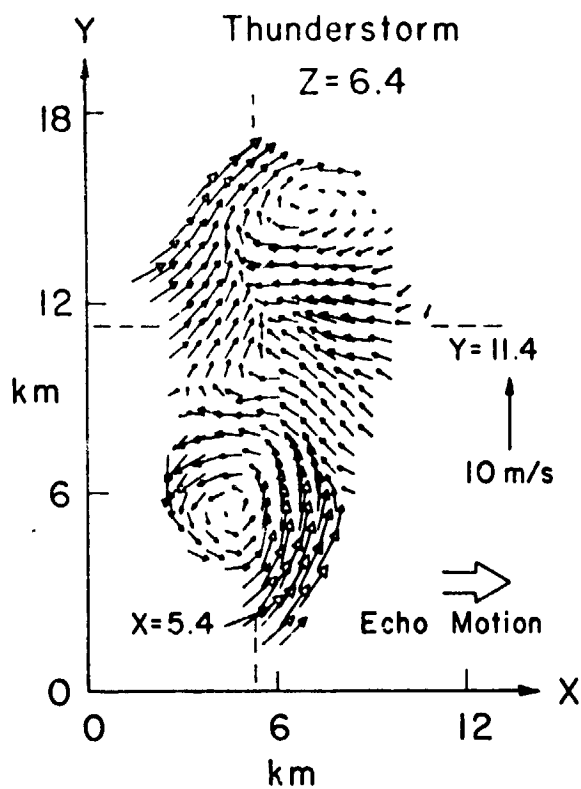
The airflow in a thunderstorm is important to the mechanics of thunderstorm development. Connell (1973) has suggested that some thunderstorms might contain a pair of contrarotating leeside vortices based on aircraft measured winds near cloud base. The existence of these vortices has been substantiated by the dual-doppler radar measured winds obtained by Kropfli and Miller as shown in Figure 11. It has been suggested that a thunderstorm might act to block the environmental winds in much the same way that a solid cylinder would. However, it is known that a thunderstorm does not completely approximate a solid cylinder but entrains some environmental air. Using the experimental results of studies of jets in crossflows by Jordinson (1956) and by McAllister (1968), and the dual-doppler radar measurements of Kropfli and Miller (1975), Connell (1976) has proposed that the interaction between a thunderstorm and its environment might be analogous to the behavior of a jet in a crossflow.

In order to produce a blocking effect in the cloud layer environmental winds, the inflowing updraft must be opposed in direction to some of the air flow above the cloud base. Since the thunderstorm itself usually moves, it is the relative updraft direction that must oppose the relative environmental winds.

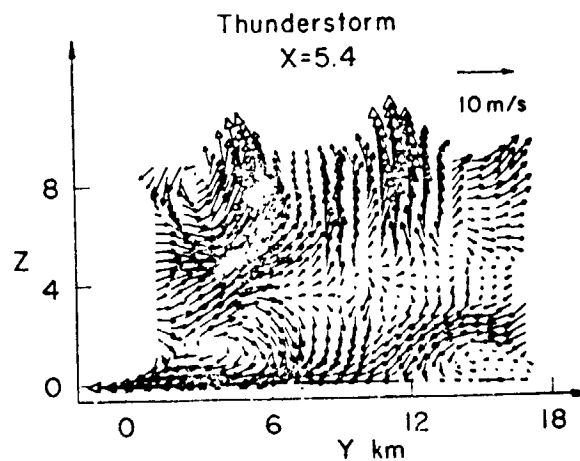
Thunderstorms usually develop in environments with strong wind shear; and, in fact, the double vortex model requires some strongly sheared environment. As the low-level updraft enters the clouds, it encounters upper-level winds from an opposing direction. The intrusion of the updraft into the upper level wind will produce a blocking effect and environmental air will flow around it with some momentum mixing which causes the updraft to bend downwind. Flow around the updraft core will

produce a lee-side wake where contrarotating vortices develop. Figure 12 is a schematic of a double vortex thunderstorm. The intensity and vertical extent of these vortices is in part dependent upon the extent to which the cloud layer winds oppose the updraft inflow.

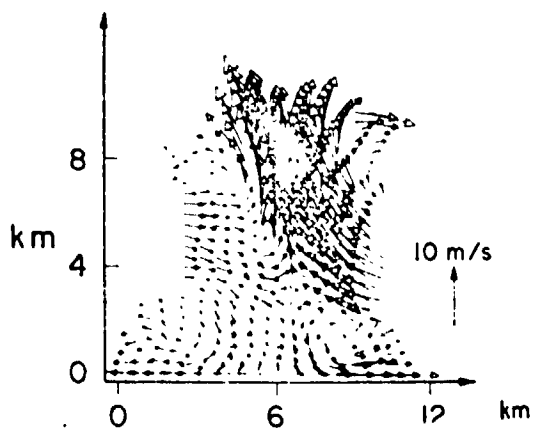
A review of the literature has revealed a thunderstorm model developed by J. R. Eagleman (Eagleman, 1975) that is very similar to the one just described. Eagleman had used his model to develop an index for predicting the occurrences of tornadoes. This predictive scheme, which will be described in the next chapter, was applied to the AVE IV data, and results are given in Chapters V and VI.



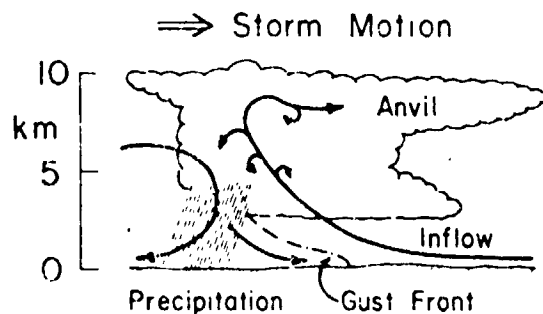
a. Horizontal flow relative to moving storm at 6.4 km above ground. Lengths at arrows are proportional to relative wind speed.



b. Vertical flow in y, z plane at $x = 5.4$ km.



c. Vertical flow in x, z plane at $y = 11.4$ as indicated in Figure 11a.



d. Schematic representation of flow pattern in vertical plane corresponding to Figure 11c.

Figure 11. Three-dimensional velocity structure within a severe thunderstorm measured by dual-doppler radar (from Kropfli and Miller).

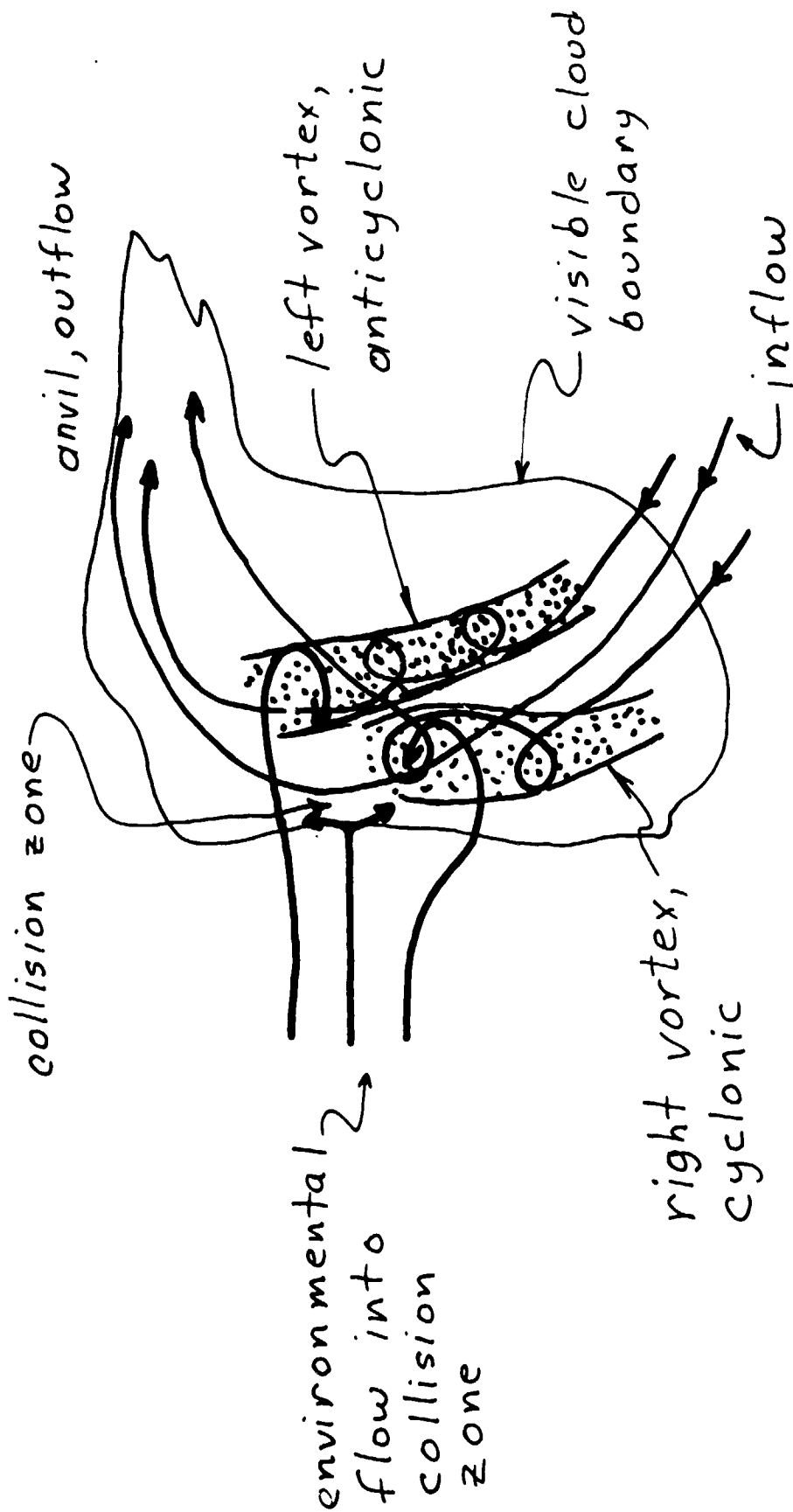


Figure 12. Schematic of air flow for the main feature of the double vortex of a thunderstorm.

IV. The Predictive Indices

The accurate forecasting of tornadoes is of importance to the protection of life and property. At the present time forecasting techniques are not accurate. Today a tornado will occur forty percent of the times the National Severe Storms Forecasting Center issues a tornado forecast. Furthermore, only thirty-five percent of tornadoes that do occur are within the tornado watch area. The need for more accurate predictions is evident.

A predictive index has been devised by J.R. Eagleman which incorporates both atmospheric thermodynamics and environmental wind conditions hypothetically leading to double-vortex thunderstorm formation. Darkow's Energy Index is used as an indicator of the potential instability of the atmosphere. It is combined with a Shear Index, which reflects the shear in the relative winds between the surface-to-850 mb layer and the cloud layer, to produce an Energy Shear Index. Each of these indices will be explained in the remainder of this chapter. The Severe Weather Threat Index (SWEAT) and the Surface Potential Index (SPOT), which were also calculated for the AVE IV data for comparison with the Energy Shear Index, will also be explained in this chapter.

1) The Energy Index (EI)

The total specific energy of a mass of air may be expressed as $E(T) = c_p T + gZ + Lq + v^2/2$, the sum of specific enthalpy, potential energy, latent energy, and kinetic energy, where c_p is the specific heat of air at constant pressure, T the temperature, gZ the geopotential, L the latent heat, q the specific humidity, and V the scalar velocity of the wind.

Darkow (1968) points out that the kinetic energy term is usually two orders of magnitude smaller than the other terms and may be neglected.

The errors in reported upper air humidity values allow the additional approximations $q = w$ and $L = L_0$, where w is the mixing ratio and L_0 a constant latent heat of condensation. The total energy or static energy is then expressed as $E(T) = C_p T = gZ + L_0 w$. The total energy defined by this equation is conservative with respect to both unsaturated and saturated adiabatic processes. Thus, the potential convective instability of atmospheric layers is indicated by the amount of decrease of total energy in the layers. Using the values of $c_p \approx 1.00 \text{ J g}^{-1} \text{ K}^{-1}$, $L_0 \approx 2500 \text{ J g}^{-1}$, and $g \approx 980 \text{ cm sec}^{-2}$ yields $E(T) \approx T(K) + 9.8 \times 10^{-3} Z(m) + 2.5 w (\text{g kg}^{-1})$ which may be approximated as $E(T) \approx T(^{\circ}\text{K}) + 2.5 w (\text{g kg}^{-1}) + Z(m)/100$.

A stability index, the Energy Index, which reflects the contribution to total atmospheric energy of both ascending potentially warm air and descending potentially cold air is defined as the algebraic difference between the total energy of the air at the 500 and 850 mb levels, expressed as $EI = E(T)_{500} - E(T)_{850}$. This difference is shown schematically in Figure 13. The 850 and 500 mb values are chosen as representative of the low-level air and mid-tropospheric air entering the storm as dictated by the routine availability of data at these levels.

Quantitative values of the Energy Index had been assigned to various degrees of thunderstorm intensity. In the range of 0.0 to -1.0, thunderstorms are possible but will not be severe. In the range of -1.0 to -2.0, isolated severe thunderstorm activity is possible, particularly as a continuation of severe activity moving into the regions. For Energy Index values less than -2.0, severe thunderstorms and tornado

activity are highly probable, providing an adequate triggering mechanism to release the potential instability is present.

Shear Index

One triggering mechanism that is present in the environment of a cloud is the vertical shear in the relative winds between the low levels and the mid-troposphere. In this regard, Eagleman (1975) has developed a Shear Index to reflect vertical changes in relative vector velocity. Figure 14 shows the relationships between cloud motion, measured winds relative to earth, and the winds measured relative to the moving cloud. The mean environmental wind is calculated by finding the vector mean of the 850, 700, 500, and 300 mb reported winds. These are interpolated so that the relative velocity through each 50 mb layer can be calculated.

In order to calculate relative velocities, storm speeds and directions must be known. For the calculation of the Shear Index, seven storm speeds of 50, 55, 60, 65, 70, 75 and 80 percent of the mean environment wind speed and 26 storm directions ranging from 60 degrees to the left to 60 degrees to the right of the mean environmental wind direction, incremented every 5°, were used. This produced 182 variations of storm movement as shown in Figure 15.

Since the model requires blocking of the inflowing low level air in the mid-level, layers 150 mb deep are examined to see if they oppose the relative winds of the low level.

The surface-850 mb layer is used as the low level inflow layer. Six layers were chosen as the critical mid-level layers for the occurrence of opposing component velocities; these were the 650-500 mb, the 400-250 mb, the 550-400 mb, the 500-350 mb, the 450-300 mb, and the 400-250 mb layers. The opposing components in the six mid-level layers were considered to produce blocking if they were between 75 and 125 percent of the magnitude of the surface-850 mb wind.

Thus the Shear Index (SI) for a trial storm and speed was defined as the number of consecutive mid-level layers whose opposing components were between 75 and 125 percent of the surface-850 mb wind speed. Therefore, the Shear Index can vary from zero to six; a maximum Shear Index of 6 is shown in Figure 16. The Shear Index of a sounding was defined as the largest SI for all 182 trials obtained for the 7 storm speeds and 26 directions. The direction of movement of an actual storm should correspond to one of the calculated storm directions which yields the maximum SI.

The Energy Shear Index

The Shear Index measures only the atmospheric wind profile; the proper thermodynamics must be present also for storm development. Therefore, the Shear Index is combined with the Energy Index to produce the Energy-Shear Index. To determine the best empirical combination of the indices, the SI was graphed versus the EI for 59 soundings as shown in Figure 17. Twenty-seven of these soundings were proximity soundings; twelve were precedence soundings, and twenty were nonproximity soundings. A proximity sounding was defined as a sounding within the warm air sector and less than 120 miles from a confirmed tornado touchdown, and within two hours before the tornado or no more than one-half hour after the first report of a tornado. A nonproximity sounding is for the same time period but located over two hundred miles away from a tornado

occurrence. Precedence soundings are those taken in the warm air ahead of the cold front but removed from it in either time or distance.

A line can be drawn that separates the proximity and precedence sounding from the nonproximity soundings. The equation of this line is $EI = 1/2 SI - 2$ or $2EI - SI + 4 = 0$. The Energy Shear Index can thus be calculated from the equation $ESI = 4 - SI + 2EI$. If the ESI is negative and a cold front is nearby, tornadoes are predicted; if it is positive, tornadoes are not indicated. For a more detailed description of the Shear Index and the Energy-Shear Index, see Eagleman (1975).

Sweat and Spot Indices

As a basis of a comparison of the accuracy of the Energy-Shear Index, two currently used indices, the Severe Weather Threat Index (SWEAT) and the Surface Potential Index (SPOT) were calculated. These indices are used in conjunction to produce short-term (three to six hour) depictions of areas with high potential for severe storm development or occurrence. The soft SWEAT was calculated in this study since parameters from AFGWC Fine Mesh and Boundary Layer Models were not available.

The Sweat Index is computed using the equation $SWEAT = 12 t_e + 20 (T - 49) + 2W_e + W_{500} + 125 f/2$ where

t_e = low level dew point in °C, the level used is 850 mb

in the soft SWEAT and 900 meters in the BLM computations.

T = Total totals (T = 850 mb temperature plus 850 mb dew point temperature minus twice the 500 mb temperature, all °C); for complete details on this stability index see Miller (1972).

W_e = low level wind speed in knots; the level used is once again either 850 mb or 900 meters.

W_{500} = 500 mb wind speed in knots.

$f(\alpha)$ = a step function of the veering angle W_e to W_{500}

See Figure 18a for a plot of this function.

This term is set to zero if both W_e and W_{500} are not equal to or greater than 15 knots. The term is not computed unless the 850 mb wind direction is within the range 130° to 250° and the 500 mb wind direction is within the range 210° to 310° .

All negative terms are set to zero.

The SPOT index is computed from the equation $SPOT = (t-60) + (t_d-55) + 100(30.00 - p) + f(v)$ where

t = surface temperature in $^\circ F$.

t_d = surface dew point in $^\circ F$.

P = altimeter setting in inches.

$f(v)$ = wind speed term which is determined from the table shown in Figure 18b.

Negative values are allowed to occur. The altimeter term is reduced by 50 percent when temperatures are less than $50^\circ F$ and altimeter settings are below 29.50 inches. Regions where high values of the index lie in close proximity to very low values are suspect areas.

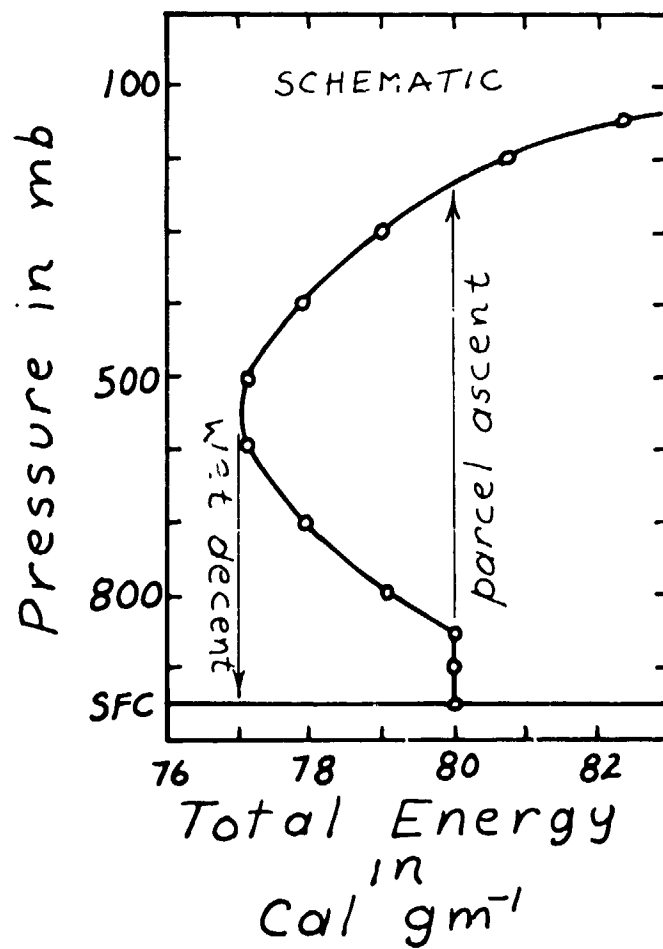


Figure 13. Schematic total energy profile in late afternoon prior to the outbreak of severe thunderstorm activity (from Darkow, 1968).

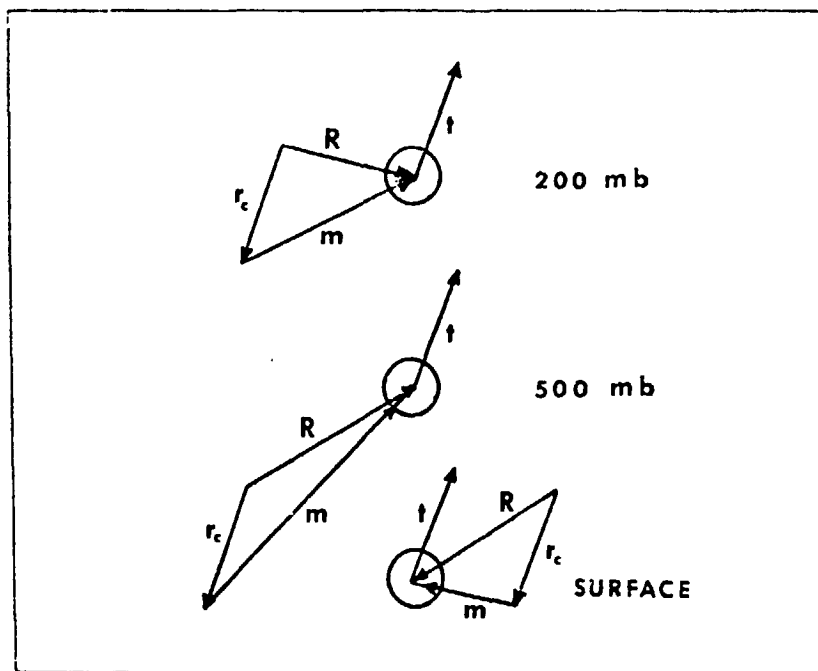


Figure 14. Vectors for a tornado proximity sounding showing the wind (R) relative to a moving thunderstorm as determined by the movement of the storm (t), which creates a wind (r_c) opposite to the direction of movement of the storm. The combination of (r_c) with the measured winds (m) relative to a fixed point results in the relative winds (R) for a moving thunderstorm (from Eagleman, 1975).

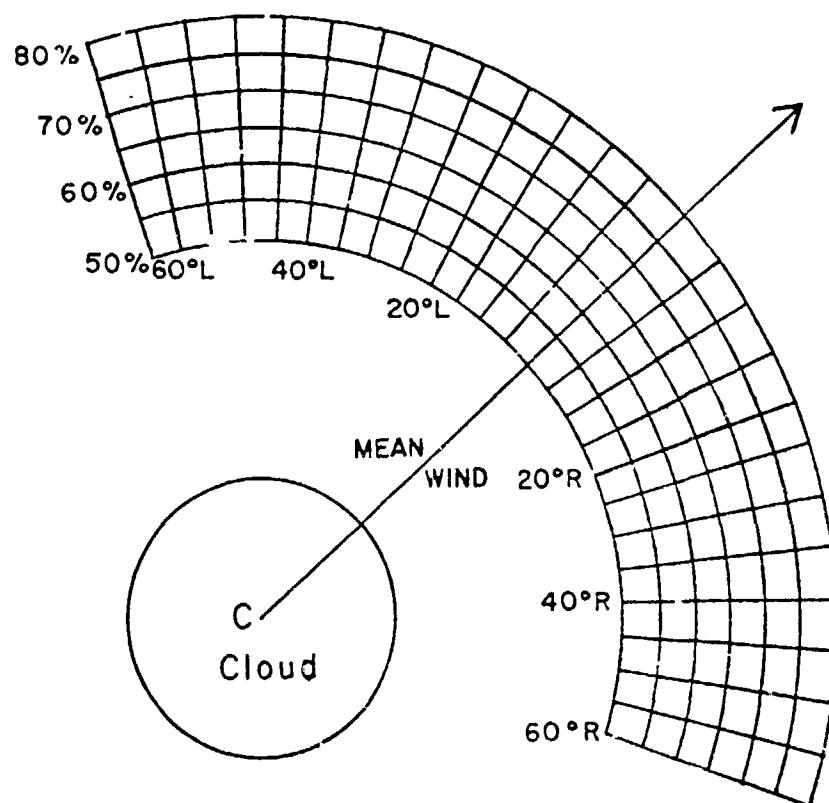


Figure 15. Combinations of storm speeds and storm directions used for making calculations of relative winds and shear index (from Eagleman, 1975).

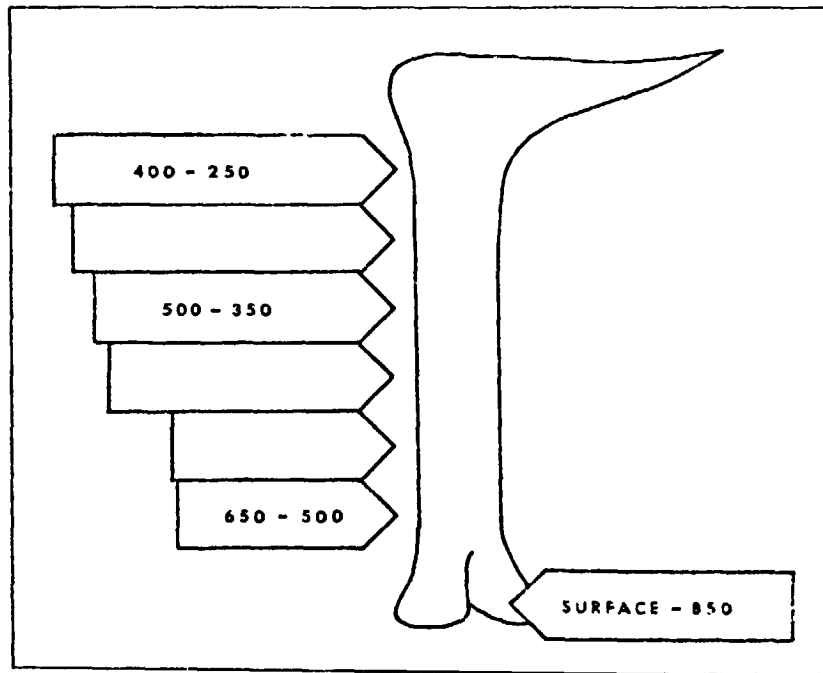


Figure 16. Example of a shear index of six (from Eagleman, 1975).

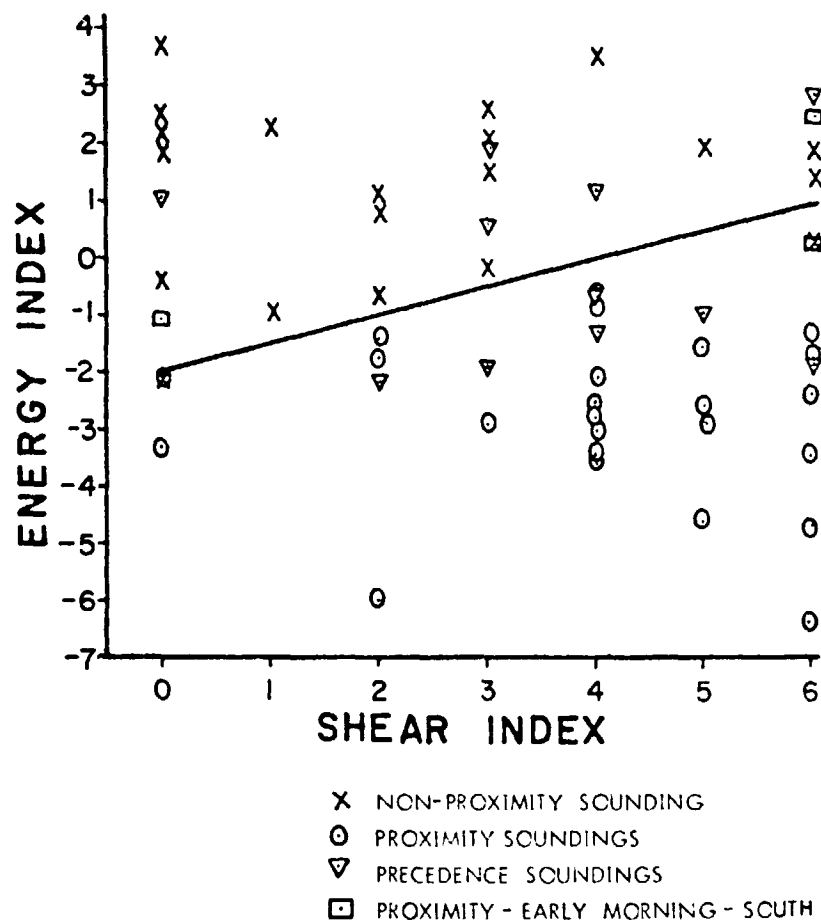


Figure 17. Scatter diagram of SI versus EI used in determination of equation for ESI (from Eagleman, 1975).

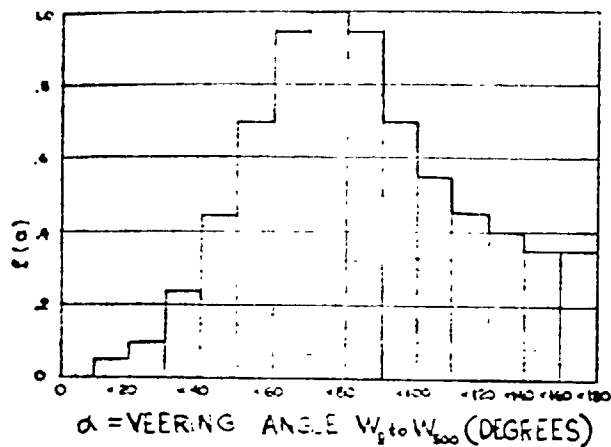


Figure 18a. Step function used to determine $f(2)$ term in SWEAT equation (from Miller and Maddox, 1975).

		WIND DIRECTION					
		GT360°	GE070°	GT140°	GT200°	GT230°	GT260°
		LT070°	LE140°	LE200°	LE230°	LE260°	LE360°
SFC Td °F	Td ≥ 60	0	VV	If P ₂ at station VV If not 2 × VV	VV	VV	-2 × VV
	55 ≤ Td < 60	0	VV	same as above	$\frac{VV}{2}$	-VV	-2 × VV
	Td < 55	0	VV	VV	0	-2 × VV	-2 × VV

NOTE: VV = greatest of VV and GG where VV = reported wind speed in knots and GG = gust speed if reported

Figure 18b. Table used to determine $f(v)$ term in SPOT equation (from Miller and Maddox, 1975).

V. Applications of Indices to AVE IV Data

A computer program was obtained from Dr. Eagleman for computing the Energy Index, the Shear Index, and the Energy-Shear Index. The input format parameters were changed to read the AVE IV data, and the section of the program which determines the atmospheric variables at 50 mb intervals by linear interpolation was removed since data at these intervals are directly available from the AVE IV data. The program as received did not execute properly on the IBM 360. For certain angles between the assumed storm direction and the measured winds, division by zero was produced. Also the accumulation of computer-generated round-off errors sometimes produced values of the sine or cosine of an angle whose absolute value was greater than one. After these problems were eliminated, a subroutine was added to calculate the SWEAT and SPOT indices, and the program was run with the AVE IV data from 29 stations at all nine times. Figures 19 through 54 show the results of these computations. The shaded areas on the maps of Energy Index are those areas in which EI has a value more negative than -2 and severe thunderstorms and tornadoes are probable. The weather types associated with other values of EI have been explained in Chapter IV. Shaded areas on the ESI maps indicate those regions with ESI values less than zero. Severe event locations and types are indicated. The time of the sounding was between two hours before and one hour after any severe events marked at a sounding time.

The following comments summarize the tests using AVE IV data:

A summary of the number of occurrences of each type of severe weather is given in Table 1, along with the number that was correctly predicted by each index. The sweat and spot index predictions are not included because it was felt that the criteria for both are not sufficiently definitive to permit an objective prediction. As we gain experience with their use we will better trust our subjective use of these indices and may use them for comparison.

Table 1

Events Reported		Events Correctly Predicted by	
Type	Number	EI	ESI
Hail	4	4	4
Tornadoes	9	4	6
Wind	5	4	3
TOTAL	18	12	13

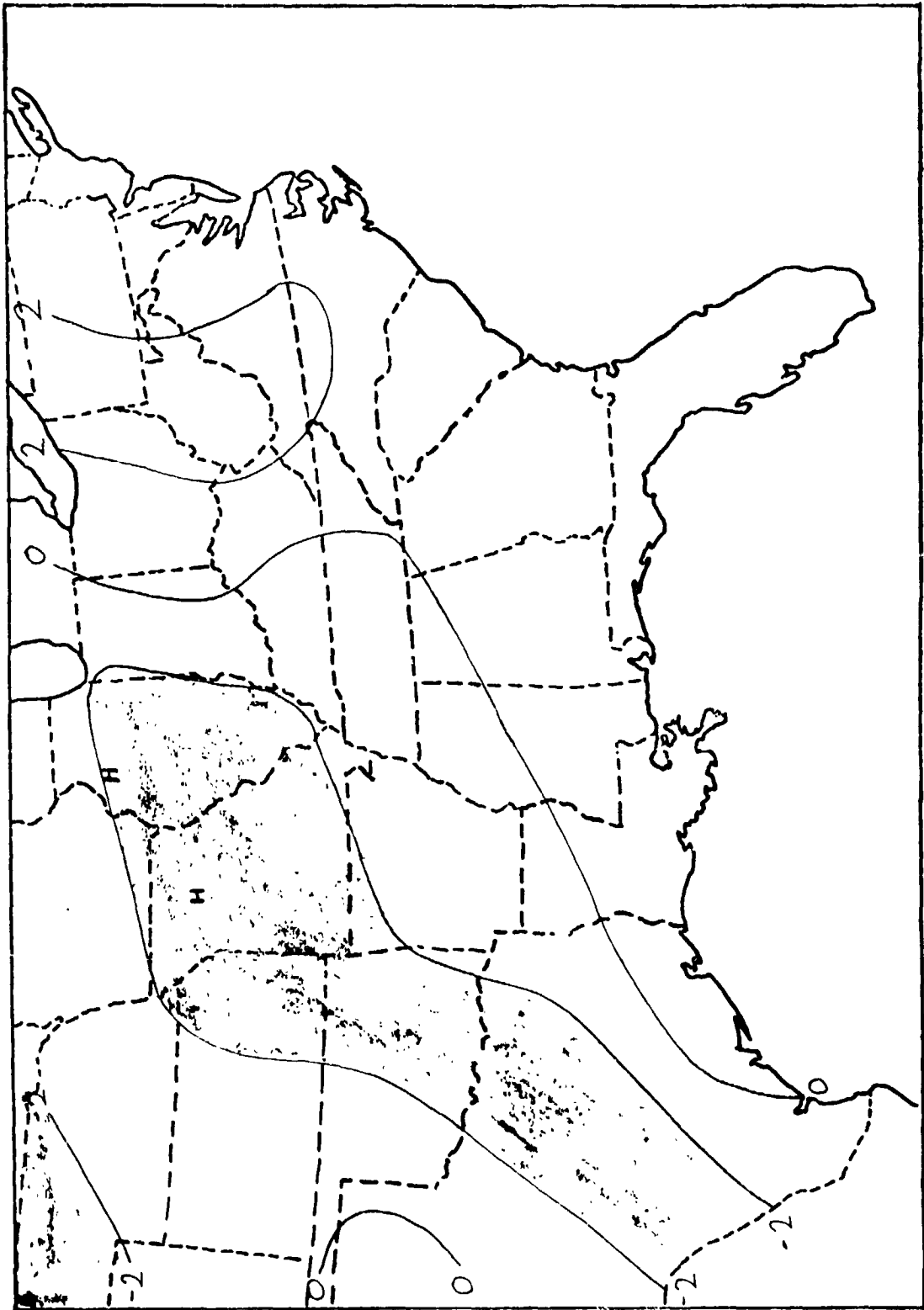


Figure 19. Map at 0000 GMT April 24, 1975 for Energy Index.

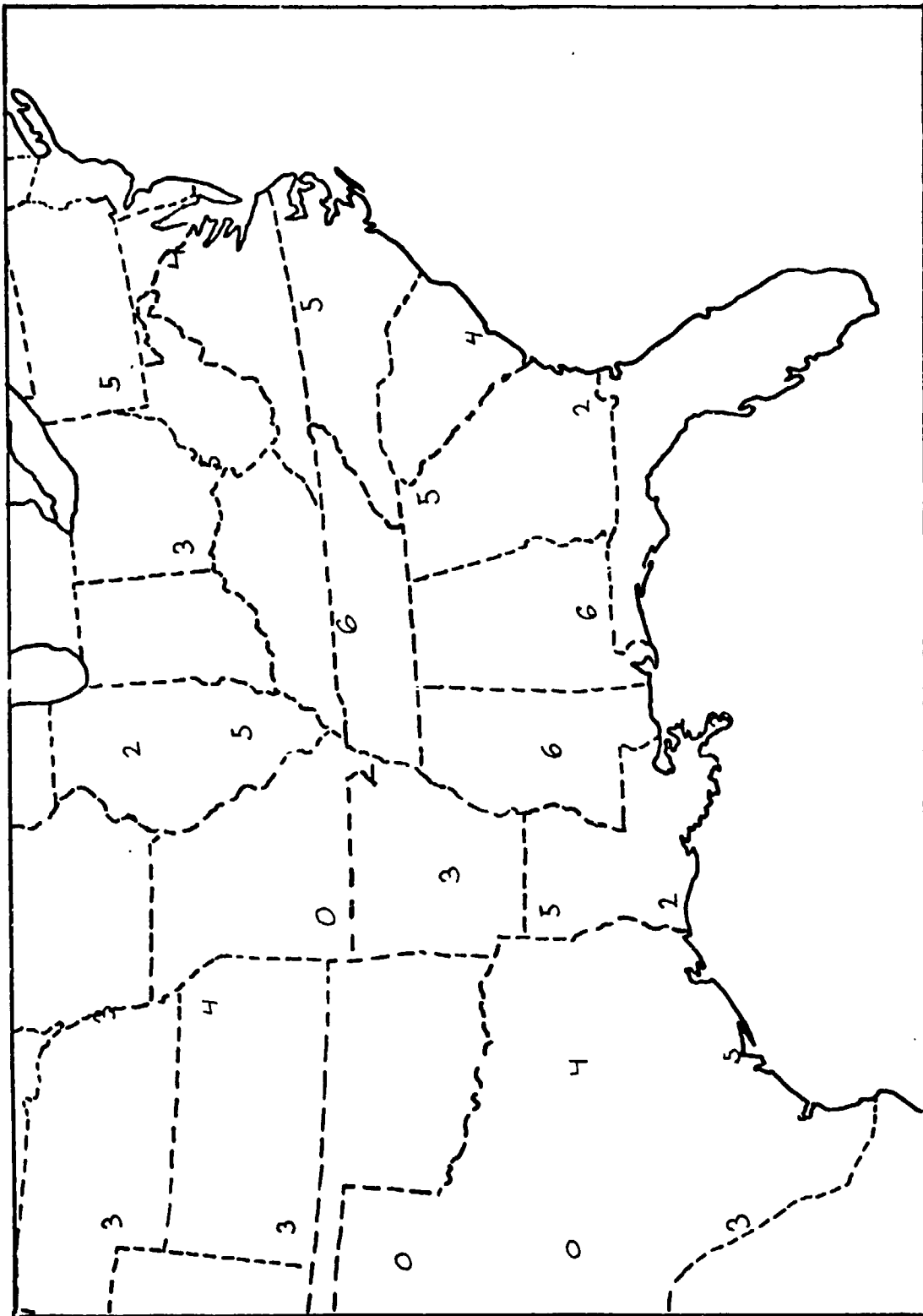


Figure 20. Map at 0000 GMT April 24, 1975 for Shear Index.

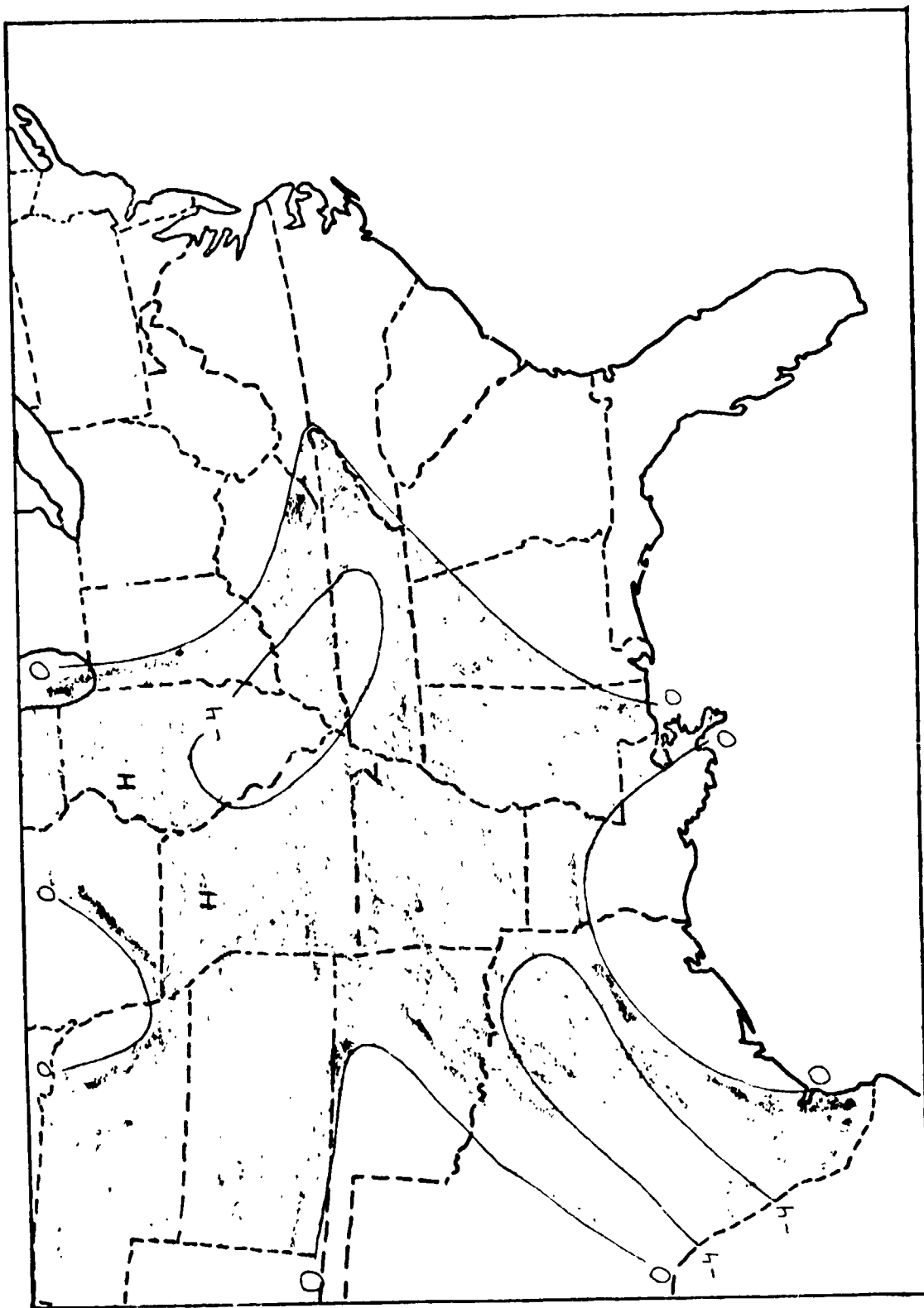


Figure 21. Map at 0000 GMT April 24, 1975 for Energy Shear Index.

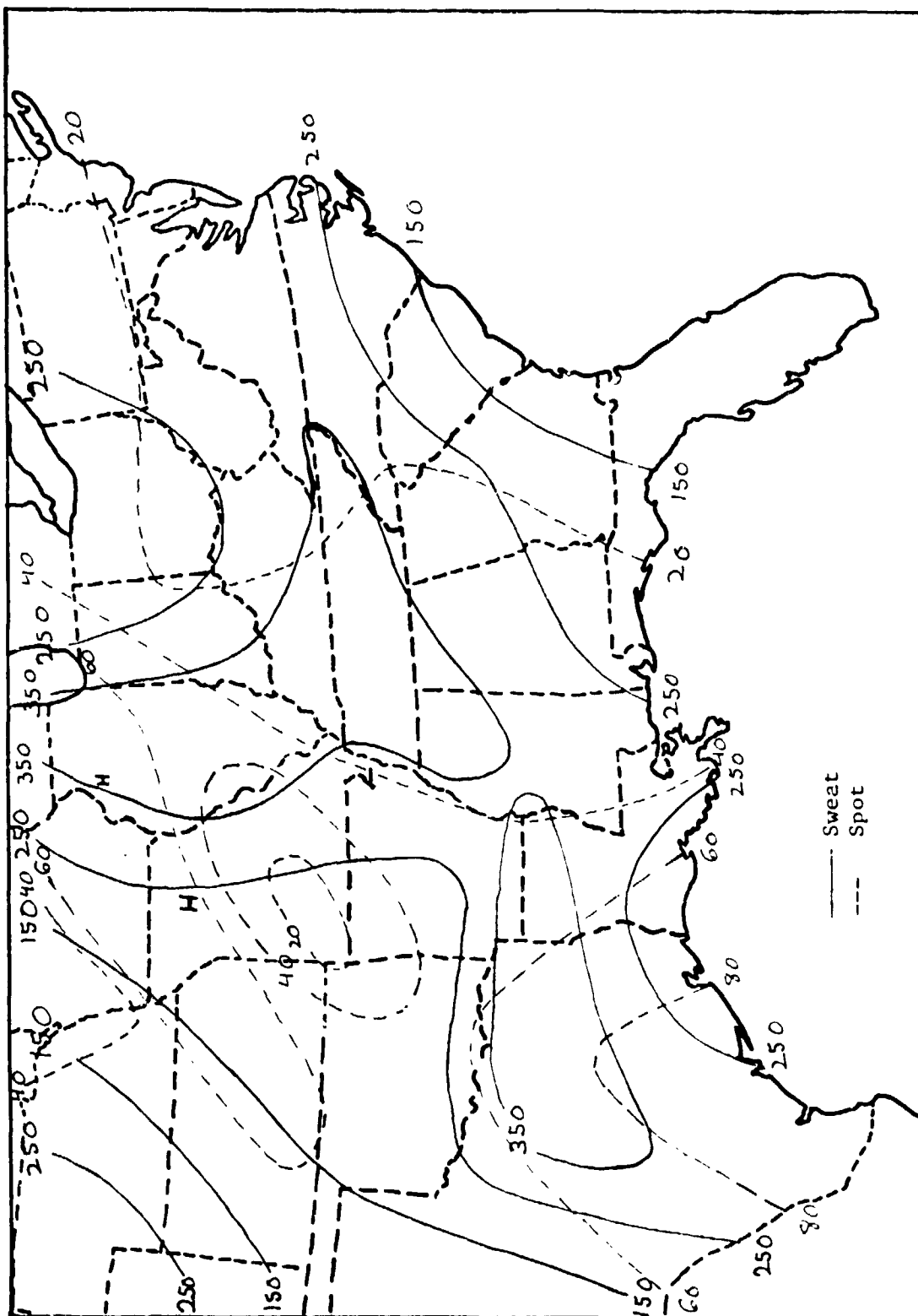


Figure 22. Map at 0000 GMT April 24, 1975 for Sweat and Spot indices.

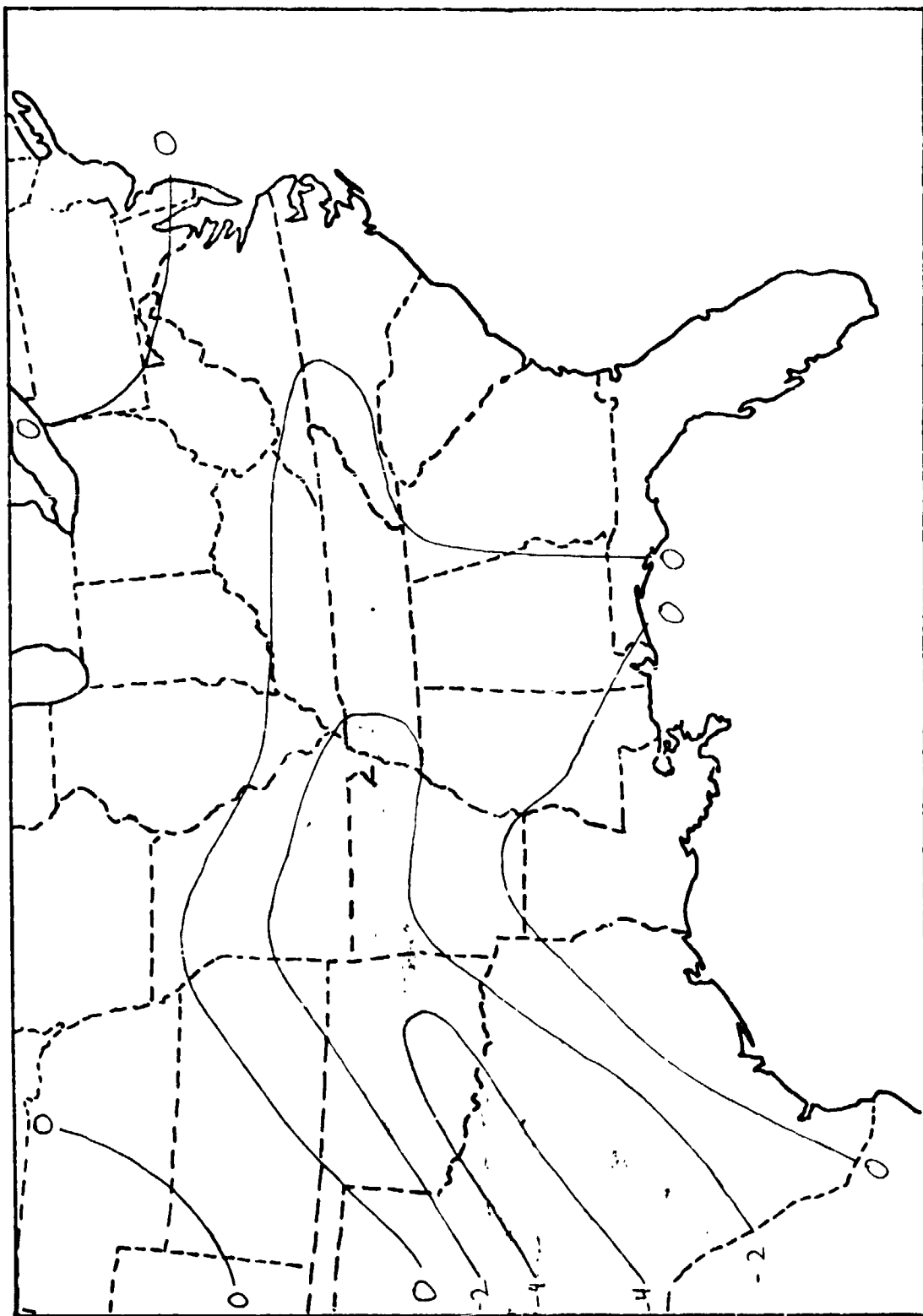


Figure 23. Map at 0600 GMT April 24, 1975 for Energy Index.

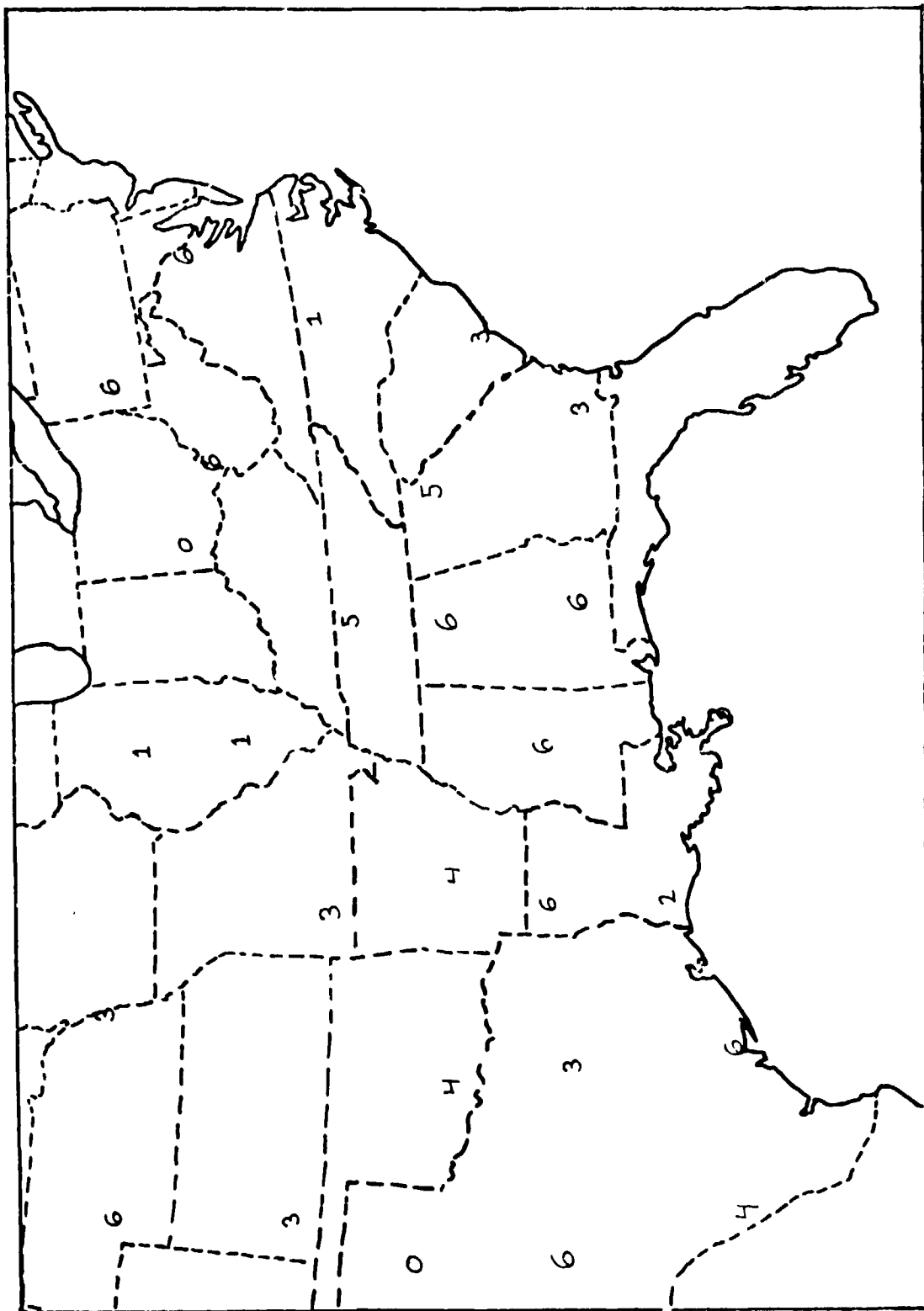


Figure 24. Map at 0600 GMT April 24, 1975 for Shear Index.

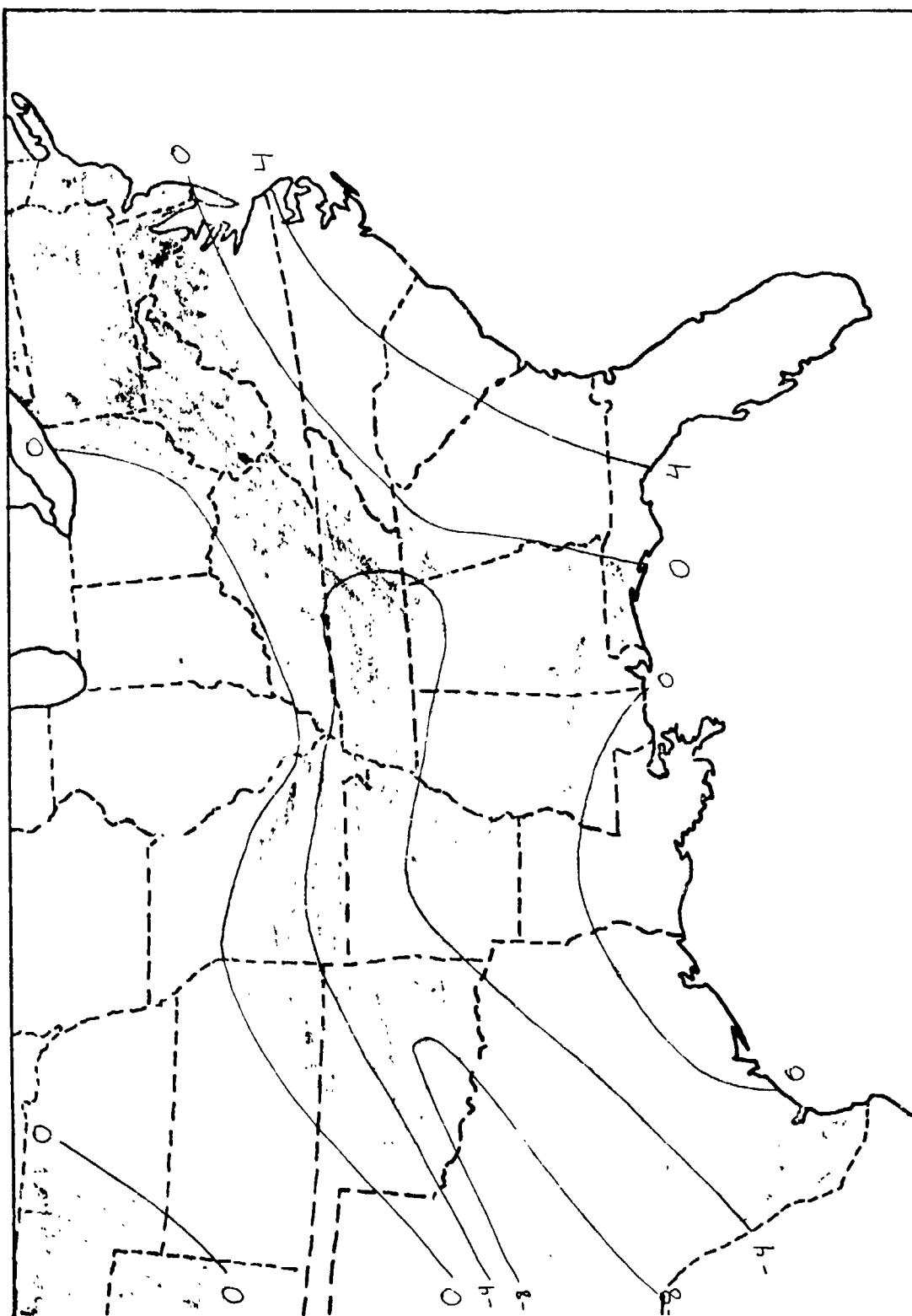


Figure 25. Map at 0600 GMT April 24, 1975 for Energy Shear Index.

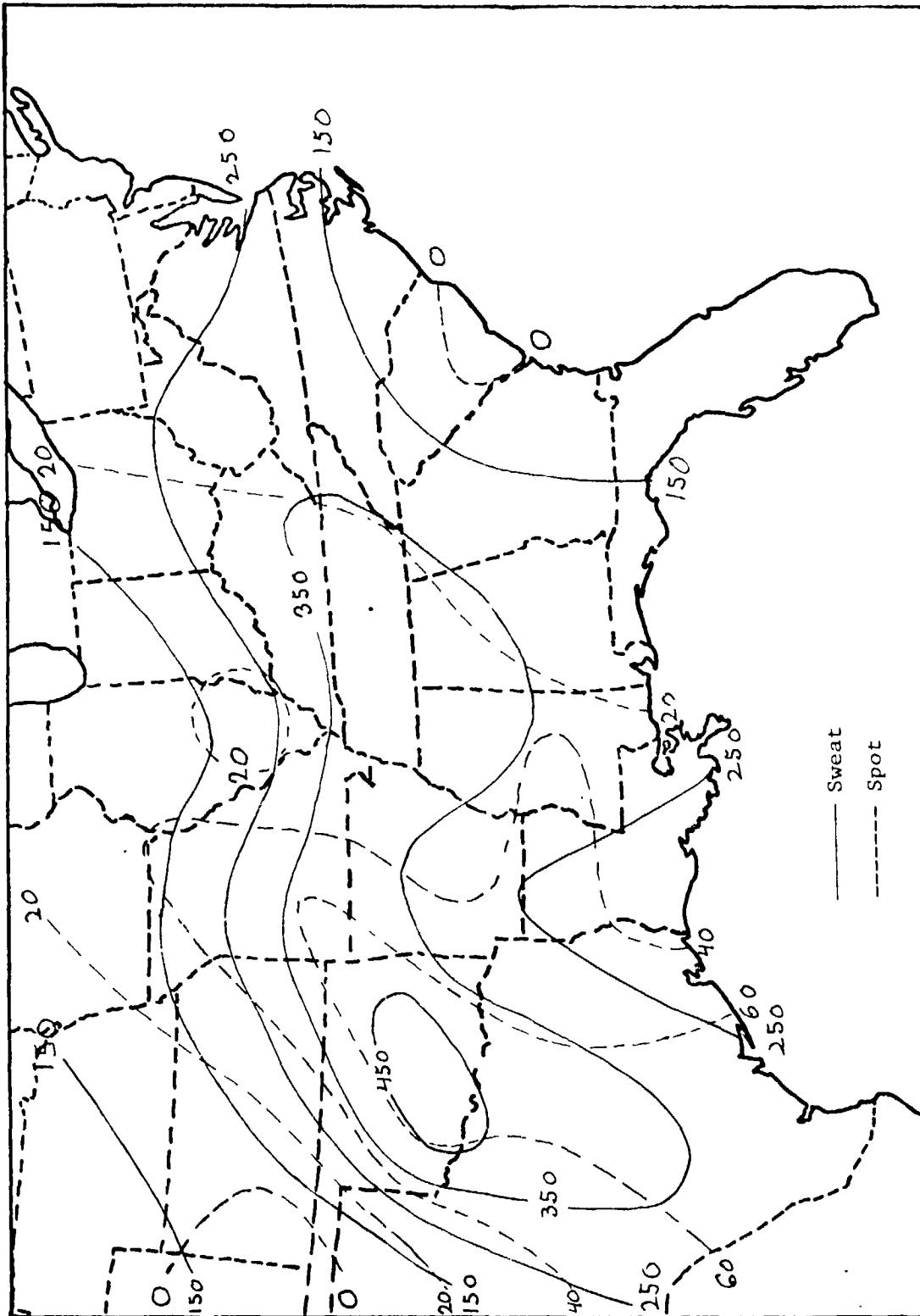


Figure 26. Map at 0600 GMT April 24, 1975 for Sweat and Spot indices.

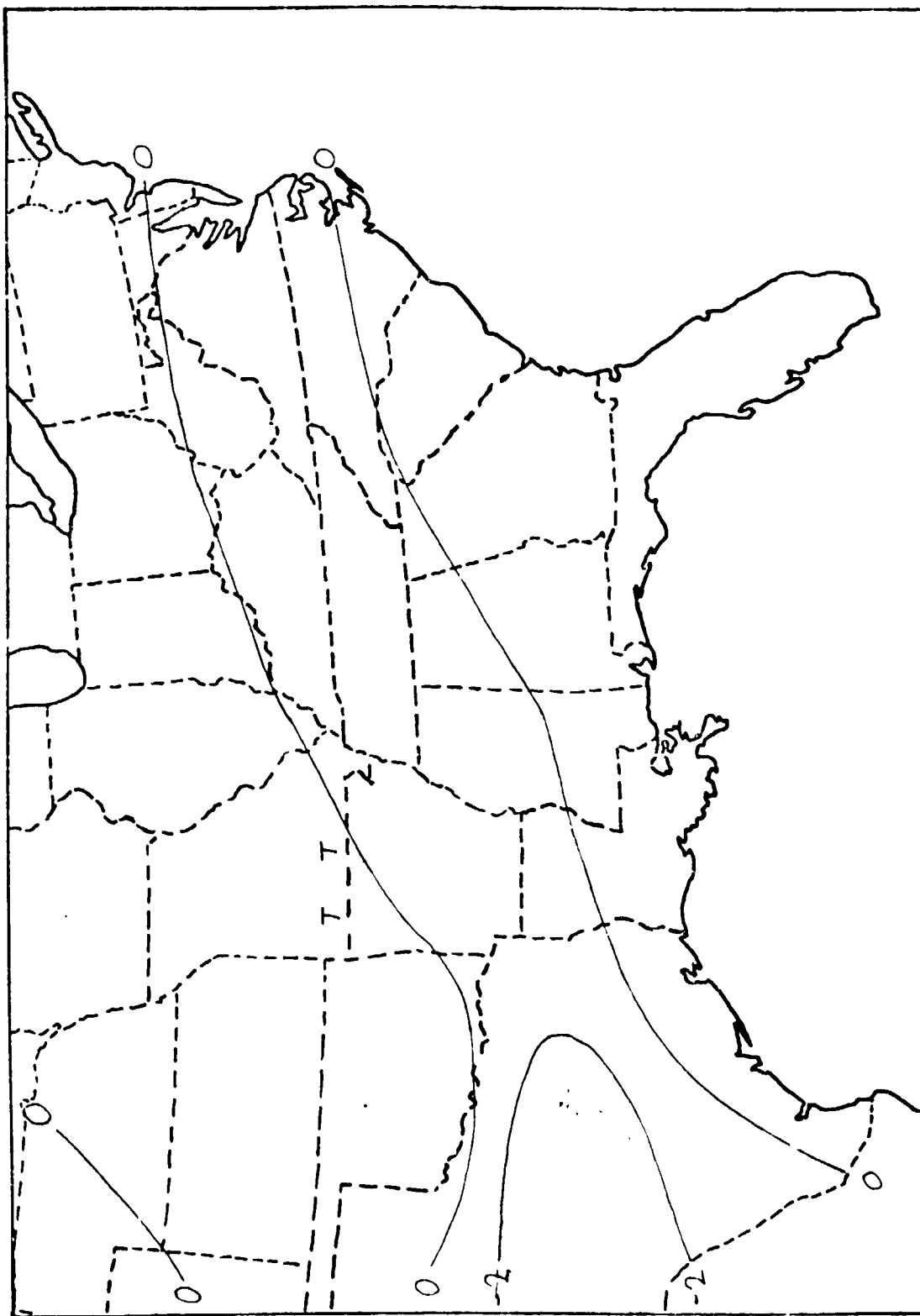


Figure 27. Map at 1200 GMT April 24, 1975 for Energy Index.

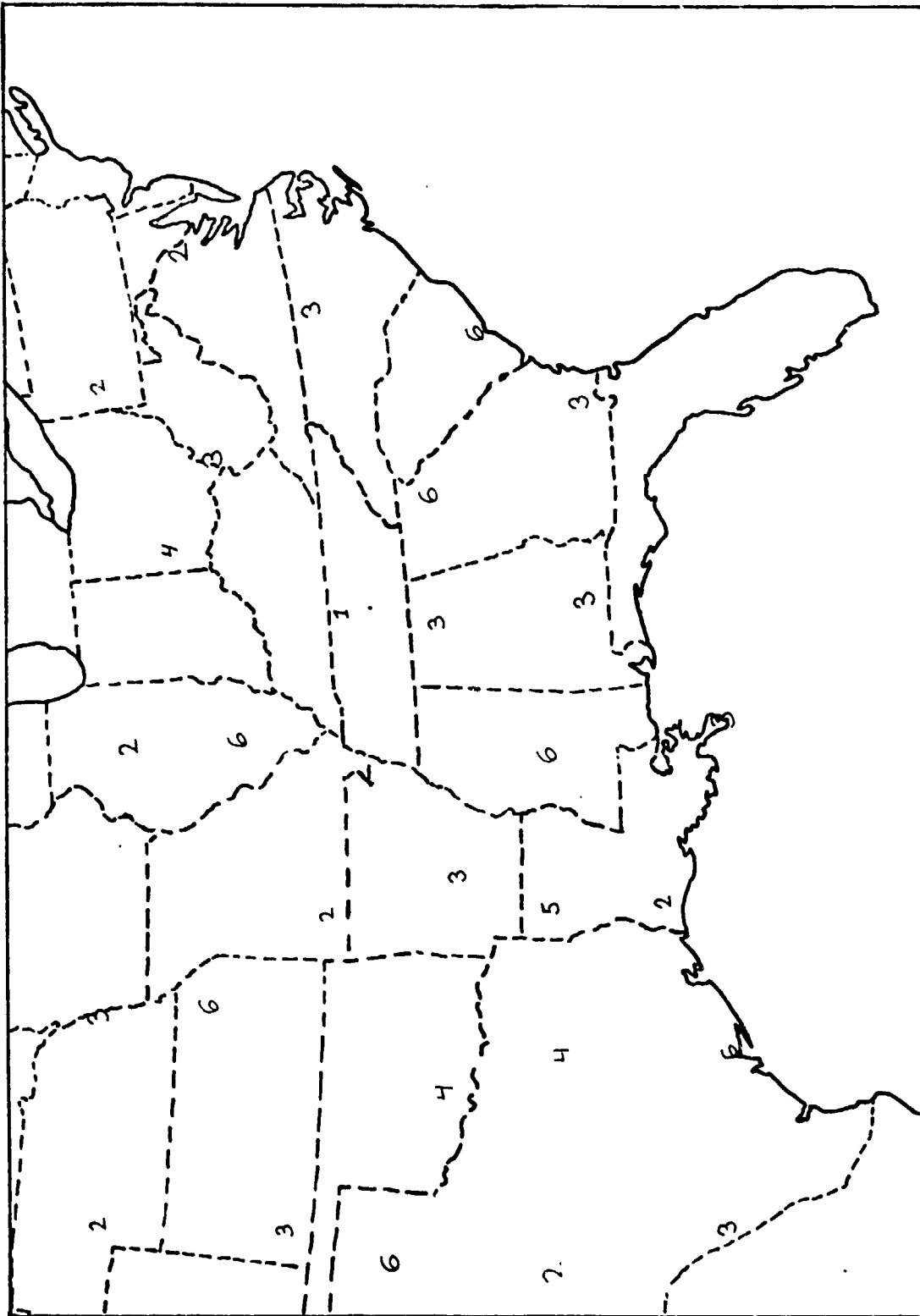


Figure 28. Map at 1200 GMT April 24, 1975 for Shear Index.

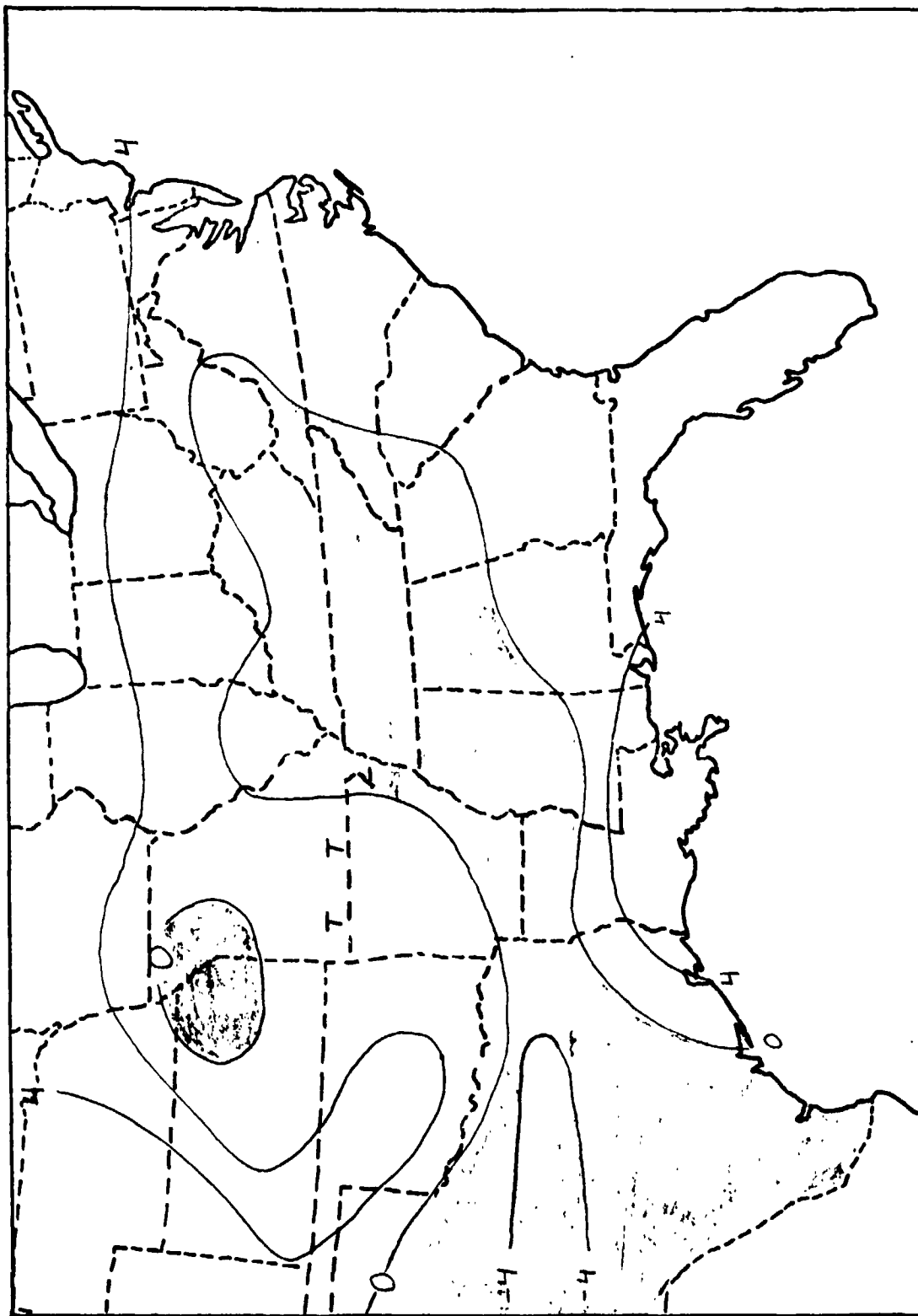


Figure 29. Map at 1200 GMT April 24, 1975 for Energy Shear Index.

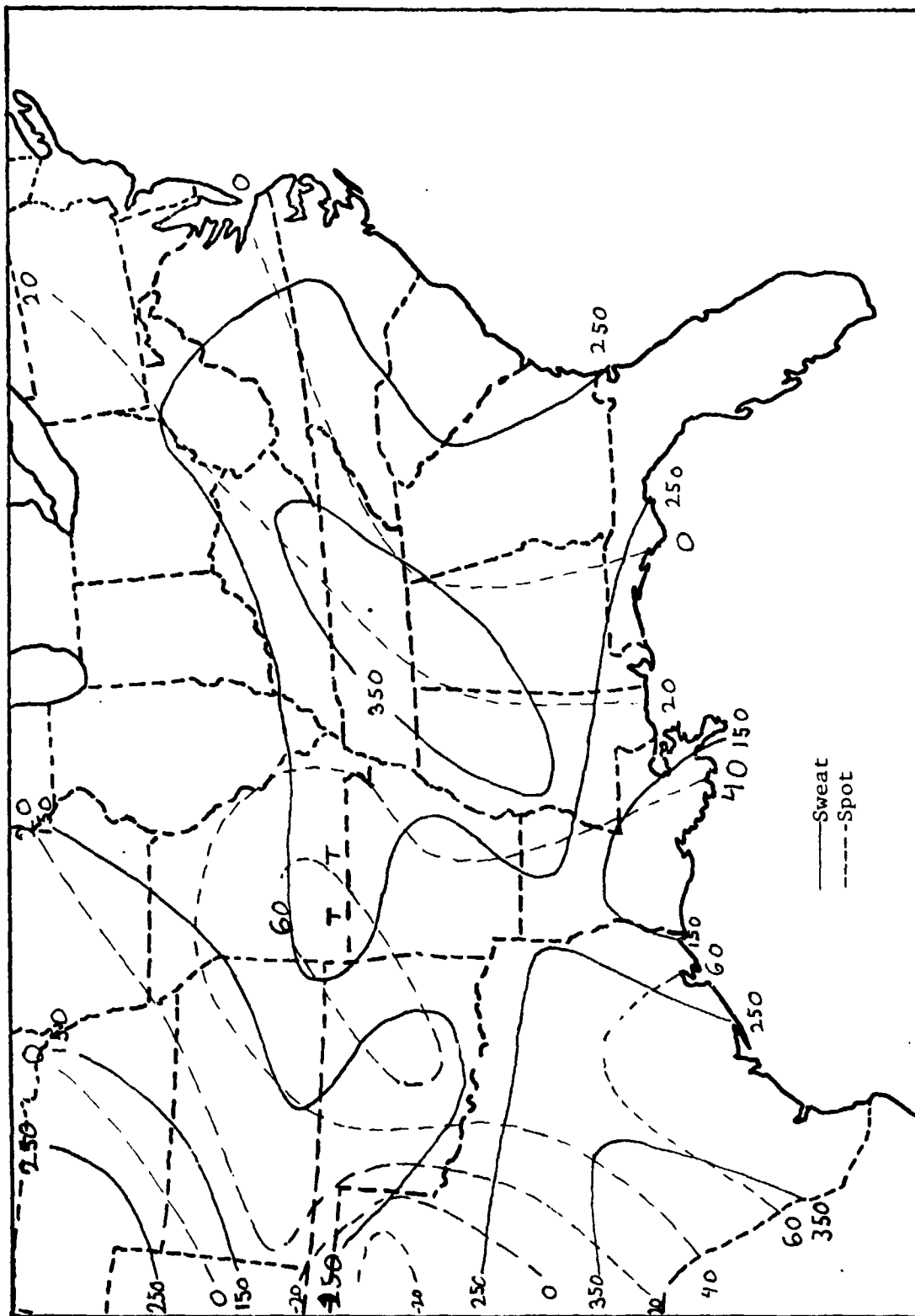


Figure 30. Map at 1200 GMT April 24, 1975 for Sweat and Spot indices.

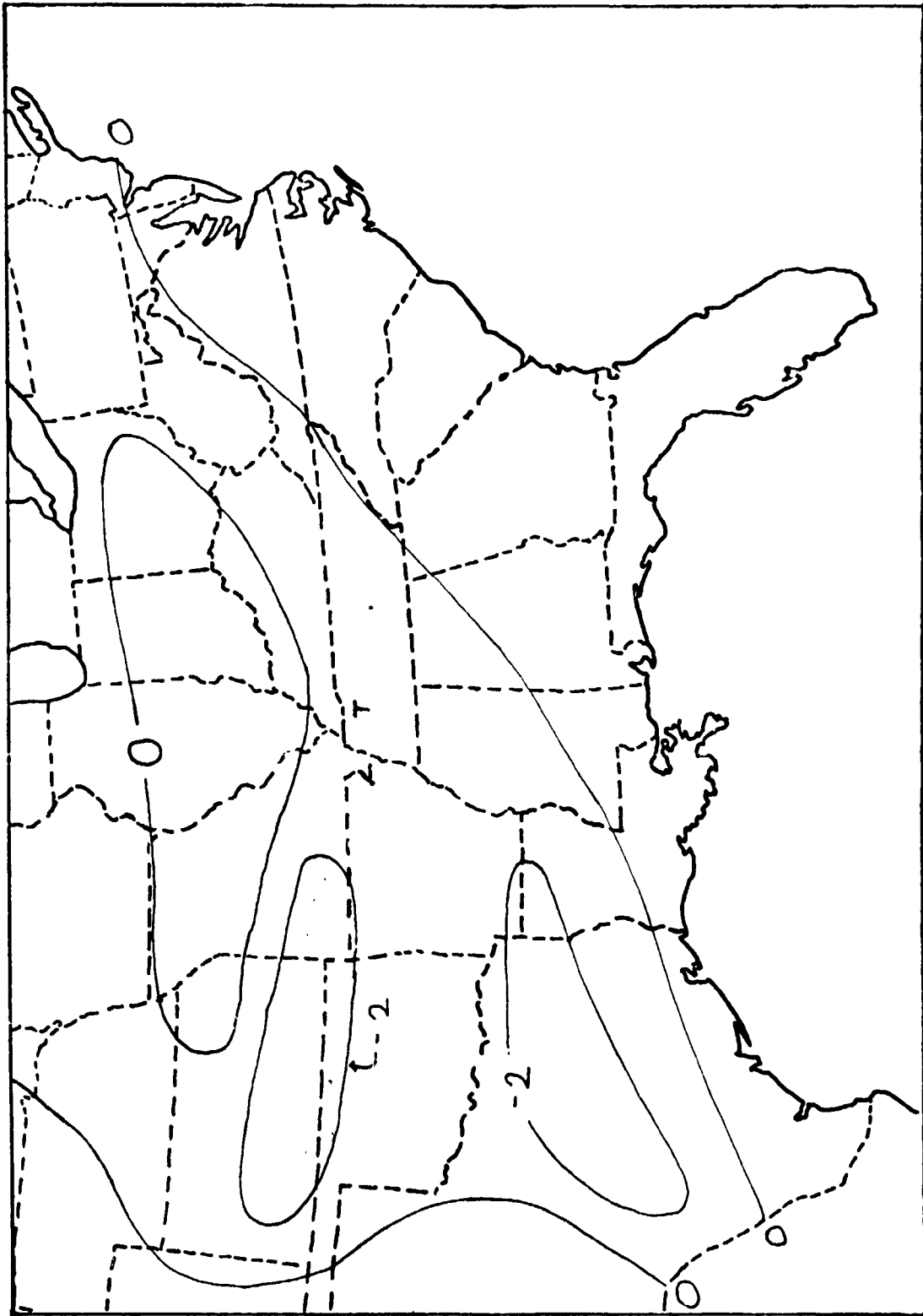


Figure 31. Map at 1500 GMT April 24, 1975 for Energy Index.

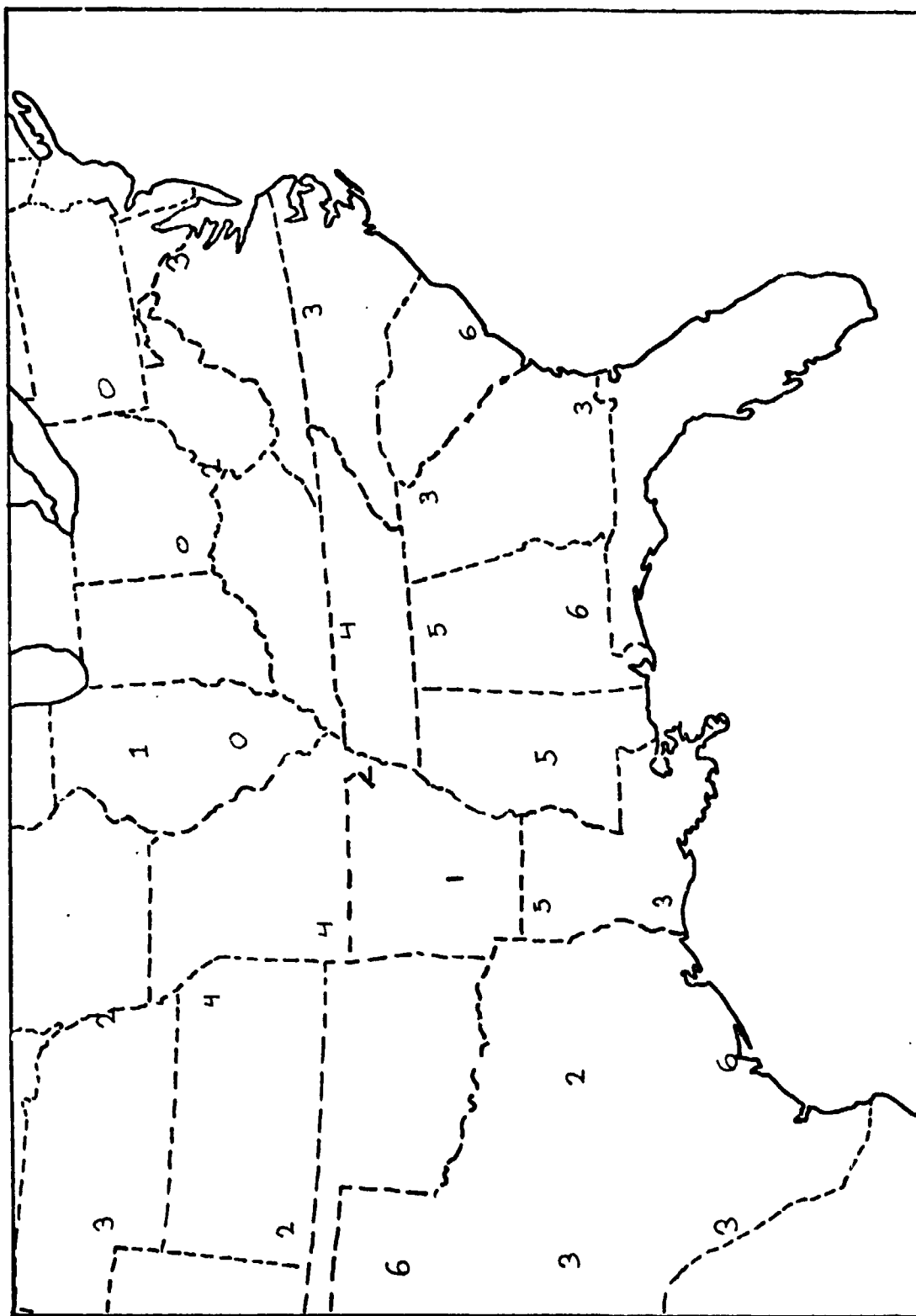


Figure 32. Map at 1500 GMT April 24, 1975 for Shear Index.

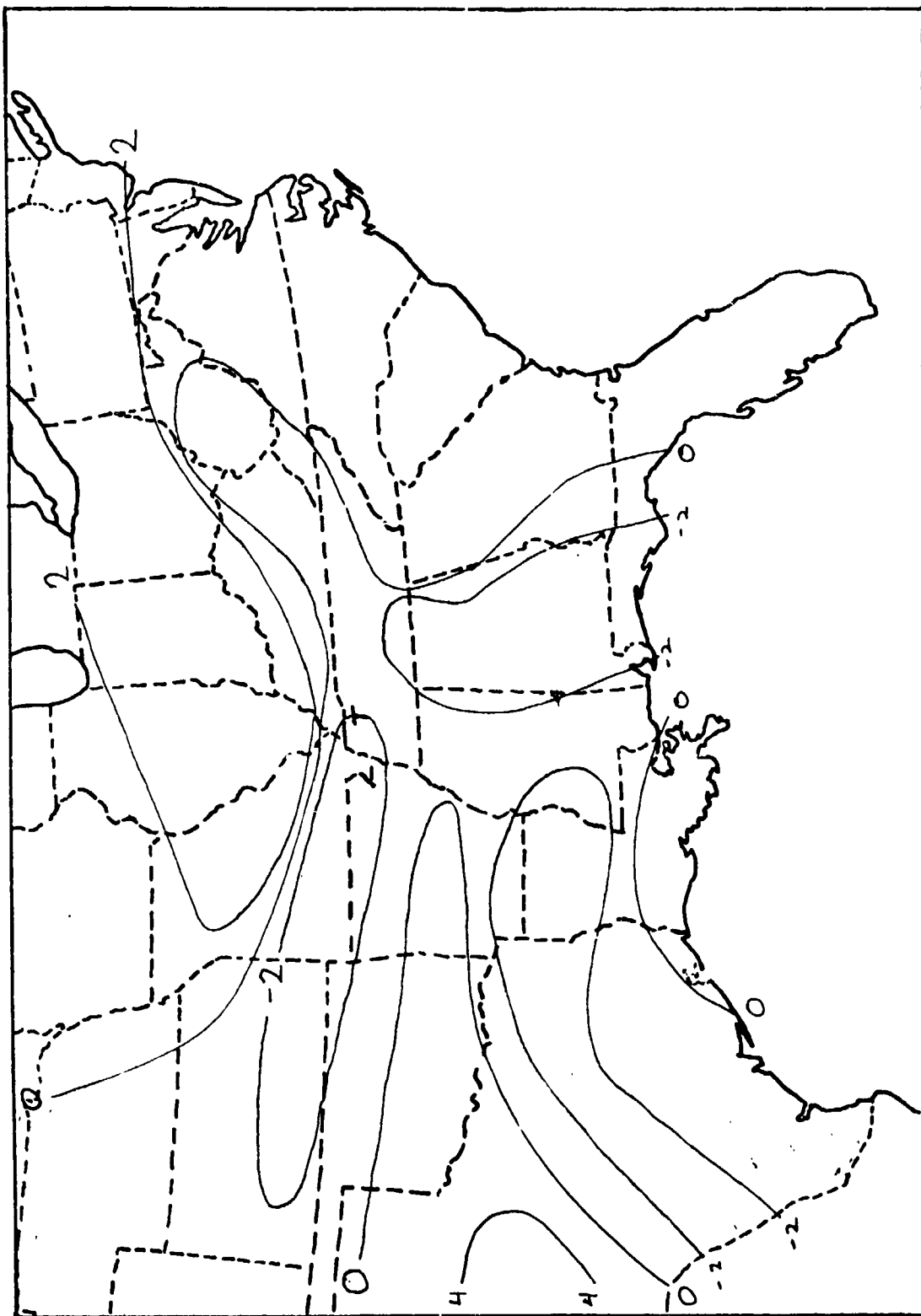


Figure 33. Map at 1500 GMT April 24, 1975 for Energy Shear Index.

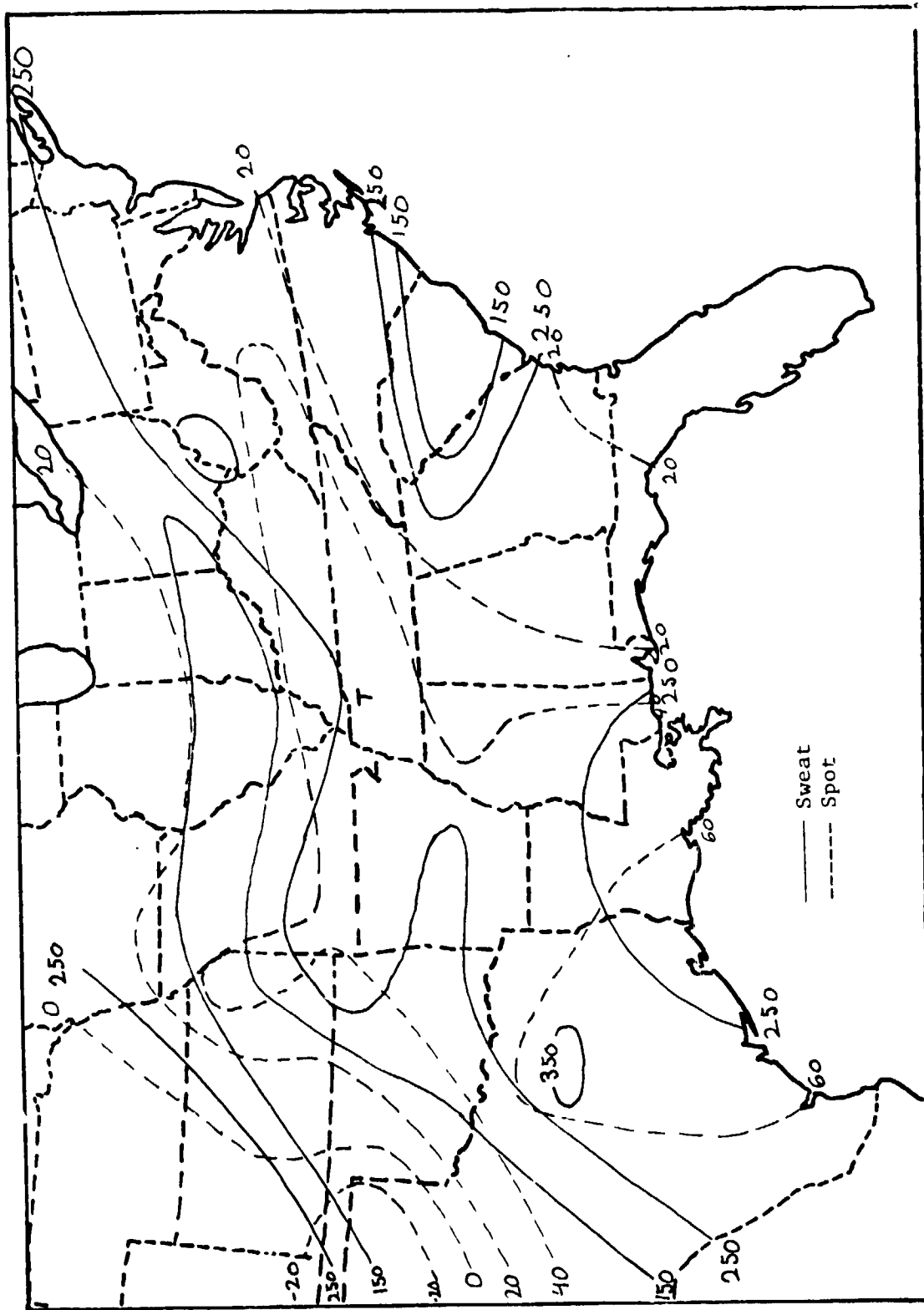


Figure 34. Map at 1500 GMT April 24, 1975 for Sweat and Spot indices.

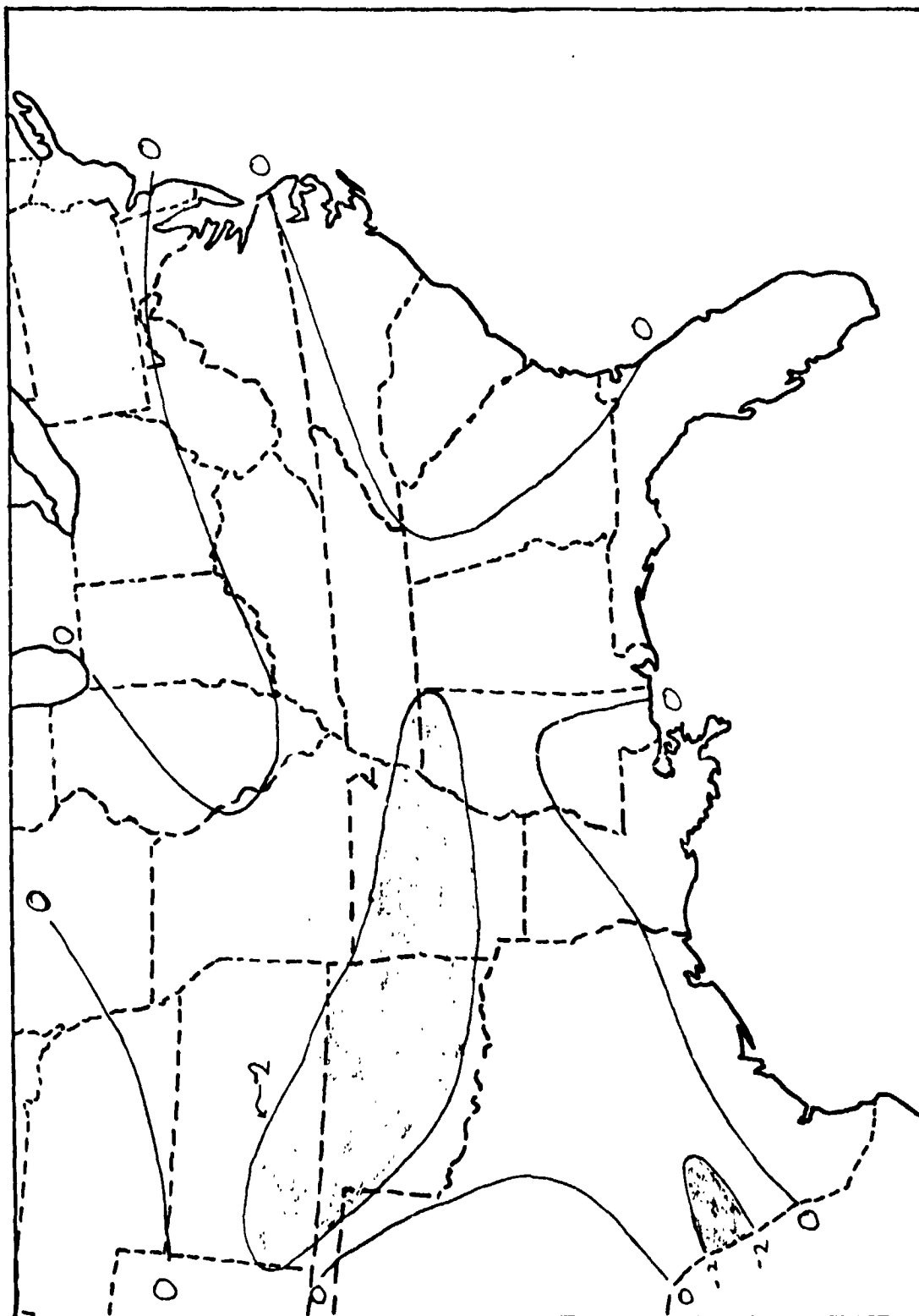


Figure 35. Map at 1800 GMT April 24, 1975 for Energy Index.

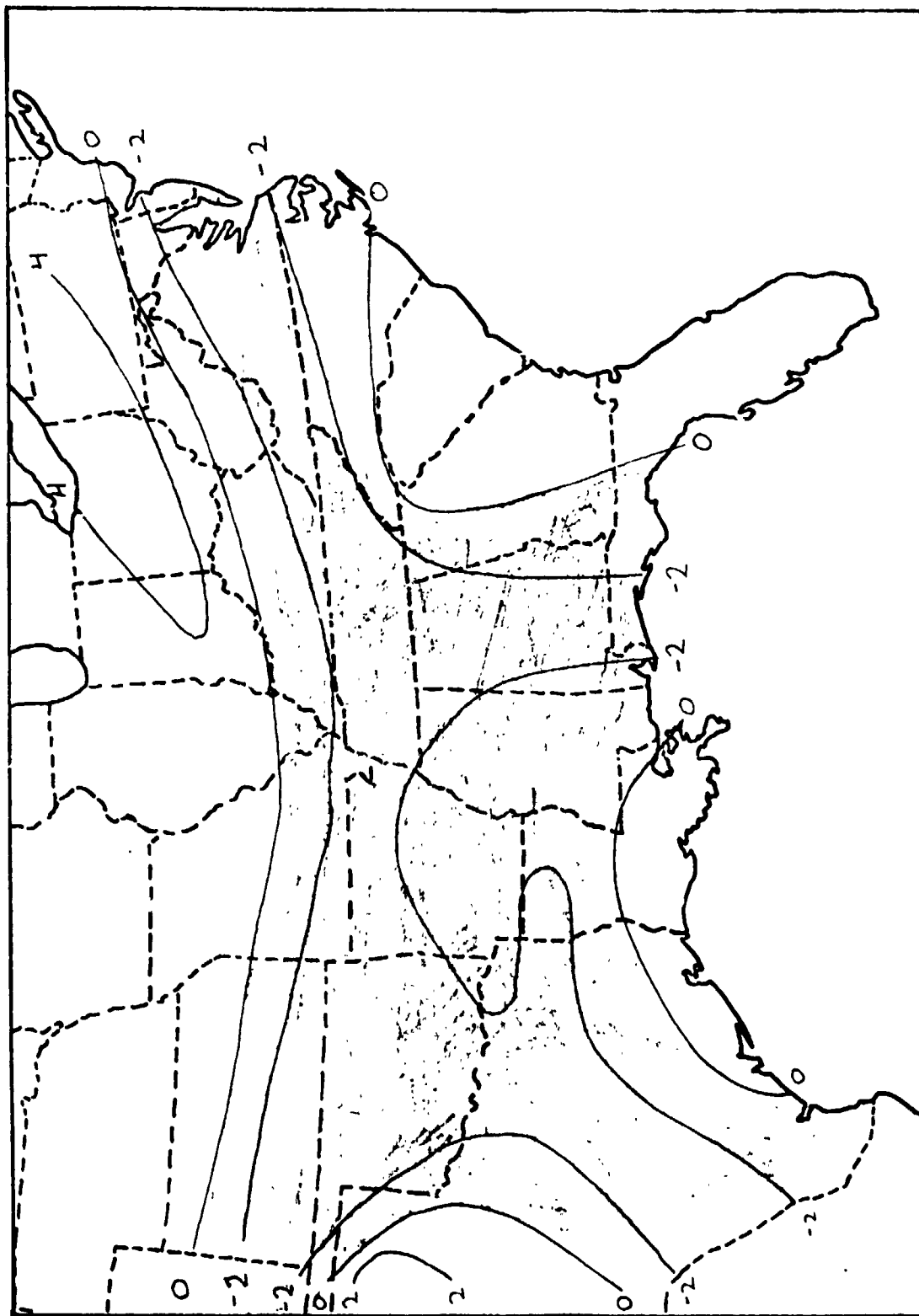


Figure 36. Map at 1800 GMT April 24, 1975 for Energy Shear Index.

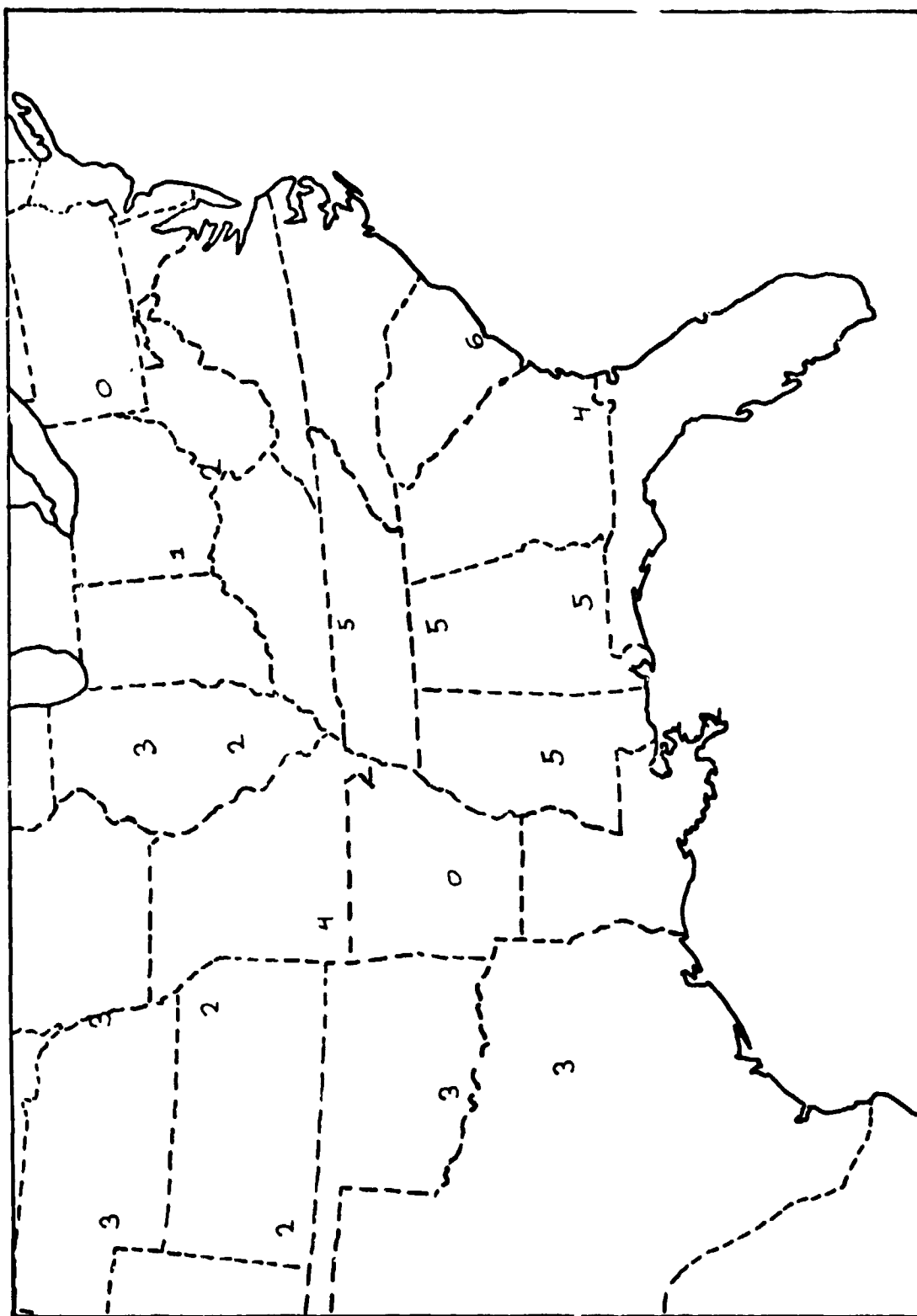


Figure 37. Map at 1800 GMT April 24, 1975 for Shear Index.

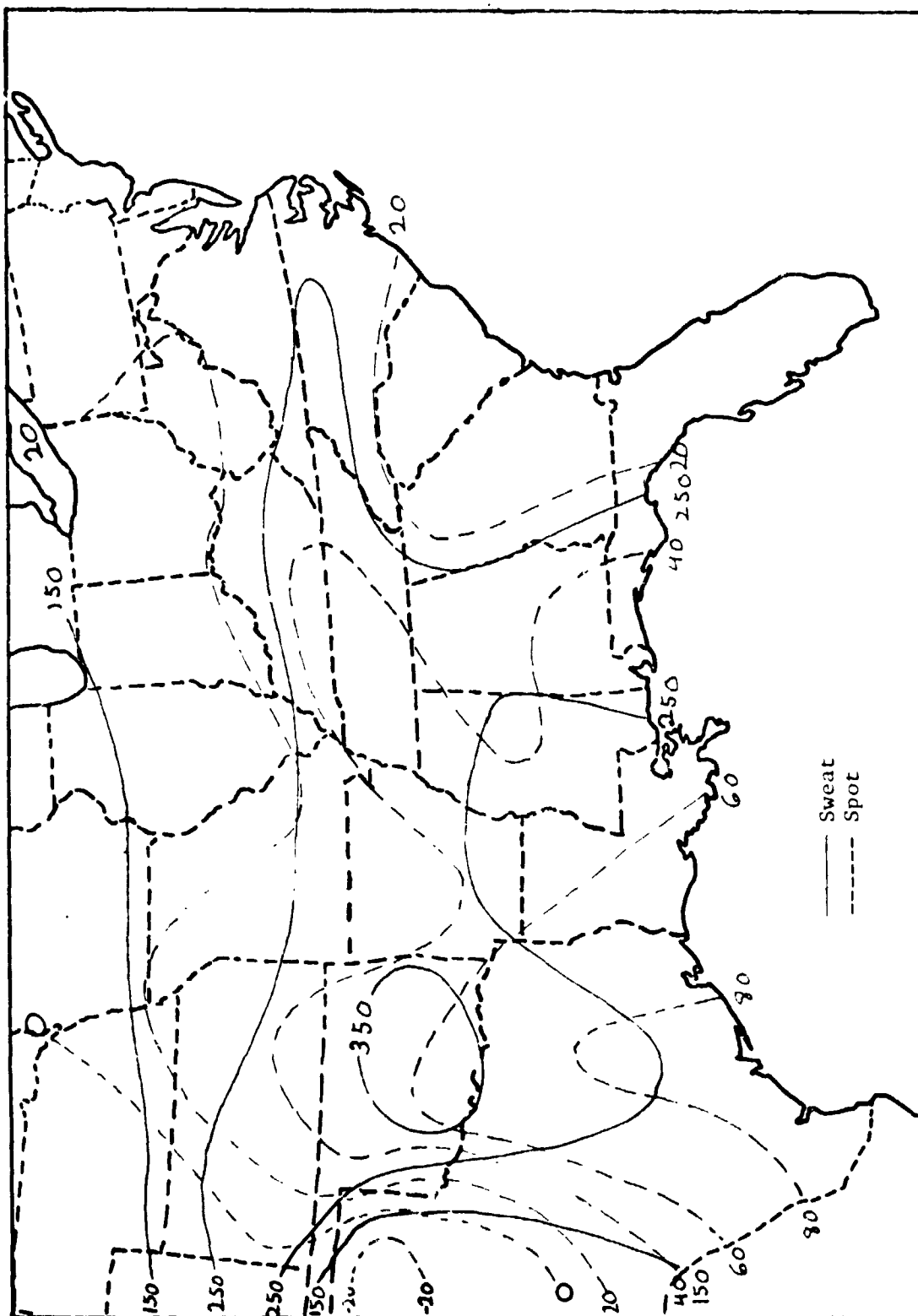


Figure 38. Map at 1800 GMT April 24, 1975 for Sweat and Spot indices.

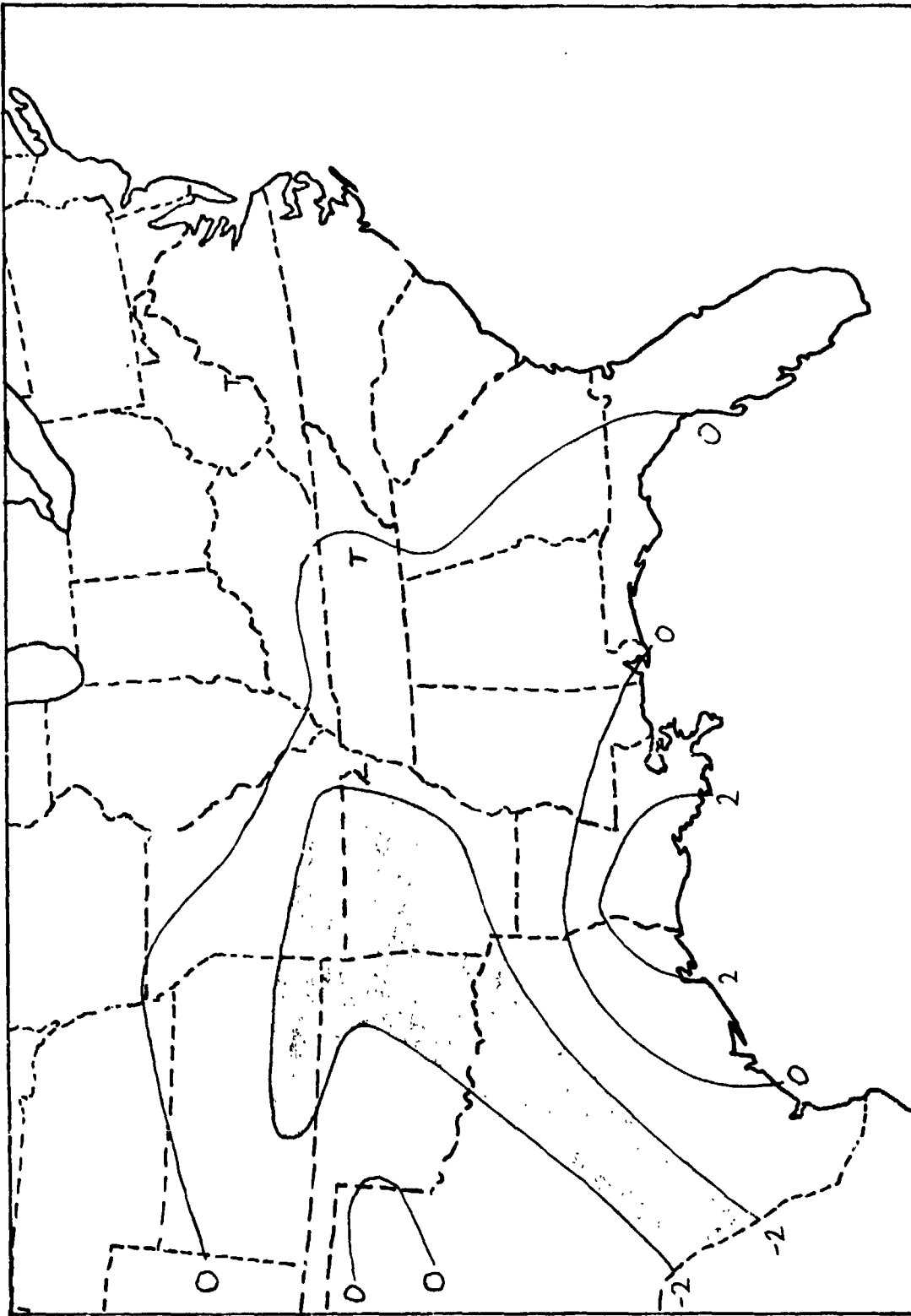


Figure 39. Map at 2100 GMT April 24, 1975 for Energy Index.

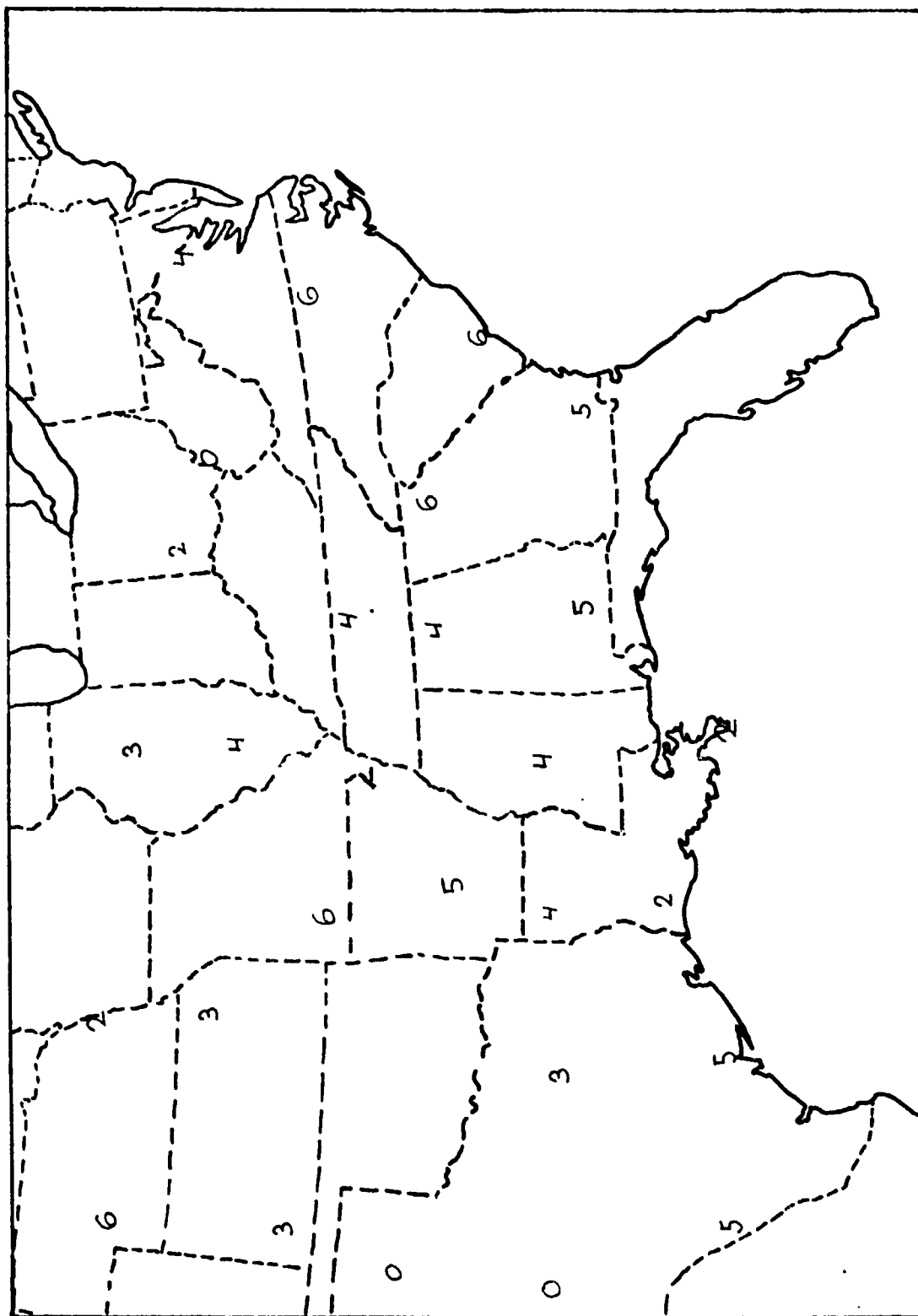


Figure 40. Map at 2100 GMT April 24, 1975 for Shear Index.

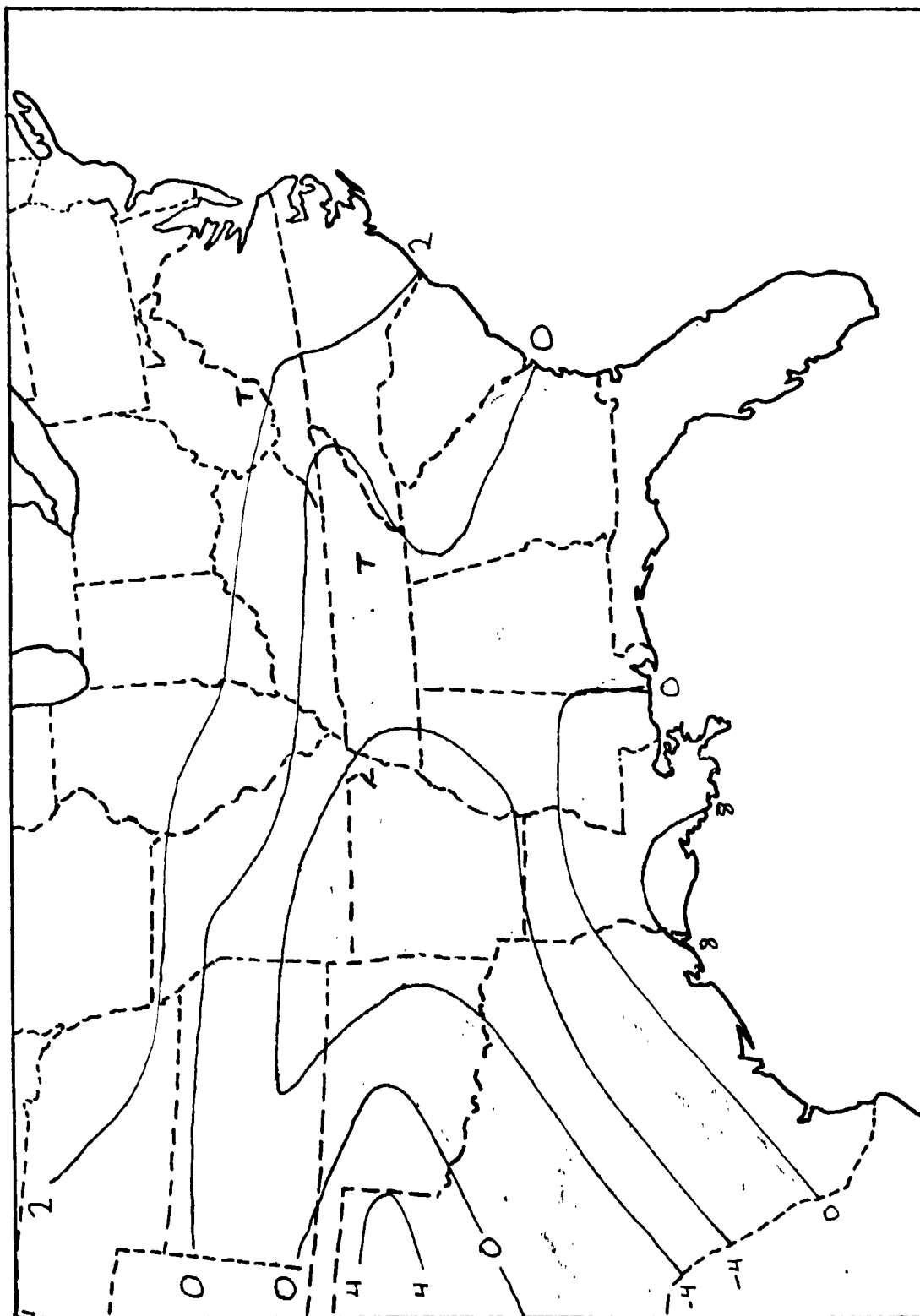


Figure 41. Map at 2:00 GMT April 24, 1975 for Energy Shear Index.

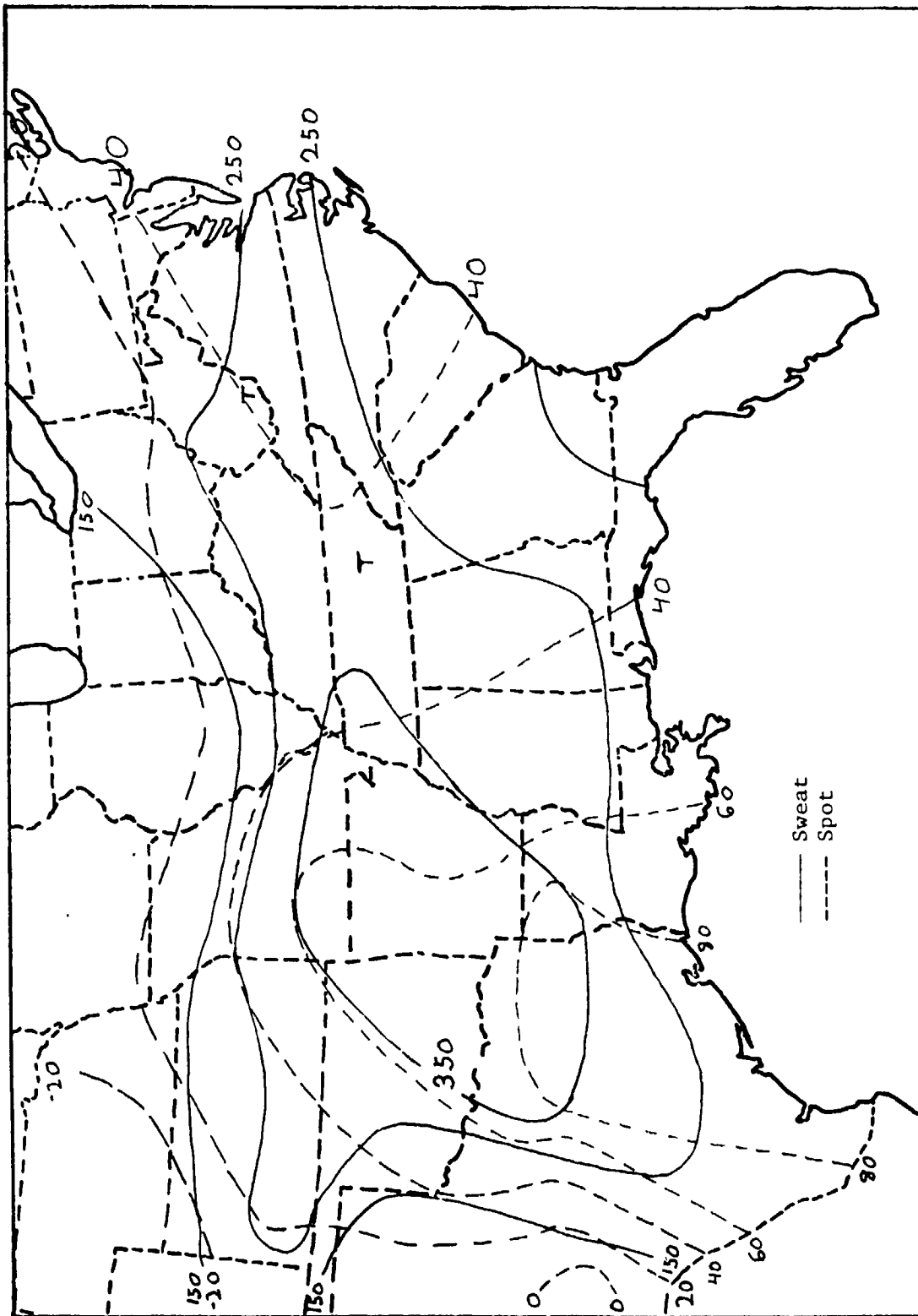


Figure 42. Map at 2100 GMT April 24, 1975 for Sweat and Spot indices.

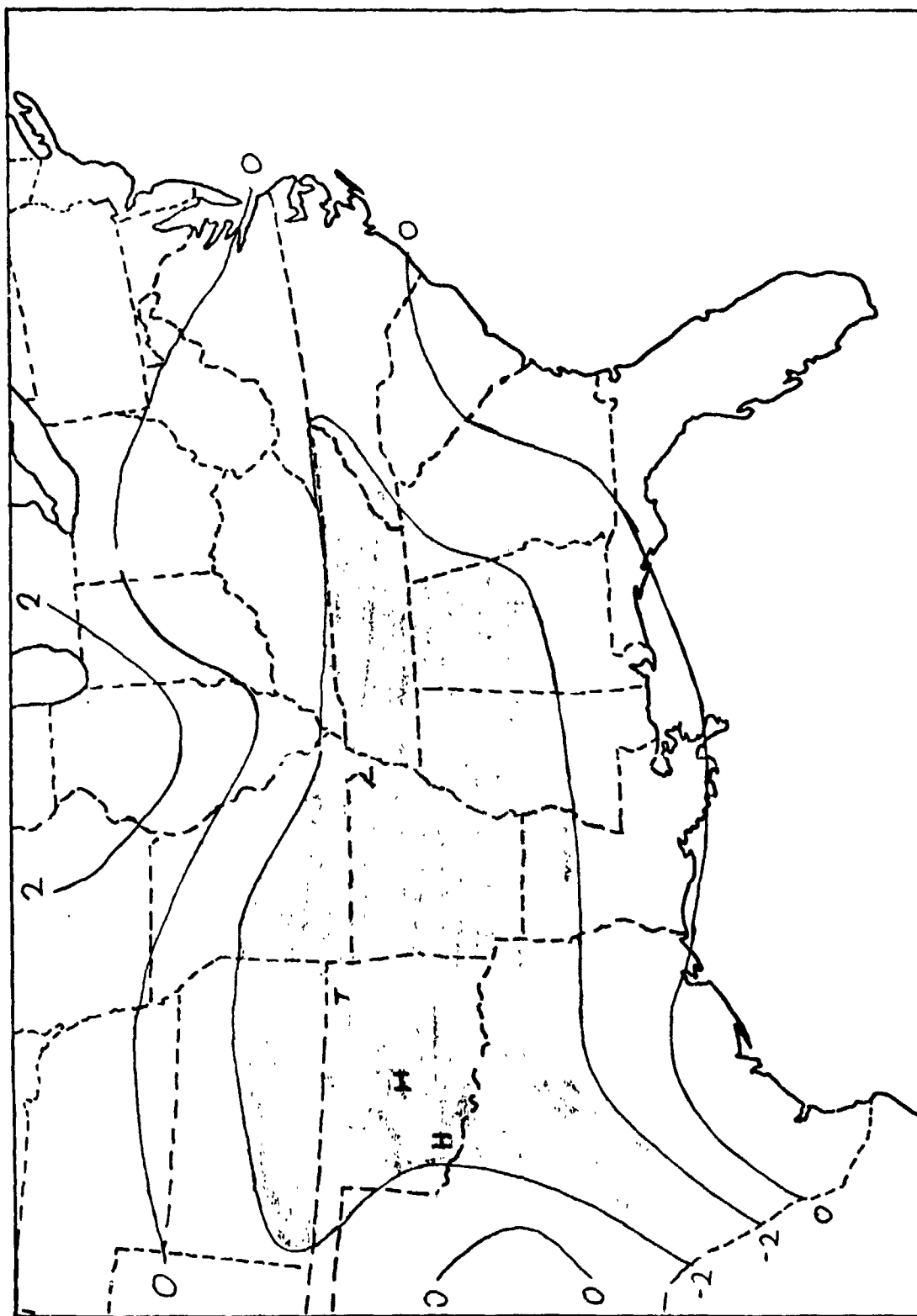


Figure 43. Map at 0000 GMT April 25, 1975 for Energy Index.

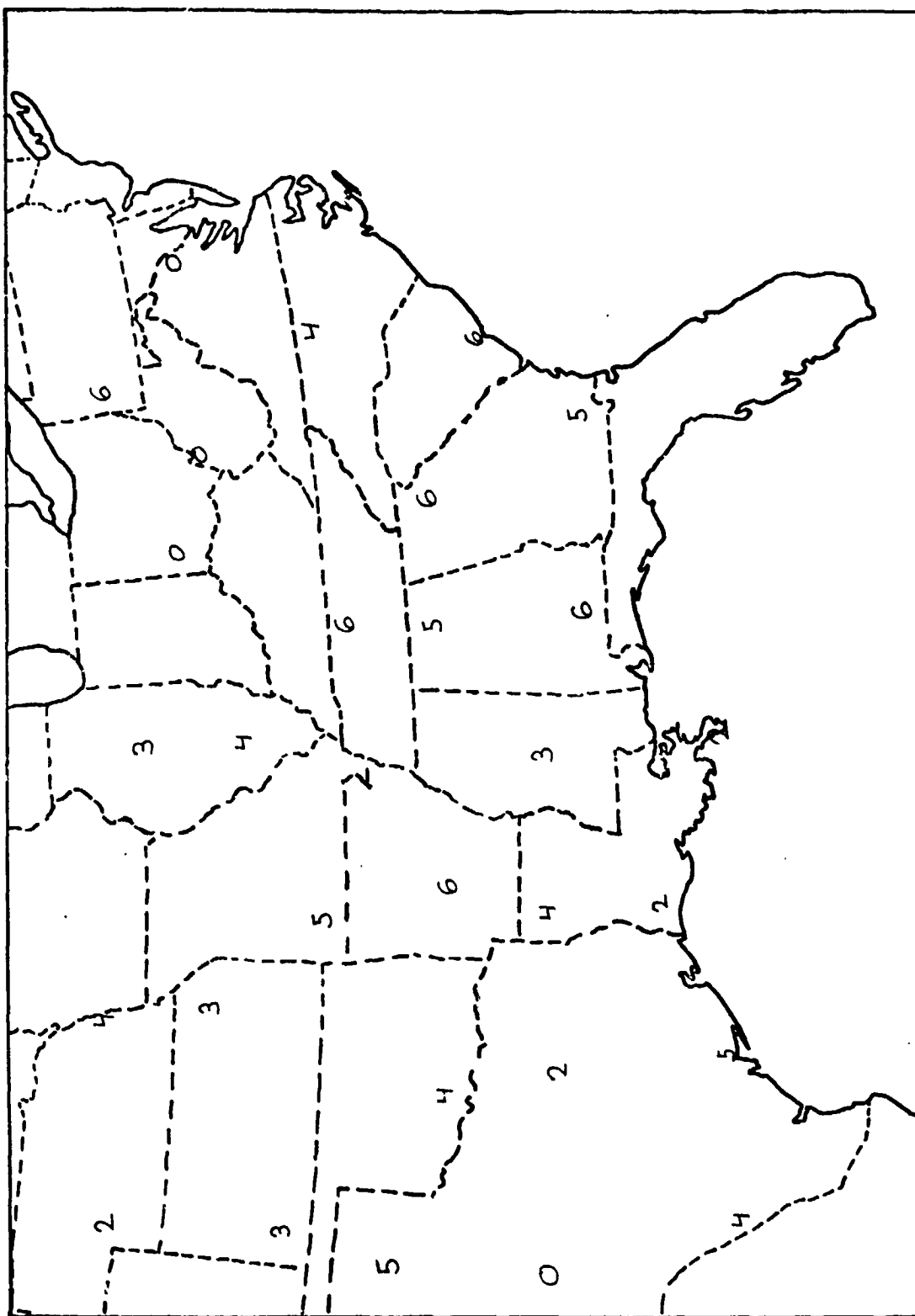


Figure 44. Map at 0000 GMT April 25, 1975 for Shear Index

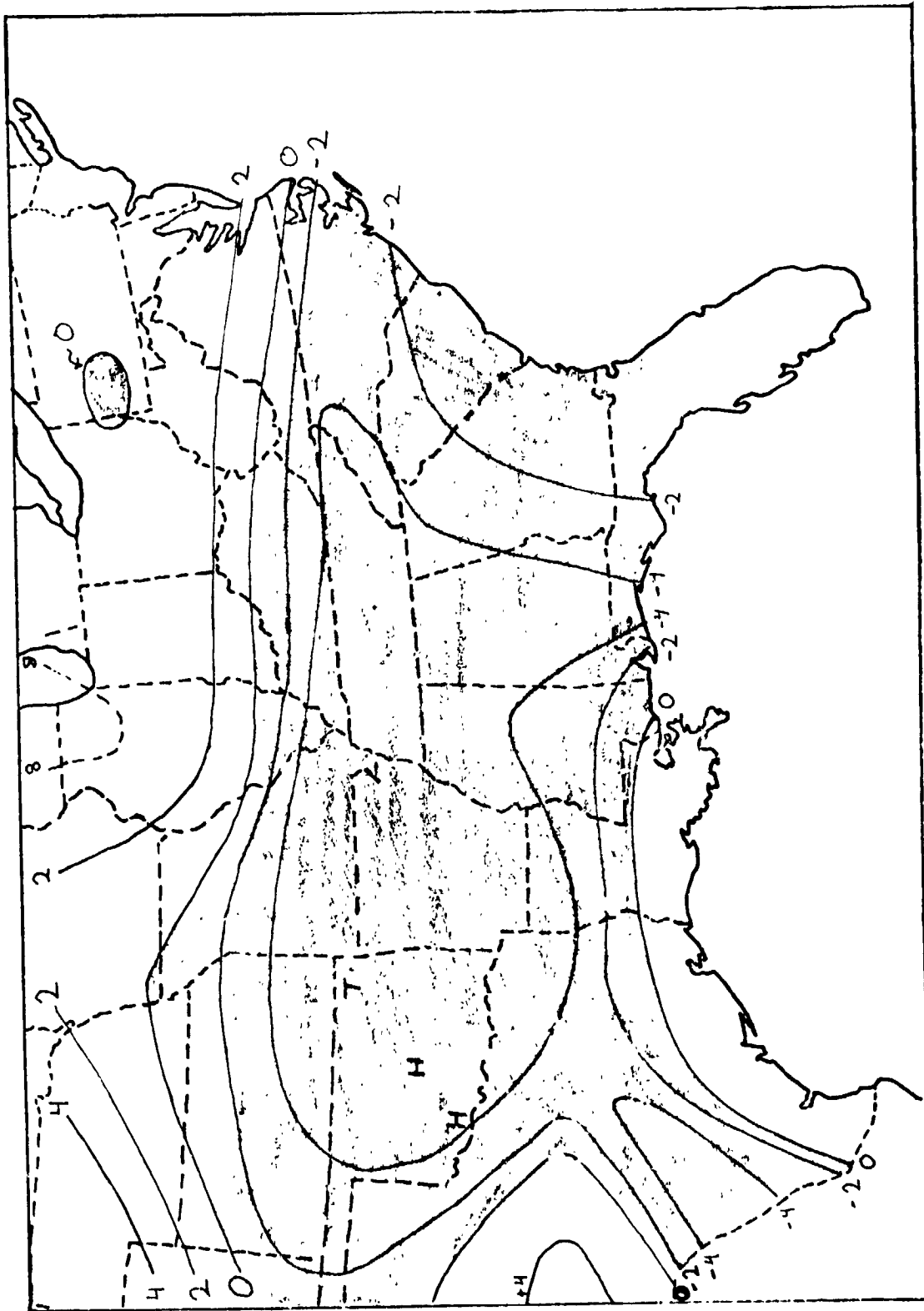


Figure 45. Map for 0000 GMT April 25, 1975 for Energy Shear Index.

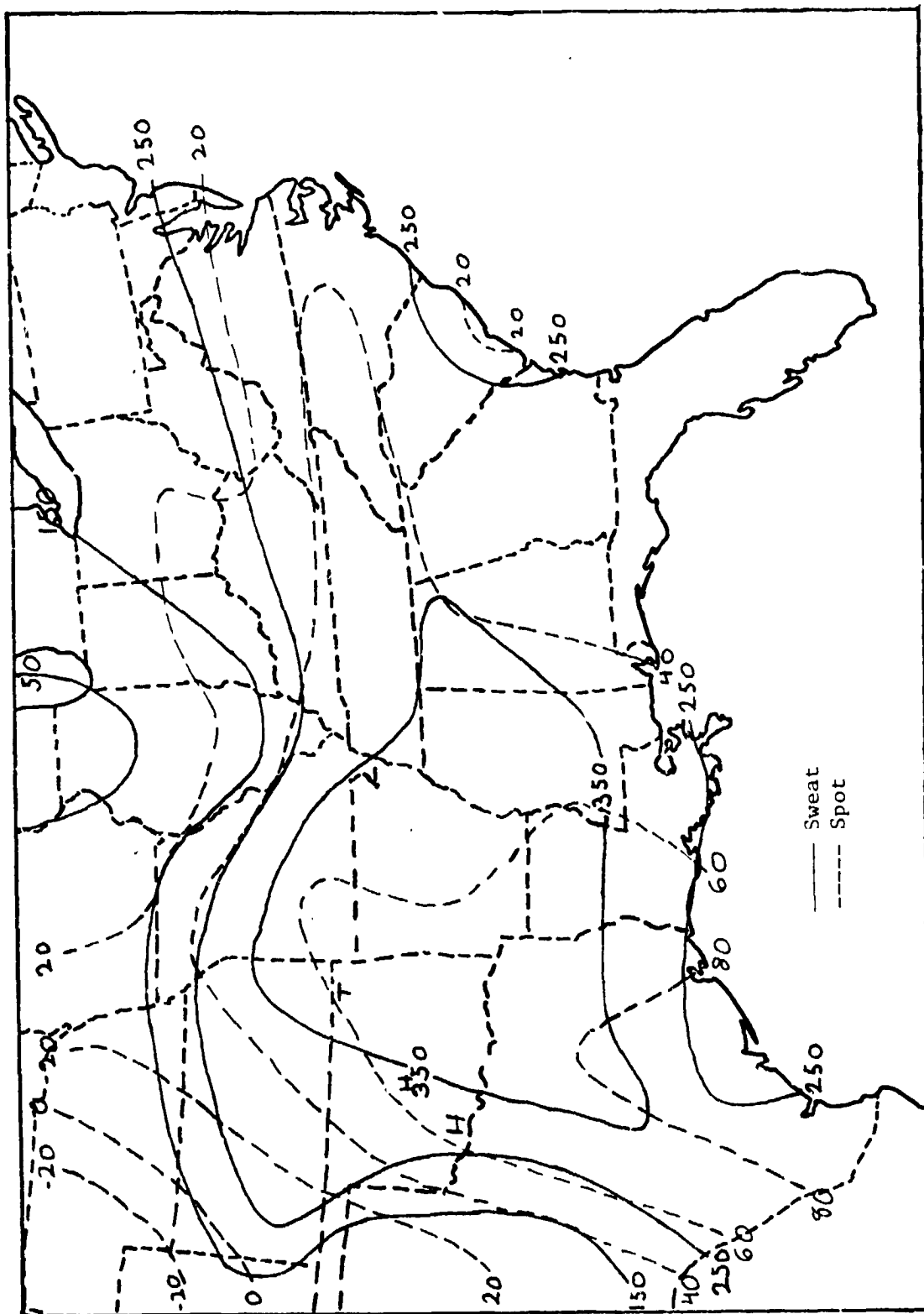


Figure 46. Map at 0000 GMT April 25, 1975 for Sweat and Spot indices.

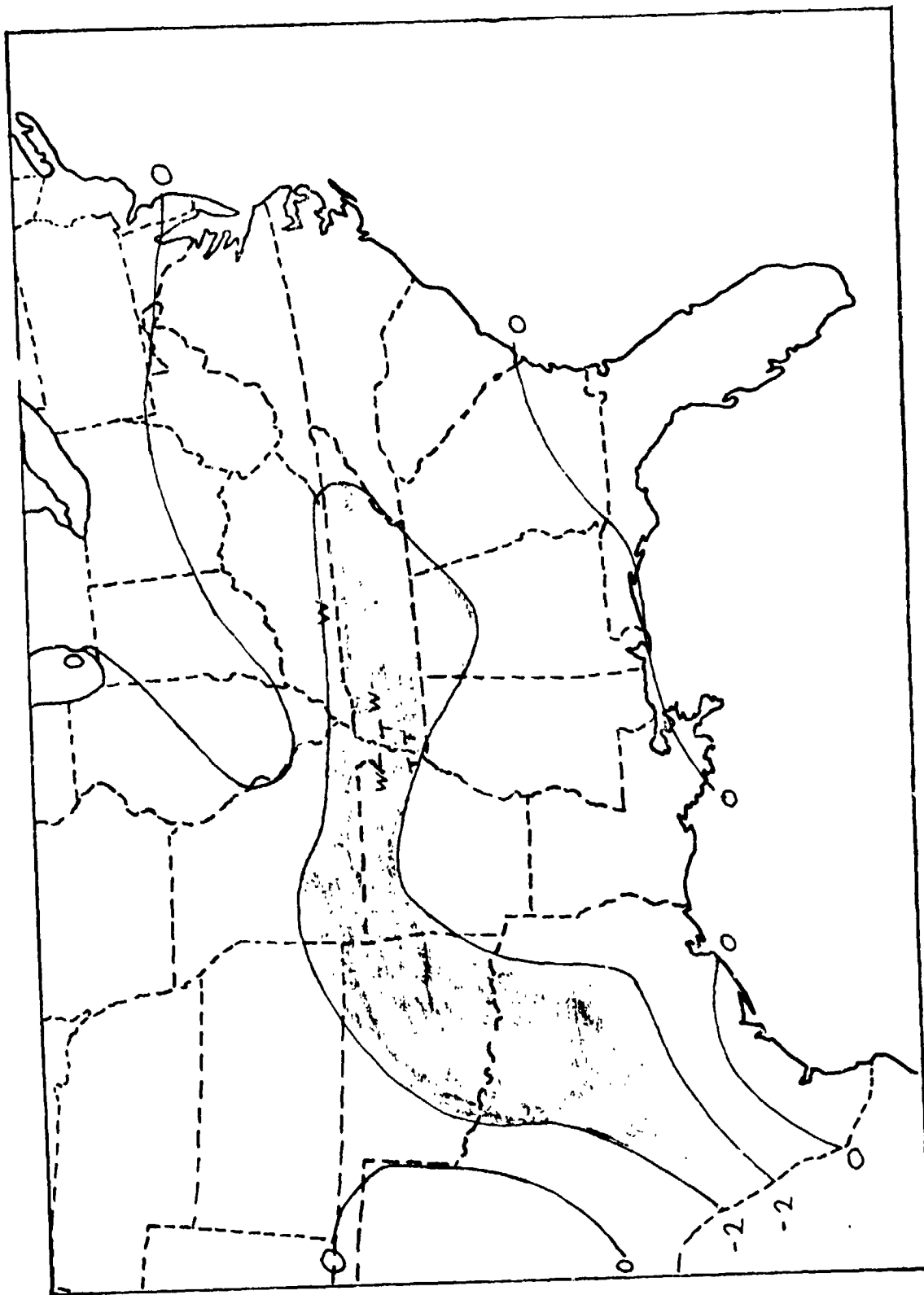


Figure 47. Map at 0600 GMT April 25, 1975 for Energy Index.

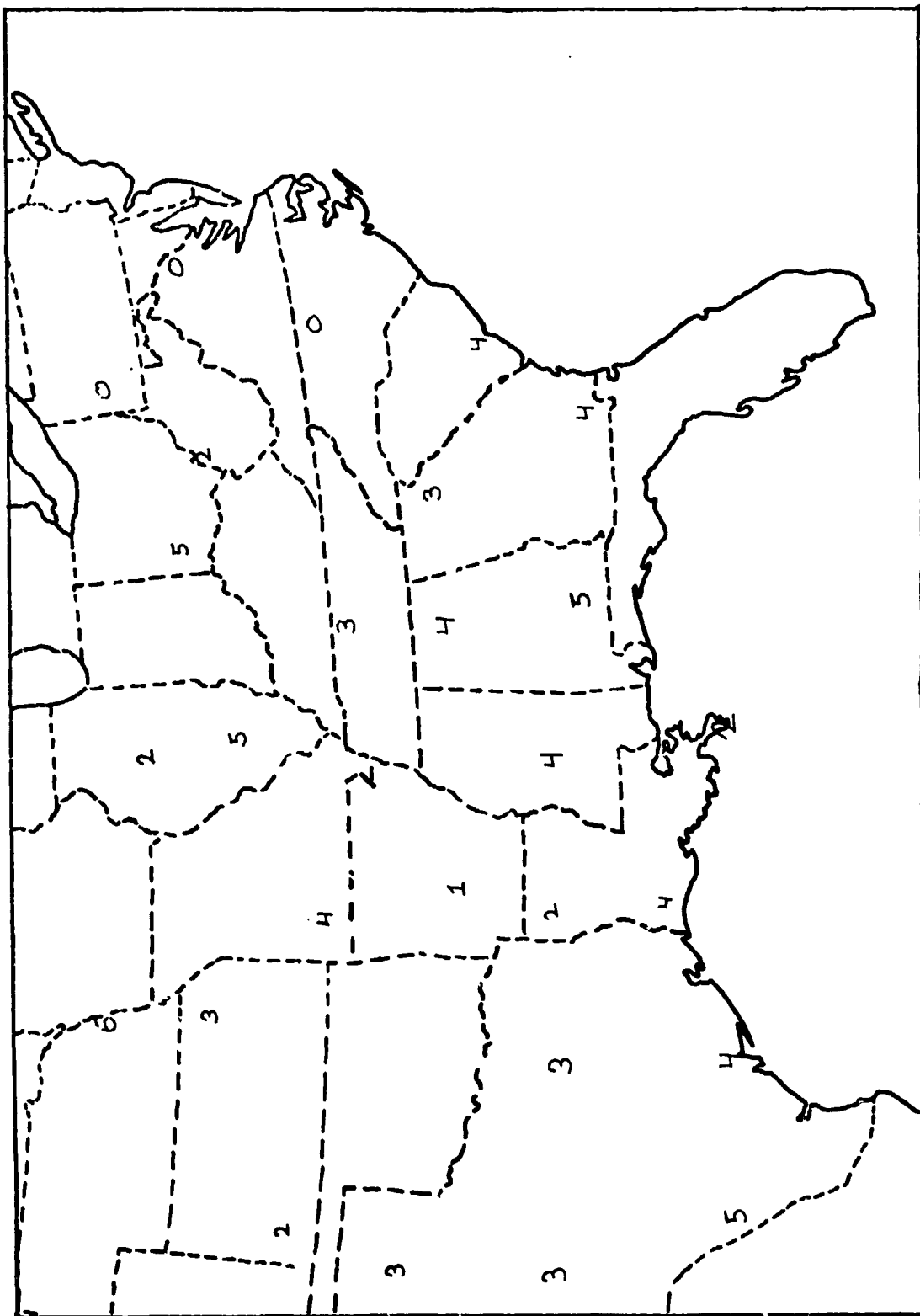


Figure 48. Map at 0600 CMT April 25, 1975 for Shear Index.

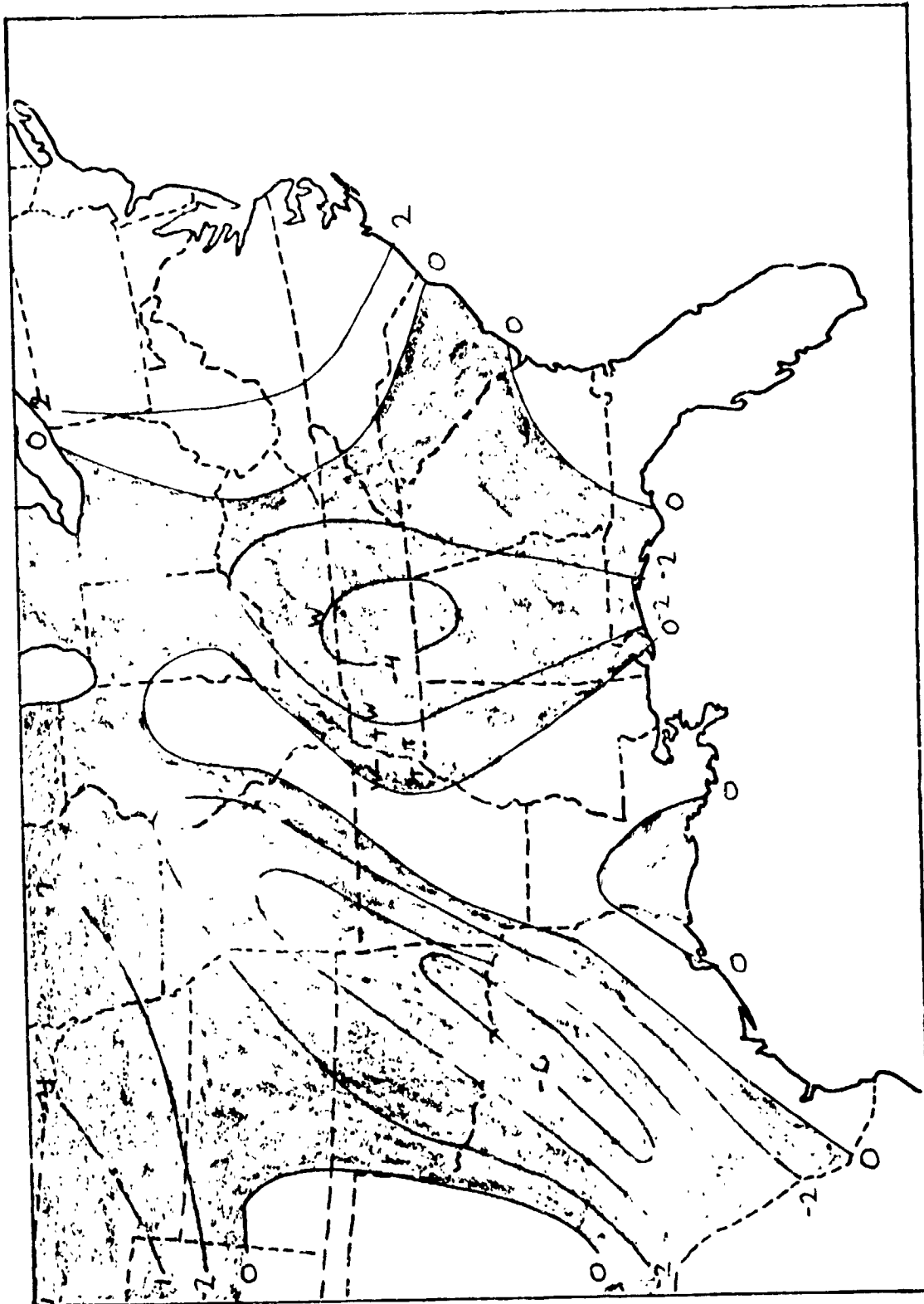


Figure 49. Map at 0600 GMT April 25, 1975 for Energy Shear Index.

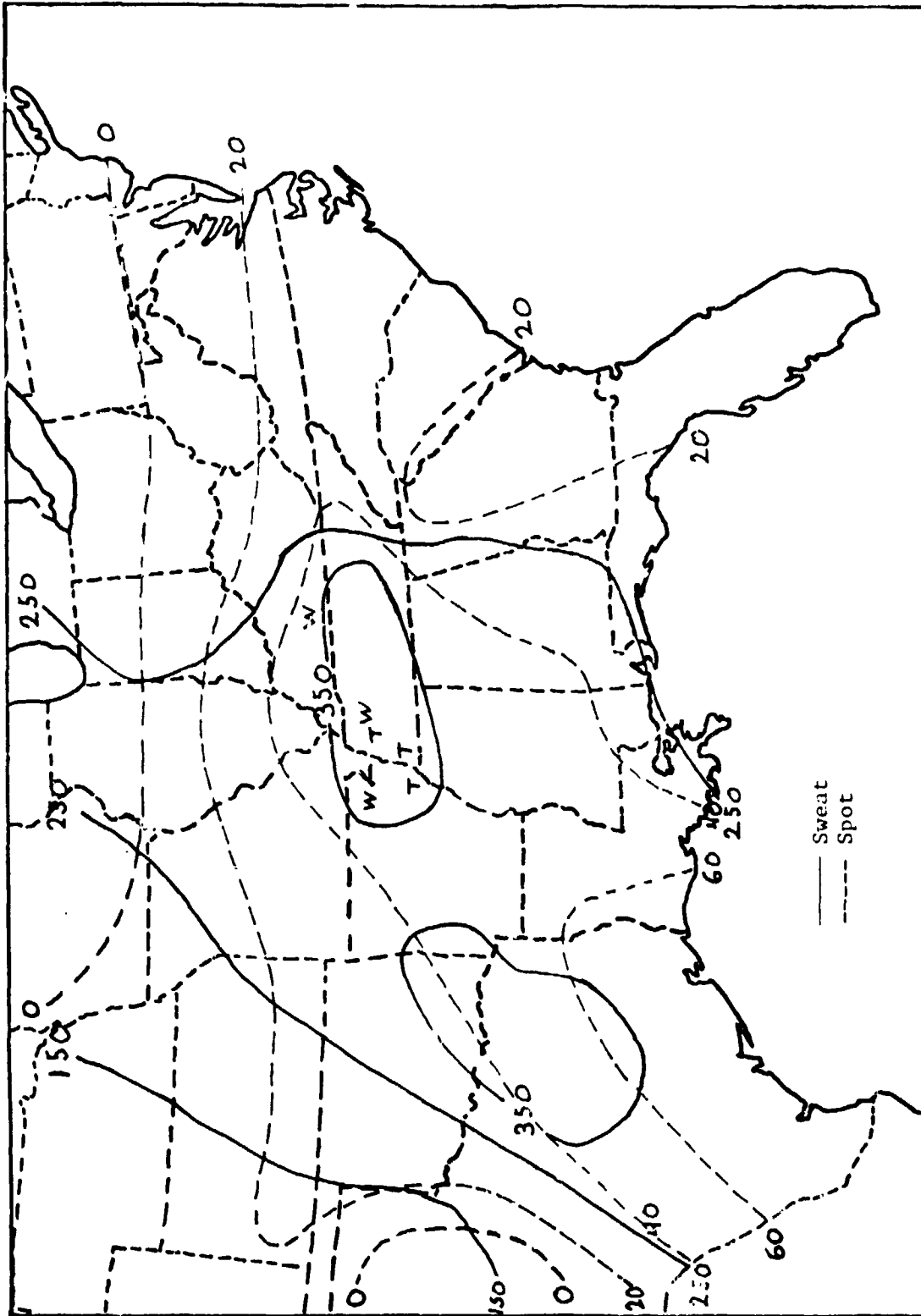


Figure 50. Map at 0600 April 25, 1975 for Sweat and Spot indices.

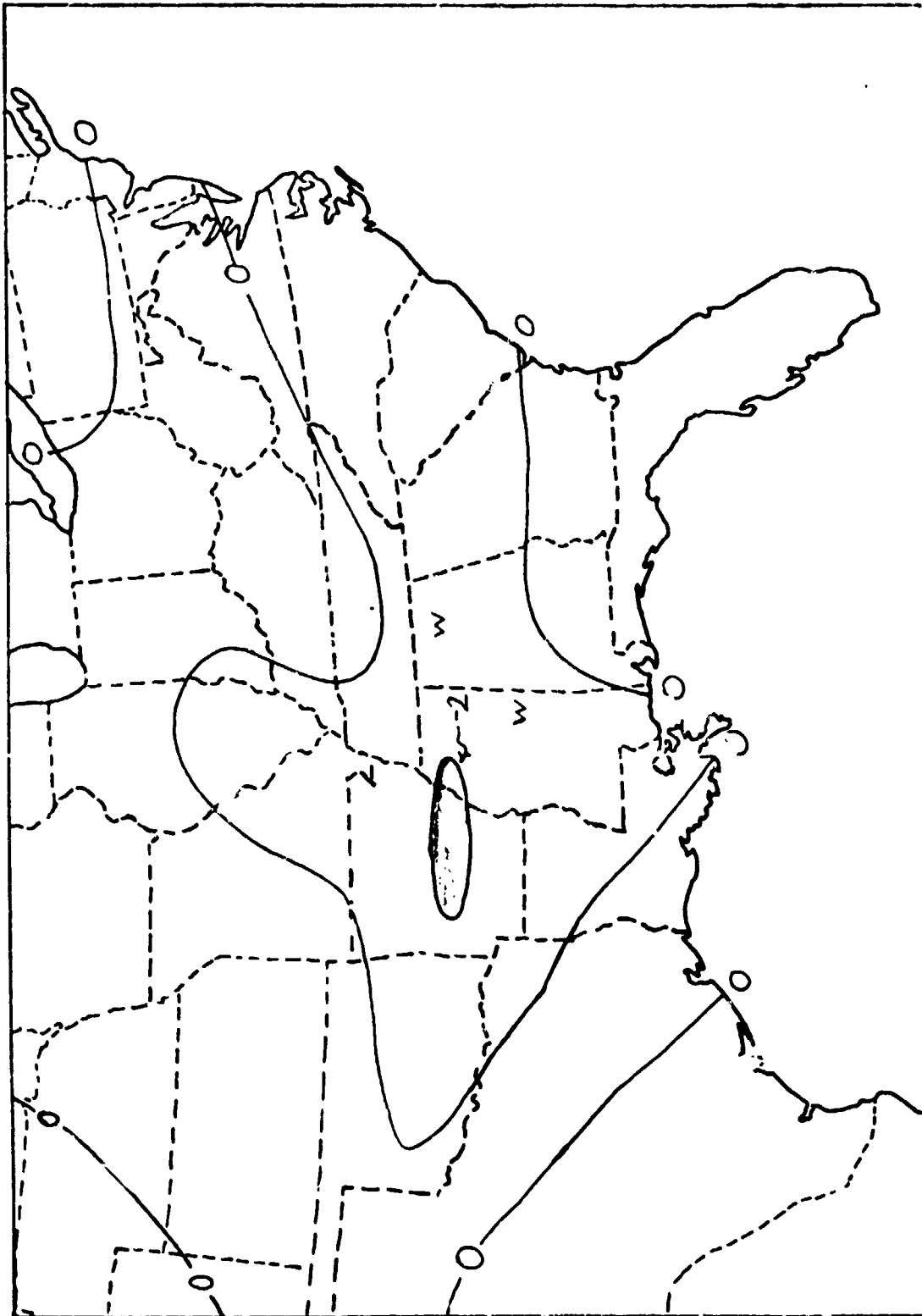


Figure 51. Map at 1200 GMT April 25, 1975 for Energy Index.

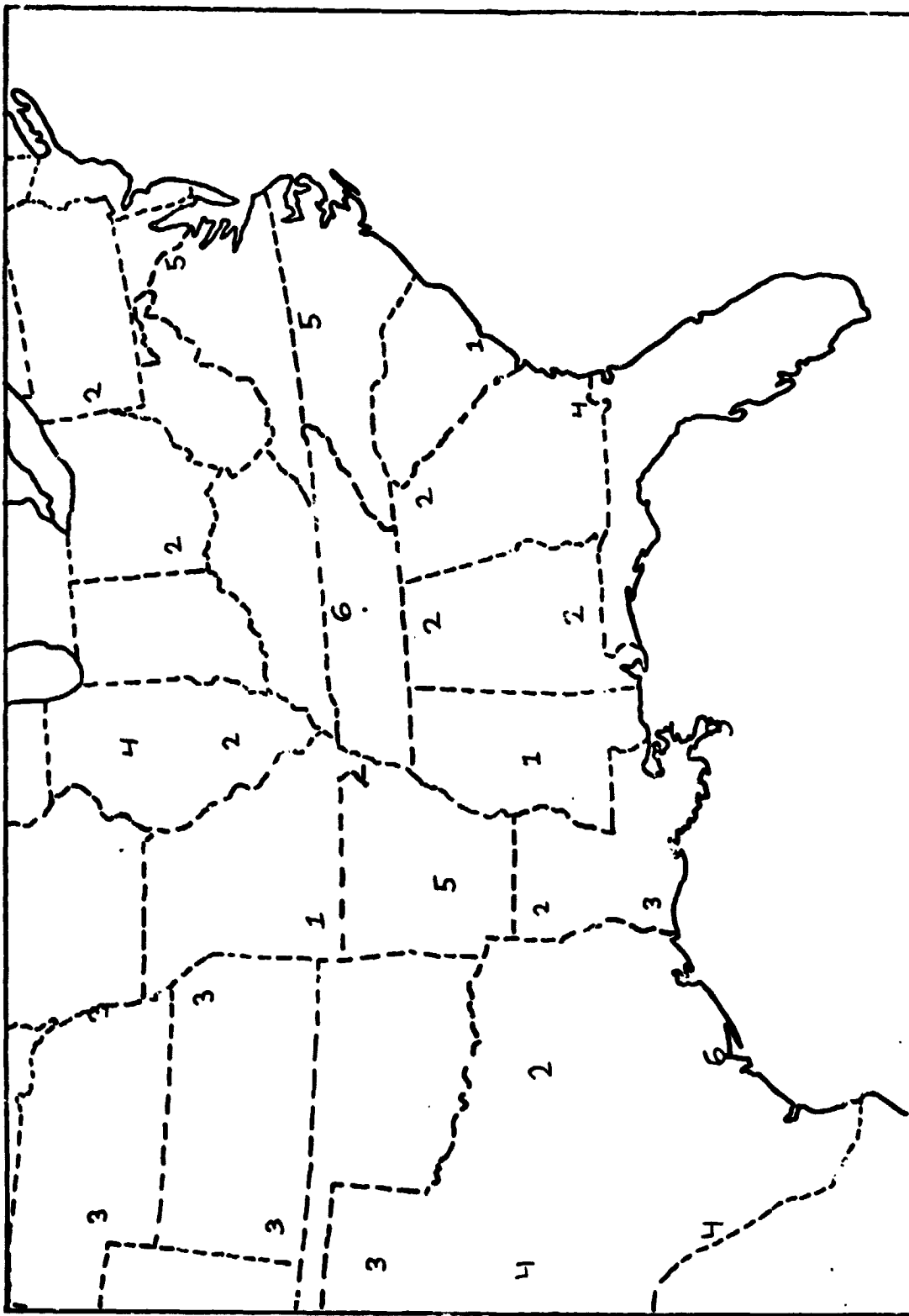


Figure 52. Map at 1200 GMT April 25, 1975 for Shear Index.

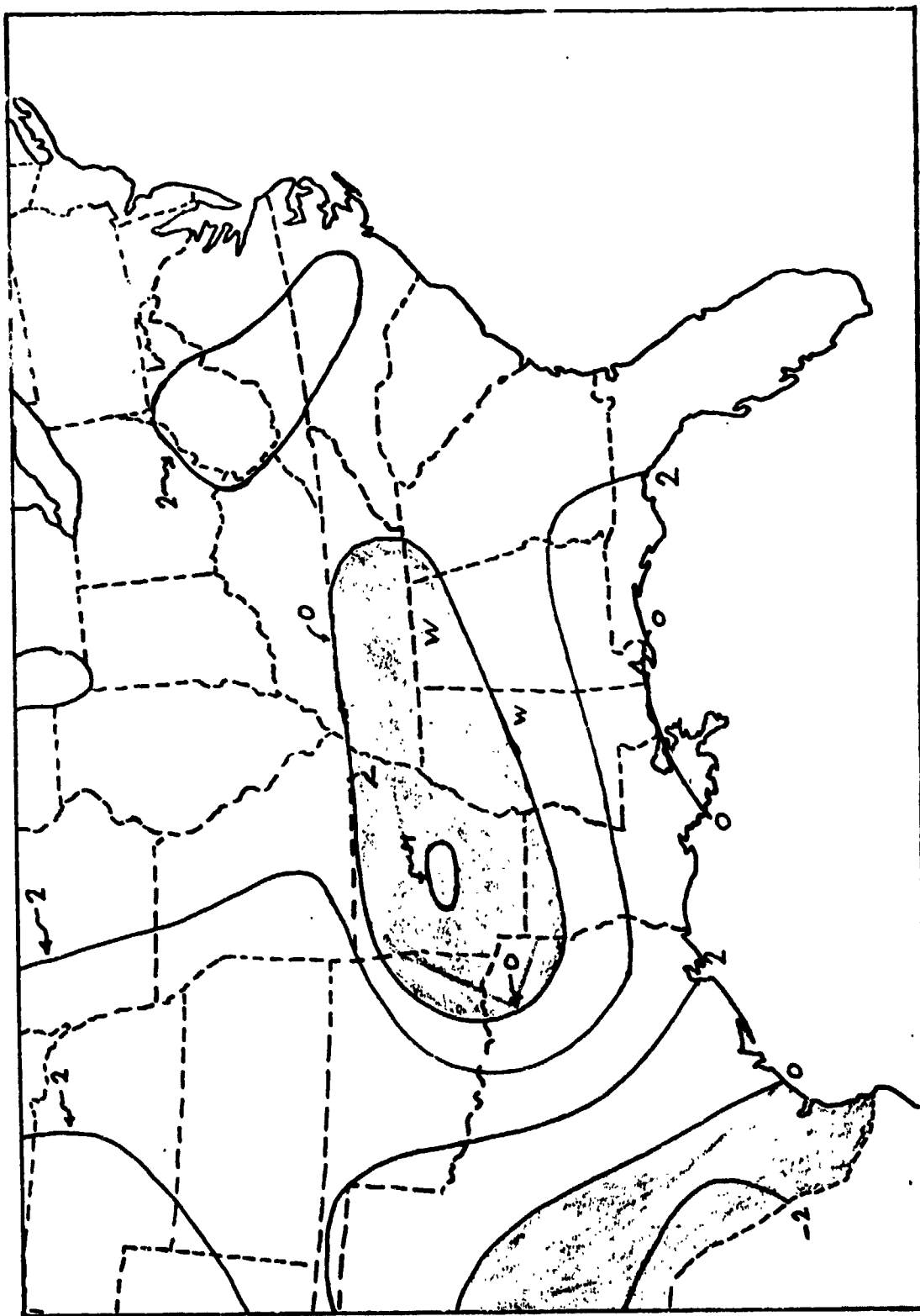


Figure 53. Map at 1200 GMT April 25, 1975 for Energy Shear Index.

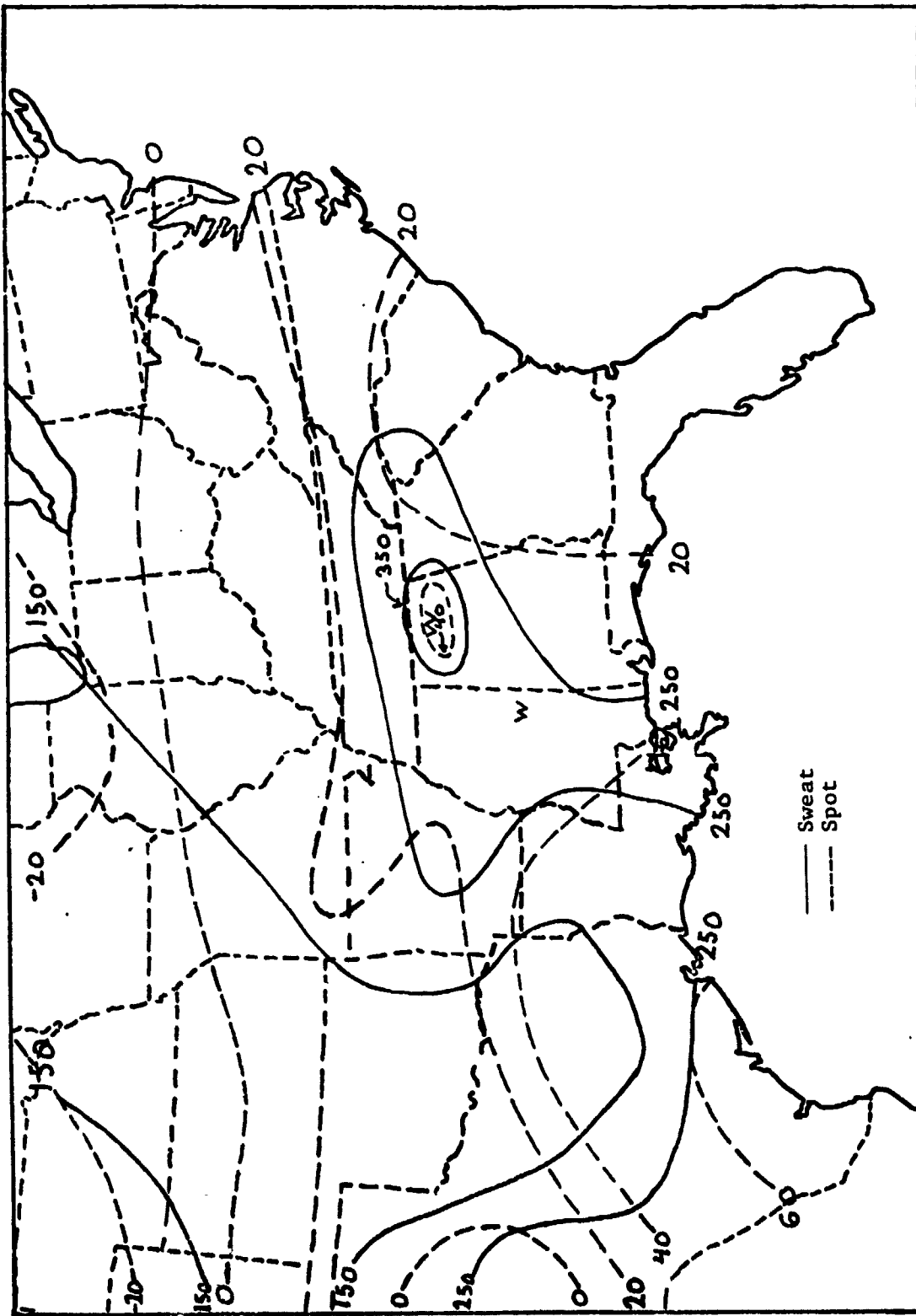


Figure 54. Map at 1200 GMT April 25, 1975 for Sweat and Spot Indices.

VI. Summary of Results

A graph of the EI's computed in this study versus the SI's is shown in Figure 55. While nine of the twelve proximity soundings and all but one of the precedence soundings fall below the line $EI = 0.5 SI - 2$, this line does not uniquely separate these soundings from the nonproximity soundings as it did for the soundings studied by Eagleman. (See Figure 17, Chapter IV, for comparison.) A linear relation between an ESI and SI and EI is not clearly indicated. However, the tests of the ESI computed on this basis do show that the ESI so computed does improve the forecast of severe wind events due to thunderstorms (such as tornado and linear winds). It is slightly better than just the energy index which has no windshear component. It also is better than the SWEAT which does include an average wind shearrelated factor. The results with the small sample from AVE IV are not as striking as those shown by Eagleman. (See Chapter IV Reference, Eagleman, et al. 1975.)

VII. Conclusions and Recommendations

The incorporation of vertical shear of horizontal environmental wind (1) in smaller layers (~200 mb thick) and (2) in a manner consistent with a double vortex model of a thunderstorm does produce slightly improved prediction of/or positive correlation with severity of thunderstorm winds and velocity of thunderstorm motion. It is still true that many thunderstorm severe events and velocities of movement are not predicted by this or any current method and the false alarm rate is high.

The method of Eagleman requires making a large number of guesses of the direction and magnitude of the motion of the predicted storm. Further, it does not prevent prediction of several directions of motion

at the same time. Finally, the choices of positions of significance for vortices and the thickness of layers for computing wind shear are neither as refined nor as physically based as now seems desirable.

It is recommended that steps be taken to improve physical insight into the mechanisms set into operation by the interaction between the thunderstorm and the sheared environment. However, even without the detailed understanding of these processes it is possible to test an improved Shear Index. Several suggestions follow:

- (1) Use thinner layers of atmosphere for computing shears.
- (2) Reduce the amount of guessing of storm vector velocity which is required in the present method.
- (3) Improve the form of the energy shear index relation.
- (4) Eliminate cloud zones of probable irrelevance from the shear index calculation scheme.
- (5) Utilize more field experiment data both for developing better correlations among prediction parameters and for testing the predictive schemes.

AVE IV CASE

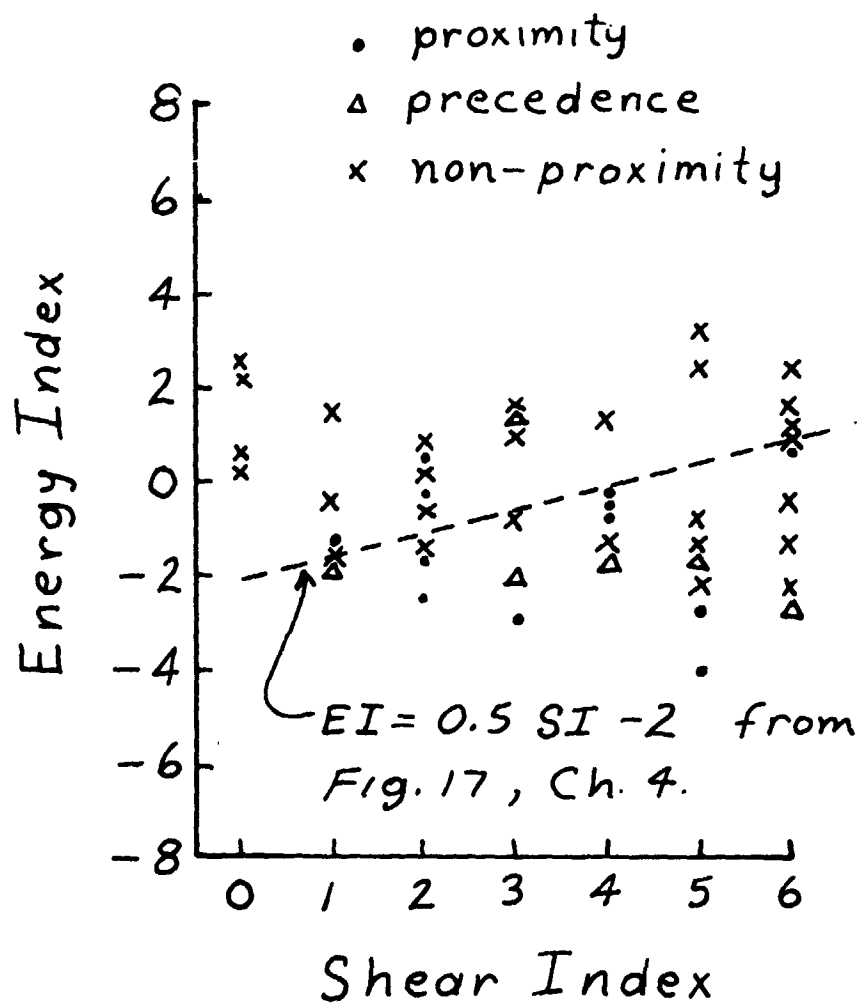


FIGURE 55

Appendix A

1. A printout of the computer printout is attached as exhibit A-1.
2. Program Checkout.

To insure that the Energy-Shear program was making the desired calculations for the shear index correctly, the program was run with the data from Charleston, South Carolina, at 2100 GMT on April 24, 1975. An assumed storm speed and direction of 50% of the cloud layer average windspeed and 10 degrees to the left of the average wind were chosen for a test calculation. These parameters gave a computed storm velocity of 5.45 meters sec^{-1} from 274.63 degrees. The shear index was 5 with surface to 850 mb average winds of 8.10 meter sec^{-1} from 179.97 degrees and a 550 to 300 mb average wind of 9.92 meters sec^{-1} from 315.47 degrees.

Instead of following the computer program step by step, vectors were used to calculate the relative mean wind velocities for each 150 mb layers and the component of these velocities opposed to the surface-850 mb mean velocity.

The components of the cloud layer average wind were calculated by finding the average of the u and v wind components at the 850, 700, 500, and 300 mb levels as given in Fucik and Turner (1975). The average winds for each 150 mb layer were also found using the published u and v values. Table 1 gives the components of the mean wind and the average wind through each layer, and the 550-300 mb average wind.

The mean cloud layer wind was calculated from $\bar{V}_{cl} = (u_{cl}^{-2} + v_{cl}^{-2})^{\frac{1}{2}}$ and the direction from $\theta = \text{Arctan}(\frac{\bar{v}_{cl}}{\bar{u}_{cl}})$. This yielded $\bar{V}_{cl} = 10.8783$ and $\theta = -14.643$. It must be remembered that this θ is the angle in

the usual mathematical coordinate system and must be converted to the meteorological system.

Remembering that the assumed storm speed and direction correspond to 50% of the cloud layer average speed and move 10 degrees to the left, the assumed storm moves at $5.44 \text{ meters sec}^{-1}$ from 274.64 degrees. This velocity was also resolved into u and v components to facilitate calculation of the relative mean wind in each layer. Relative velocities were calculated using the equation $\vec{V}_L - \vec{V}_S = \vec{V}_R$. The components of the relative wind are given by Table 2.

The component of the relative wind in the upper layers which directly opposed the surface-850 mb relative wind was then found by

$$V_{u-B} = \frac{\vec{V}_u - \vec{V}_B}{V_B}. \text{ This component is also given in Table 2.}$$

The magnitude and direction of the surface to 850 mb layer relative mean wind were calculated from the components by the method described earlier for the cloud layer average wind. The resultant relative wind was $8.1050 \text{ meter sec}^{-1}$ from 182.04 degrees.

Since the model assumes that the component of the relative mean wind velocity of an upper layer that directly opposes the surface-850 mb relative wind must be between 75 and 125% of the magnitude of that wind in order to produce blocking, the value of V_{u-B} should be between 6.075 and 10.125 if the layer is to have a blocking effect. From Table 2 five consecutive layers have values of V_{u-B} within this range; therefore the shear index is 5. Table 3 gives a summary of the values computed from the IBM 360 and those calculated using vectors and the HP-65 calculator. Discrepancies between these values are probably due to sounding differences in the two machines and are well within the accuracies of the data.

Exhibit A-1. The Computer Program

-----SJOB

TIME=4,PAGES=99

-----C THIS PROGRAM CALCULATES THE ENERGY-SHEAR-INDEX FROM RAWINSUNDE-DATA

C
C
C

```
1  DIMENSION DTEMP(3),DATE(5), PRESS(3),GPHT(3),TEMP(3),ET(2),WS(41)
2  DIMENSION WD(41),DIRMID(6,200),SPDMID(6,200),RWS(40),RAD(40)
3  DIMENSION CWS(40),WS525(6,200),MSD25(6,200),DEV25(6,200)
4  DIMENSION SRWS25(6,200),SRAD25(6,200),SS25(6,200),SD25(6,200)
5  DIMENSION ISAVE(6)
6  INTEGER HOUR
```

C

```
7  DATA ALEFT/4HLEFT/
8  DATA RIGHT/4HRIGHT/
```

C

```
9  COMMON TEMP, DTEMP, WD, WS, HOUR, NDAY, PRESS, GPHT
10 COMMON ISTA
```

C

```
READ IN A DATA SET
```

C

```
11 100 READ (5,1102) ISTA, DATE
12 IF (ISTA.EQ. 99999) STOP
13 READ (5,1104) GPHT(1), PRESS (1), TEMP (1), DTEMP(1), WD(1), WS(
14 1 1),HOUR,NDAY
15 DO 105 LOP1= 2,7
16 READ (5,1106) WD (LOP1), WS(LOP1)
17 105 CONTINUE
18 READ (5,1104) GPHT(2), PRESS (2), TEMP (2), DTEMP(2), WD(2), WS(
19 1 2)
20 DO 110 LOP2= 9,21
21 READ (5,1106) WD (LOP2), WS(LOP2)
22 110 CONTINUE
23 READ (5,1104) GPHT(3), PRESS (3), TEMP (3), DTEMP(3), WD(3), WS(
24 1 3)
25 DO 115 LOP3= 23,41
26 READ (5,1106) WD (LOP3), WS(LOP3)
27 115 CONTINUE
28 1107 FORMAT (15,2PX,5A4)
29 1106 FORMAT (2F7.1,3F6.1,F5.1,35X,15,13)
30 1106 FORMAT (26X,F6.1,F5.1)
31 C IF DATA IS MISSING, PRINT MESSAGE
32 IF ( GPHT(2).EQ. 99.9 .OR. GPHT(3).EQ. 99.9) GO TO 299
33 IF ( TEMP(2).EQ. 99.9 .OR. TEMP(3).EQ. 99.9) GO TO 299
34 IF ( DTEMP(2).EQ. 99.9 .OR.DTEMP(3).EQ. 99.9) GO TO 299
```

C

C

C

C

-----C
CALCULATE THE ENERGY INDEX

```
31 DO 240 I=2,3
32 TEMPA = DTEMP (1) +273.16
33 TEMPA = TEMP (1) +273.16
34 IF (TEMPA.LT. 273.16) GO TO 220
35 EXP = ((17.2693882 +ITEMPA-273.16))/(ITEMPA-35.66)
36 GO TO 230
37 220 EXP = ((17.2745588+ITEMPA-273.16))/(ITEMPA-7.66)
38 230 F = 8.10789*(2.71424+EXP)
39 AMIXRA = (622.0/E)/(PRESS(1)-E)
40 J=1
```

ORIGINAL PAGE IS
OF POOR QUALITY

```

41      ET(J) = .24*(TEMPR +2.5*AVIXRA*GPHT(I)/100.)
42      240 CONTINUE
43      EI= ET(2)-ET(1)
44      GO TO 300
45      299 WRITE (6,1012) DATE, ISTA
46      1012 FORMAT (42HTHE ENERGY INDEX CANNOT BE CALCULATED FOR ,5A4,1X,15)
47      - GO TO 100
C
C*****
C
C CALCULATE THE MEAN WIND VELOCITY OF THE CLOUD LAYER
C
48      300 WRITE (6,1122) DATE, ISTA
49      1122 FORMAT(1H1,////,17X,5A4,1X,15,40X,18H$HEAR INDEX VI MOD,/)
50      ICI= 0
51      IFOUR = 0
52      DO 304 I=1,20
53          IM=I
54          IF (I .NE. 1) IM=2*I-2
55          IF (WS(IM).NE. 99.9) GO TO 304
56          ICI= ICI+1
57          IF (IM.EQ.8 .OR. IM.EQ.14 .OR. IM.EQ.22 .OR. IM.EQ.30) GO TO 302
58          GO TO 304
59      302 IFOUR = IFOUR+1
60      304 CONTINUE
61      304 N = 20-ICI
62      XWIND = 0.
63      YWIND = 0.
64      DO 312 J=1,20
65          JM=J
66          IF (J.NE. 1) JM=2*J-2
67          IF (WS(JM).EQ. 99.9) GO TO 312
68          IF (JM.EQ.8 .OR. JM.EQ.14 .OR. JM.EQ.22 .OR. JM.EQ.30) GO TO 310
69          GO TO 312
70      310 RADWS = WCI(JM)/57.296
71          XWIND = XWIND + WS(JM)*COS(RADWS)
72          YWIND = YWIND + WS(JM)*SIN(RADWS)
73      312 CONTINUE
74      320 AVXW = XWIND/(4.-FLOAT(IFOUR))
75      AVYW = YWIND/(4.-FLOAT(IFOUR))
76      THXS= SQRT(AVXW**2 +AVYW**2)
77      DD = AVYW/AVXW
78      THWD = ATAN(DD)*57.296
79      IF(AVXW.GE.0.) GO TO 350
80      THWD = THWD +180.
81      350 IF (THWD .LT. 0.) THWD = THWD+360.
82      IF ( THWD .GT. 360.) THWD = THWD-360.
83      DO 365 V=1,6
84          ISAVEIN= 1
85      365 CONTINUE
86      INDSM? = 0
87      DO 699 III= 1,2
88      699 K = 1.61,5
89      DO 699 L = 1,31,5

```

```

C
C*****
C
C CALCULATE RELATIVE WIND VELOCITIES BASED ON DEVIATIONS
C OF STORM DIRECTIONS FROM THE MEAN WIND VELOCITY
C

```

ORIGINAL PAGE IS
OF POOR QUALITY

```

90      IMUNPR= 50*L-1
91      IDEVIT = K-1
92      SS = TVWS *FLOAT(50*L-1)/100.
93      IF (III.EQ.1) DIR= RIGHT
94      IF (III.EQ. 2) DIR= ALEFT
95      IF ( DIR.EQ. ALEFT) IDEVIT= IDEVIT+9
96      IF (III.EQ.2) GO TO 401
97      SD= TMWD *FLCAT(K)-1.
98      GO TO 402
99      401 SD= TMWD*FLOAT(K)-4.
100     402 DO 430 LL=1,20
101         LLM = LL
102         IF (LL.EQ.1) LLM=2*LL-2
103         GAMMA =SD*RDILLM)
104         RADGA= GAMMA/57.296
105         RWS(LLM) = SORT(W5(LLM)**2+SS**2-2.0*W5(LLM)*SS*COS(RADGA))
106         SINSS = (SS*SIN(RADGA))/RWS(LLM)
107         NSIN =0
108         IF (SINSS.LT.0.0) NSIN=-1
109         IF (ABS(SINSS).GE. .9999998 .AND. ABS(SINSS).LT.1.00001) SINSS=1.0
110         IF (SINSS.GT.1.) GO TO 1224
111         IF (NSIN.EQ.1 .AND. SINSS.EQ. 1.0) SINSS = -1.0
112         IF (1.0-ABS(SINSS)**2.) .GT. 0.0) GO TO 405
113         WRITE(6,5302) III,K,L,LLM,SINSS,COSSS
114         COSSS=0.0
115         GO TO 410
116         405 COSSS =SORT(1.0- ABS(SINSS)**2.0)
117     5302 FORMAT (4I4,2E14.6)
118     410 IF (COSSS .LE. .000001) GO TO 415
119         TANSS= SINSS/COSSS
120         BETA = ATAN(TANSS)*57.296
121         GO TO 420
122     415 WRITE (6,5302) III,K,L,LLM,SINSS,COSSS
123         IF (SINSS = 0.0) *16.416.417
124     416 BETA = 270.
125         GO TO 420
126     417 BETA = 90.
127     420 RWD(LLM) =SD (LLM)-BETA
128         IF (RWD(LLM).LT.0.) RWD(LLM)= RWD(LLM)+360.
129         IF (RWD(LLM).GT.360.) RWD(LLM)= RWD(LLM)-360.
130     430 CONTINUE
131         IDI = 0
132         DO 440 M= 1,5
133             MM=V
134             IF (MM.EQ. 1) MM=2*V-2
135             IF (W5(MM).NE. 99.9) GO TO 440
136             IDI = IDI+1
137     440 CONTINUE
138         XSUM = 0.
139         YSUM = 0.
140         NN = 5-IDI
141         DO 450 II=1,5
142             IIV=II
143             IF (IIV.EQ.1) IIV= 2*II-2
144             IF ( W5(IIV).EQ. 99.9) GO TO 450
145             RWWD = RAD(IIV)/57.296
146             XSUM= XSUM+W5(IIV)*COS (RWWD)
147             YSUM = YSUM+W5(IIV)*SIN(RWWD)
148     450 CONTINUE

```

```

C.....
C
C  CALCULATE LAYER AVERAGES
C
149  AVXSUM = XSUM/FLOAT(NN)
150  AVYSUM = YSUM/FLOAT(NN)
151  AVRS = SORT( AVXSUM**2+AVYSUM**2)
152  D = AVYSUM/AVXSUM
153  AVRWD = ATAN(D)*57.296
154  IF (AVXSUM.GE. 0.) GO TO 501
155  AVRWD = AVRWD+180.
156  501 IF ( AVRWD .LT. 0.) AVRWD = AVRWD+360.
157  IF (AVRWD .GT. 360.) AVRWD = AVRWD-360.0
158  CWD = AVRWD +180.
159  IF ( CWD.GT. 360.) CWD = CWD-360.
160  DO 570 KK= 16,38*2
161  KKJ =0
162  XRW =0.
163  YRW = 0.
164  KKI = KK-6
165  KKK=KK
166  DO 520 KKL= KKI, KKK*2
167  IF (ABS(KKL).EQ.99.9) GO TO 510
168  RRRWD =RWD(KKL)/57.296
169  XRA = XRA+R*(KKL)*COS(RRRWD)
170  YRW = YRW +R*(KKL)*SIN(RRRWD)
171  GO TO 520
172  510  KKL= KKJ+1
173  520  CONTINUE
174  57* IF (KKJ.EQ.4) GO TO 550
175  XAVRW = XRW/16.=FLOAT(KKJ)
176  YAVRW = YRW/16.=FLOAT(KKJ)
177  AAVRW = SORT(AAVRW**2+YAVRW**2)
178  E = YAVRW/XAVRW
179  XAVRWD = ATAN(E)*57.296
180  IF ( XAVRW.GE.0.) GO TO 530
181  XAVRWD = XAVRWD+180.
182  530 IF (XAVRWD.LT.0.) XAVRWD = XAVRWD+360.
183  IF ( XAVRWD.GT. 360.) XAVRWD = XAVRWD-360.
184  CDEG1 = (CWD-XAVRWD)
185  IF (CDEG1.GT.90.) GO TO 560
186  CDEG2 = CDEG1 + 90.
187  IF (CDEG2.LT.0.) GO TO 560
188  540 CDEG = CDEG1/57.296
189  CWS(KK) =XRA/KWS*COS (CDEG)
190  GO TO 570
191  550 CWS(KK) =-1.
192  GO TO 570
193  560 XAVRWD = XAVRWD + 360.
194  CDEG1 = XAVRWD-CWD
195  XAVRWD = XAVRWD-360.
196  IF (CDEG1.LT. 0.) GO TO 540
197  CWD = CWD +360.
198  CDEG1 = CWD -XAVRWD
199  CWD = CWD-360.
200  IF (CDEG1 .LT. 90.) GO TO 540
201  CWS (KK) =-1.
202  570 CONTINUE
203  YMID =0.
204  XMID =0.

```

FINAL PAGE IS
 OF POOR QUALITY

```

205 JJJJ=0
206 DO 587 JJJ=20,30,2
207 IF (N5(JJJ).EQ. 99.9) GO TO 575
208 RRRWD = RWD(JJJ)/57.296
209 XVID = XVID +RWS(JJJ)*COS (RRRWD)
210 YVID = YVID +RWS(JJJ)*SIN(RRRWD)
211 GO TO 580
212 575 JJJ=JJJJ+1
213 580 CONTINUE
214 IF (JJJJ.EQ. 6) GO TO 590
215 XAVVID = XVID/(6.-FLOAT(JJJJ))
216 YAVVID = YVID/(6.-FLOAT(JJJJ))
217 AVMSPD = SQRT(XAVVID**2+ YAVVID**2)
218 G = YAVVID/XAVVID
219 AVMDIR = ATAN(G)*57.296
220 IF (XAVVID.GE.0.) GO TO 595
221 AVMDIR = AVMDIR +180.
222 595 IF ( AVMDIR .LT.0.) AVMDIR = AVMDIR +360.
223 IF ( AVMDIR .GT. 360.) AVMDIR = AVMDIR-360.
224 GO TO 600
225 590 AVMSPD = -1.
226 AVMDIR = -1.
C
C.....
C
C CALCULATE SHEAR INDEX
C
227 600 IC25C = 0
228 DO 611 IJK = 16,20,2
229 IF (CN5(IJK).LT. 0.) GO TO 611
230 DIFF = CAS(IJK)-AVRMS
231 IF (DIFF.GT. 0.) GO TO 670
232 611 CONTINUE
233 DO 614 IKJ = 22,32,2
234 IF (CN5(IKJ).GT. 0.) GO TO 620
235 615 CONTINUE
236 GO TO 670
237 620 M= IKJ
238 F = 1.
239 INC25C = 0
240 DO 665 JJK= M,32,2
241 IF (CN5(JJK).LT.0.) GO TO 625
242 DIFF = CAS(JJK)-AVRMS
243 ARC2 = .25*AVRMS
244 IF (ABS(DIFF).LE. ARC2) GO TO 635
245 625 F = 0.
246 GO TO 665
247 635 IF ( F .EQ. 0.) GO TO 640
248 IC25C = IC25C +1
249 GO TO 650
250 640 IC25C =1
251 650 IF ( IC25C .GT. INC25C) INC25C = IC25C
252 F = 1.
253 GO TO 665
254 665 CONTINUE
255 IF ( INC25C .GT. INDSH4) INDSH4 = INC25C
256 IF ( INC25C .EQ. 0) GO TO 670
257 GO TO 680
258 670 IF (III.EQ. 1 .AND. K.EQ.1 .AND. L.EQ.1) GO TO 690
259 GO TO 699

```

```

260 690 IZERO = 1
261 VM = ISAVE(IXC25C)
262 VSS25 (IXC25C,VM) = IMUNPR
263 MSD25 (IXC25C,VM) = IDEVIT
264 DFV25 (IXC25C,VM) = DIR
265 SRAS25 (IXC25C,VM) = AVRWS
266 SRWD25 (IXC25C,VM) = AVRWD
267 SS25 (IXC25C,VM) = SS
268 SD25 (IXC25C,VM) = SD
269 DIRWD (IXC25C,VM) = AVMDIR
270 SPDWD (IXC25C,VM) = AVMSPD
271 ISAVE(IXC25C) = ISAVE(IXC25C) + 1
272 GO TO 699
273 699 IZERO = 0
274 ISAVES = IMUNPR
275 ISAVED = IDEVIT
276 SAVEDV = DIR
277 SAVENS = AVRWS
278 SAVEDW = AVRWD
279 SAVES = SS
280 SAVED = SD
281 SAVEDD = AVMDIR
282 SAVENS = AVMSPD
283 699 CONTINUE

C
C .....
C
C CALCULATE ENERGY-SHEAR INDEX
C
284 EST = 4. - FLOAT (INDSHR) + 2. * EI
285 IF (IZEZO.EQ.0) GO TO 920
286 DO 920 I = 1,6
287 IF I ISAVE(I),EQ. 1) GO TO 910
288 MMW = ISAVE (I)-1

C
C OUTPUT RESULTS
C
289 WRITE (6,1110) I
290 1110 FORMAT (//,3X,66MTHE FOLLOWING STORM SPEEDS AND DIRECTIONS GAVE A
1SHEAR INDEX OF .11,/)
291 WRITE (6,1112)
292 1112 FORMAT (2X,15MSTORM SPEED,2X,15MSTORM DIRECTION,3X,1MDEV,6X,
1 1MSURF=950 AVERAGE,4X,15M550-300 AVERAGE )
293 WRITE (6,1114) (VSS25(I),J),SS25(I),J),MSD25(I),J),SD25(I),J),DEV25
1(I),J),SRWS25(I),J),SRWD25(I),J),SPDWD(I),J),DIRWD(I),J),J=1,MMW)
294 1114 FORMAT (2X,12,1X,F6.2,6M MPS,3X,12,1X,F6.2,6M DEG,3X,45,3X,
1F5.2,6M MPS,1X,F6.2,6M DEG,3X,F6.2,6M MPS,1X,F6.2,6M DEG)
295 GO TO 920
296 91. WRITE (6,1116) I
297 1116 FORMAT (//,31X, ' THERE WERE NO STORM SPEEDS AND DIRECTIONS THAT
1GAVE A SHEAR INDEX OF .11)
298 920 CONTINUE
299 GO TO 930
300 920 WRITE (6,1118)
301 1118 FORMAT (//,66X,66MTHE SOUNDRING HAD A SHEAR INDEX OF 0.//)
302 WRITE (6,1117)
303 WRITE (6,1117) ISAVES,SAVES,ISAVED,SAVED,SAVEDV,SAVENS,SAVEDW,
1 SAVES,SAVED,SAVENS
304 930 WRITE (6,1120) FI,INDSHR,EST

```

```

305 1120 FORMAT (//.47X,SWEAT = ,F6.2,7X, SI = ,11.12M, AND ESI = ,F5.2//)
306 CALL INDEX(TTI,SWEAT,SPOT,ERROR,MISS)
307 IF (ERROR.EQ.0. .AND. MISS.EQ.0) GO TO 1220
308 IF (ERROR.EQ.1) WRITE(6,1134) TTI,SWEAT
309 1134 FORMAT (17X,TTI = ,F10.1, 'SWEAT = ,F10.1)
310 1202 IF (ERROR.EQ.1) WRITE (6,1126)
311 1204 IF (ERROR.EQ.2) WRITE (6,1128)
312 1206 IF (ERROR.EQ.3) WRITE (6,1130)
313 1126 FORMAT (17X,'SWEAT CANNOT BE CALCULATED MISSING TEMP//)
314 1128 FORMAT (17X,'SWEAT CANNOT BE CALCULATED MISSING WS //)
315 1130 FORMAT (17X,'SWEAT CANNOT BE CALCULATED MISSING WD //)
316 IF (MISS.EQ.0)WRITE (6,1136) SPOT
317 1136 FORMAT (14X, ' SPOT = ,F10.1)
318 IF (MISS.EQ.1) WRITE(6,1132)
319 1132 FORMAT (17X, 'SPOT CANNOT BE CALCULATED MISSING DATA//)
320 GO TO 1225
321 1220 WRITE (6,1140) TTI,SWEAT,SPOT
322 1140 FORMAT (14X,TTI = ,F10.1, 'SWEAT = ,F10.1, 'AND SPOT = ,F10.1)
323 GO TO 1225
324 1274 WRITE (6,6220) TTI,K,L,LLM,TMWD,TMWS,SINSS
325 6220 FORMAT (41X,3E15.7)
326 1225 GO TO 100
327 END

```

```

328 SUBROUTINE INDEX(TTI,SWEAT,SPOT,ERROR,MISS)
329 DIMENSION T(3), TD(3), WK(3)
330 COMMON TEMP(3),DTEMP(3),WD(41),WS(41),HOUR,NDAY,P (3),M (3)
331 COMMON ISTA
332 NO=ISTA
C THIS PROGRAM CALCULATES THE SOFT SWEAT AND SPOT INDICES
C TO(1) = SURFACE DEWPOINT F
C TD(2) = 850MB DEW POINT C
C TD(3) = 500MB DEW POINT C
C T(1) = SURFACE TEMPERATURE F
C T(2) = 850 MB TEMPERATURE C
C T(3) = 500MB TEMPERATURE C
C W(1) = SURFACE WIND SPEED IN KNOTS
C W(2) = 850 MB WIND SPEED
C W(3) = 500MB WIND SPEED
C VA = WIND VEERING ANGLE 850 TO 500 MB
C WD(1) = SURFACE WIND DIRECTION
C WD(2) = 850 MB WIND DIRECTION
C WD(3) = 500 MB WIND DIRECTION
C TT = TOTAL TOTALS INDEX
C ASIN= ALTITUDE SETTING IN INCHES
C DEFINT(COF,IP**N)*A/T(1)
333 COF= 1/(1013.25**0.19028)*0.00651/258.0
334 RA= 1.0/0.19028*
335 FACT= 29.921/1013.25
336 ERROR =0.
337 MISS =0
C CONVERT TO PROPER UNITS
338 IF (TEMP(2).EQ.99.9 .OR. DTEMP(3).EQ.99.9) GO TO 165
339 IF (DTEMP(2).EQ.99.9 .OR. DTEMP(3).EQ.99.9) GO TO 165
340 IF (ASIN.EQ.99.9 .OR. WD(2).EQ.99.9) GO TO 166
341 IF (WD(1).EQ.99.9 .OR. WD(3).EQ.99.9) GO TO 167
342 IF (WD(2).EQ.99.9 .OR. WD(2).EQ.99.9) GO TO 167
343 T(1)= TEMP(1)*1.8 +32.0
344 T(2)= TEMP(2)

```

```

345      T(3)= TEMP(3)
346      KK(1)= WS(1)*1.94254
347      KK(2)= WS( 8)*1.94254
348      KK(3)= WS(22)*1.94254
349      TD(1)= DTEMP(1)*1.8+ 32.0
350      TD(2)= DTEMP(7)
351      TD(3)= DTEMP(3)
C      CALCULATE TTI
352      TTI= T(2)+TD(2)-2.0*T(3)
C      NO NEGATIVE TERMS OCCUR IN SWEAT FORMULA
353      IF (TTI .LT. 49.0) TTI=49.0
354      IF (TD(2) .LT. 0.0) TD(2)= 0.0
C      CALCULATE SOFT SWEAT
C      IF EITHER KK(2) OR KK(3) LESS THAN 15, FVA=0
355      IF ((KK(2).LT.15.0) .OR. (KK(3).LT.15.0))FVA=0.0
356      IF ((WD(1) .LT. 130.0) .OR. (WD(1) .GT. 250.0)) GO TO 150
357      IF ((WD(22).LT. 210.0) .OR. (WD(22).GT. 310.0))GO TO 150
358      XVA = WD(22)- WD(1)
359      IF ( XVA .LT. 130.0) FVA = .2606
360      IF ( XVA .LT. 140.0) FVA = .640
361      IF ( XVA .LT. 120.0) FVA = .4468
362      IF ( XVA .LT. 110.0) FVA = .5511
363      IF ( XVA .LT. 100.0) FVA = .5994
364      IF ( XVA .LT. 90.0) FVA = .9404
365      IF ( XVA .LT. 80.0) FVA = 1.0
366      IF ( XVA .LT. 70.0) FVA = .9404
367      IF ( XVA .LT. 60.0) FVA = .6894
368      IF ( XVA .LT. 50.0) FVA = .4415
369      IF ( XVA .LT. 40.0) FVA = .2340
370      IF ( XVA .LT. 30.0) FVA = .0957
371      IF ( XVA .LT. 20.0) FVA = .0532
372      IF ( XVA .LT. 10.0) FVA = .0
373      GO TO 140
374      150 FVA=0.0
C      CALCULATE SWEAT
375      160 SWEAT= 12.0*TD(2) + 20.0*(TTI-49.0) +2.0*KK(2)+KK(3)+ 125.0*FVA
376      GO TO 95.
377      165 ERROR=1.
378      GO TO 95
379      166 ERROR = 2.
380      GO TO 95
381      167 ERROR = 3.
C      CALCULATE SPOT
C      CALCULATE ALTIMETER SETTING
382      95 IF (TEMP(1).EQ.99.9 .OR. DTEMP(1).EQ.99.9) GO TO 250
383      IF ( P(1).EQ.99.9 .OR. H(1).EQ.99.9) GO TO 250
384      IF ( WS(1).EQ.99.9 .OR. WD(1).EQ.99.9) GO TO 250
385      CORR=(1+(COF*H(1)/P(1)**.190284))**KX
386      ASIN=(FACT *P(1)*CORR)
387      ALTT = 100.*(30.-ASIN)
388      IF (IT(1) .LT. 50.0) .AND. ASIN .LT.29.5) ALTT= .5*ALTT
389      IF (WD(1) .GT. 240.0) WST= 2*WK(1)
390      IF (AD(1) .LE. 260.0) GO TO 101
391      GO TO 200
392      101 IF (WD(1) .LE. 230.0) GO TO 110
393      IF (TD(1) .LT. 55.0) WST=-2*WK(1)
394      IF (TD(1) .LT. 60.0) WST =-WK(1)
395      WST=WK(1)
396      GO TO 200
397      110 IF (WD(1) .LE. 200.0) GO TO 120

```

ORIGINAL PAGE IS
OF POOR QUALITY

```

399      IF (TD(1) .LT. 55.0) WST=0
399      IF (TD(1) .LT. 60.0) WST=WK(1)/2.0
400      WST=WK(1)
401      GO TO 200
402 120 IF (WD(1) .LE. 140.0) GO TO 130
403      WST=WK(1)
404      IF (TD(1) .LT. 55.0) GO TO 200
405      IF (NDAY .NE. 24) GO TO 125
406      IF ((INC.EQ.429).AND.(HOUR.EQ.515)).OR.((INC.EQ.349).AND.(HOUR.EQ.
1115)).OR.(HOUR.EQ.2315))) GO TO 200
407 125 WST = WK(1)* 2.
408      GO TO 200
409 130 IF (WD(1) .LT. 70.0) GO TO 140
410      WST=WK(1)
411      GO TO 200
412 140 WST=0.0
413 200 SPOT= (T(1)-60.0) + (TD(1)-55.0) + ALTT + WST
414      GO TO 225
415 200 MISS = 1
416 225 CONTINUE
417      RETURN
418      END

```

SENTRY

TABLE 1

Layer	Average u	Average v
Cloud layer	10.525	-2.75
Surface-850 mb	5.42	7.66
650-500 mb	12.975	-6.275
600-450 mb	12.275	-6.7
550-400 mb	12.425	-7.65
500-350 mb	12.0	-8.45
450-300 mb	12.075	-8.125
400-250 mb	13.3	-7.9
550-300 mb	12.3667	-7.5

TABLE 2

Components of Stormspeed $u = 5.4322$ $v = 0.4399$

Layer	Relative average u	Relative average v	Vu-L
Surface-850 mb	.2878	8.0999	
650-500 mb	7.5428	-5.8351	5.4323
600-450 mb	6.8428	-6.2601	6.5371
550-400 mb	6.9928	-7.2101	6.9923
500-350 mb	6.5678	-8.0101	6.1551
450-300 mb	6.6428	-7.6851	6.6428
400-250 mb	7.8678	-7.4601	7.8678
550-300 mb	6.93448	-7.0601	

Table 3

<u>Variable</u>	<u>Computer value</u>	<u>Calculated value</u>
Storm speed	5.45	5.44
Storm direction	274.63	274.64
SURF-850 AV.REL. SPEED	8.10	8.105
SURF-850 AV.REL. DIR.	179.97	182.03
550-300 AV. REL. SPEED	9.92	9.90
550-300 AV. REL. DIR.	315.47	315.51
Shear Index	5	5

References

- Connell, J. R. Observed Inflow-Updraft Structure Related to Thunderstorms Precipitation and Dynamics. 8th Conference on Severe Local Storms, American Meteorological Society, Boston, 1973, 18-24. Unpublished manuscript.
- Darkow, G. L. Hourly Surface Static Energy Analysis as a Delineator of Thunderstorm Outflow Areas. Monthly Weather Review, Vol. 103, No. 9, 1975, pp. 817-822.
- Darkow, G. L. The Total Energy Environment of Severe Storms. Journal of Applied Meteorology, Vol. 7, No. 2, 1968, pp. 199-205.
- Darkow, G. L. and Livingston, R. L. The Evaluation of the Surface Static Energy Fields on 3 April 1974. Preprints 9th Conference on Severe Local Storms, AMS, Norman, Oklahoma, October 1975.
- Eagleman, J. R., Muirhead, Vincent M., and Willems, Nicholas. Thunderstorms, Tornadoes, and Building Damage. Lexington Books, Lexington, Mass., 1975.
- Jordinson, R. Flow in a Jet Directed Normal to the Wind. Aeronautics Department Paper No. 35, Imperial College, 1956, 17 pp.
- Kropfli, R. A. and Miller, L. J. Thunderstorm Flow Patterns in Three Dimensions. Monthly Weather Review, Vol. 103, No. 1, 1975, pp. 70-71.
- McAllister, J. D. A Momentum Theory for the Effects of Cross Flow on Incompressible Jets. Ph.D. Dissertation, University of Tennessee, Tullahoma, Tennessee, August 1968.
- Miller, R. C. and Maddox, R. A. Use of the SWEAT and SPOT Indices in Operational Severe Storm Forecasting. Preprints 9th Conference on Severe Local Storms, AMS, Norman, Oklahoma, October 1975.
- Saucier, Walter J. Principles of Meteorological Analysis. Chicago: The University of Chicago Press, 1955.
- Turner, Robert E. The Mechanics of Atmospheric Systems Derived through Vertical and Horizontal Analysis of Parametric Data. Dissertation, University of Tennessee, Knoxville, 1976.
- Storm Data. Volume 17, No. 4, National Oceanic and Atmospheric Administration, Asheville, North Carolina, April 1975.